The microbial ecology of bacterial lignocellulosic degradation in the ocean

A Dissertation Presented for the

Doctor of Philosophy

Degree

The University of Tennessee, Knoxville

Hannah Laing Yee Woo

May 2017

Copyright © 2017 by Hannah W.

All rights reserved.

Dedication

To my parents, John T. Woo and Felicia K Woo, and Jiang Liu

Acknowledgements

First and foremost, I must thank Dr. Terry Hazen for being my graduate advisor. He encouraged the necessary independent thinking and self-initiative to develop this project from scratch. Because of Dr. Hazen, I have been able to present my work in many places around the world, collect and study fascinating environmental samples, and meet the most influential microbiologists of our time. He has helped my academic career tremendously. For that, I will always be grateful.

I am fortunate to have a wonderful group of professors on my thesis committee, Dr. Nicole Labbe, Dr. Qiang He, and Dr. Chris Cox. I value their opinions highly and thank them for providing constructive feedback and support over the years.

My labmates within the Hazen lab group were supportive colleagues and friends for the past 5 years. A special thanks to Dominique Joyner and Julian Fortney who have been there for me since I was an intern at LBNL.

I must thank my sources of funding from the NSF iGERT SCALE-IT, NSF GRFP, NSF EAPSI, and PEO organization. Thank you for believing in my ideas and potential.

I am a Ph.D. today because of my supportive and loving family. Thank you, Jiang, for being my best friend. Your kindness, tenacity, and patience is unparalleled. Thank you, Brian and Andrew, for always being there for me. Thank you, Mommy and Daddy, for always letting me follow my dreams.

Abstract

The overarching theme of my dissertation is to study the role of bacteria in lignocellulose degradation. In recent years, more research has investigated the biodegradability of lignocellulose for biofuel production. The components of the lignocellulosic plant cell wall are considered intrinsically recalcitrant due to their structure. However, we hypothesize that these components are not intrinsically recalcitrant but their biodegradation is contingent on the environmental conditions, particularly the bacterial diversity. We believe bacteria will become especially important in lignocellulose degradation in conditions that are unfavorable for white-rot fungi. Therefore, we investigated the potential for lignin degradation by bacteria in the ocean where fungi would likely be rare. This knowledge would gather insight into allochthonous terrestrial organic carbon cycling in the ocean, a basic science knowledge gap in the complex ocean carbon cycle. Also, our investigation into the microbial ecology of marine lignocellulolytic bacteria may find new hosts of stress-tolerant commercial enzymes for biofuels and lignin valorization.

Table of Contents

Chapter 1 Introduction 1

Background 2

Dissertation Overview 4

Chapter 2 Comparing the lignin degrading potential of the deep ocean sediment and surface seawater microbial communities in the Eastern Mediterranean Sea 5

Abstract 7

Introduction 8

Material and Methods 10

Sample collection 10

Microcosm Enrichments and Respirometry 10

Cell counts 10

Phenol oxidase and peroxidase enzyme activity assays 11

Carbon and nitrogen measurements 11

UV-Vis spectroscopy 11

Excitation and emission (EEM) fluorescence 12

DNA extraction and 16S rRNA gene amplicon sequencing 12

Results 14

Respirometry 14

Cell Counts 14

Enzyme Activity 14

Total Carbon Measurements 15

UV-Vis 15

Excitation and Emission Matrices 16

16S rRNA gene amplicon sequencing 16

Conclusions 18

Acknowledgements 20

Appendix A: Figures and Tables 21

Chapter 3 Distinguishing keystone species and "cheaters" in the biodegradation of recalcitrant hemicellulose using polysaccharide xylan and monosaccharide xylose in enrichment microcosms 43

Abstract 45

Graphical Abstract 46

Introduction 47

Material and Methods 49

Initial enrichment of Great Australian Bight seawater on xylan 49

Respirometry of xylan-amended microcosms, xylose-amended microcosms, and control microcosms and respirometry data analysis 49

Optical Density at 600nm (OD 600nm) 50

Real-Time qPCR quantification of bacterial 16S gene copy number 50

High performance liquid chromatography (HPLC) measurement of xylose sugars 50

Ad-hoc Swapped Microcosm Community Test 50

Statistical Analysis 51

16S rRNA gene amplicon sequencing using the Illumina MiSeq and QIIME analysis 51

Alpha diversity, Beta Diversity, and Differential Abundance analysis using various R packages 51

Phylogenetic Tree analysis of Pseudoalteromonas OTUs 52

Results 53

Conclusions 56

Acknowledgements 59

Conflict of Interest 59

Appendix B: Figures and Tables 60

Chapter 4 Bacterial dominate lignin degradation via the phenylacetyl-CoA pathway in the Eastern Mediterranean Sea 90

Abstract 92

Introduction 93

Material and Methods 95

Lignin and Xylan amended enrichments of Eastern Mediterranean Seawater 95

Respirometry 95

DNA extraction 95

Metagenomics 96

16S rRNA gene amplicon sequencing 96

Results 97

Mineralization of lignin and xylan as measured by carbon dioxide production 97

Shifts in functional gene structure 97

Changes in microbial community composition 98

Potential lignin-degrading species in lignin-adapted consortia 99

Discussion 101

Acknowledgements 103

Conflict of Interest 103

Appendix C: Figures and Tables 104

Chapter 5 Conclusions 123

References 125

Vita 135

List of Tables

Table 1 Total Organic Carbon measurements 32

Table 2 Non-adjusted total production of carbon dioxide 60

Table 3 Sequencing Reads of 16S rRNA gene amplicons..... 70

Table 4 ADONIS tests of the main effects 80

Table 5 ADONIS tests of the interaction effects 82

Table 6 ADONIS tests of focused tests between Substrate and Concentration..... 83

Table 7 Alpha Diversity and statistics of sampled based on respiration group 84

Table 8 Metagenome sequencing results and accession numbers on MG-RAST 107

Table 9 The relative abundance of phyla detected in metagenomic shotgun reads..... 116

List of Figures

Figure 1 Photo of microcosms after 2 wk of incubation 21

Figure 2 Sampling Approach 22

Figure 3 Organosolv lignin UV-VIS spectrum 23

Figure 4 Beer's Law of Organosolv lignin dilution series 24

Figure 5 Photo of DNA extraction of mock samples with Organosolv lignin 25

Figure 6 Total carbon dioxide production 26

Figure 7 Respiration curves 27

Figure 8 Total carbon dioxide production and total inorganic carbon 28

Figure 9 Cell counts 29

Figure 10 Enzyme activity on model lignin L-Dopa 30

Figure 11 Total Carbon (TC) and Total Inorganic Carbon (TIC) Measurements 31

Figure 12 UV-Vis Spectroscopy 33

Figure 13 Excitation-emission matrix (EEM) spectroscopy 34

Figure 14. Chao1 Richness 35

Figure 15 Shannon's Diversity 36

Figure 16 Faith's Phylogenetic Diversity 37

Figure 17 Phylum level taxonomy 38

Figure 18 Class level taxonomy 39

Figure 19 Family level taxonomy 40

Figure 20 Beta Diversity 41

Figure 21 Relative abundance of lignin-associated species identified in previous Eastern Mediterranean Study 42

Figure 22 Carbon dioxide production from initial xylan-amended Australian Bight seawater 62

Figure 23 Dominant taxa in initial xylan-amended Australian Bight seawater 63

Figure 24 Production of carbon dioxide by substrate-amended microcosms 64

Figure 25 Xylan adapted consortia during the three consecutive incubations periods 65

Figure 26 Quantification of bacterial 16S rRNA gene copies in xylan-amended microcosms 66

Figure 27 Optical Density at 600 nm (OD 600 nm) of xylan-amended and control microcosms 67

Figure 28 Swapped Community Test Carbon Dioxide Production 68

Figure 29 Xylose adapted consortia during the three consecutive incubations periods 69

Figure 30 Relative abundances of dominant taxa 71

Figure 31 Chao1 Richness 72

Figure 32 Simpson Diversity 73

Figure 33 Faith's phylogenetic diversity 74

Figure 34 One-way ANOVA analysis of timepoint, substrate and concentration on Chao1 Richness Index 75

Figure 35 One-way ANOVA analysis of timepoint, substrate and concentration on Simpson Diversity Index 76

Figure 36 One-way ANOVA analysis of timepoint, substrate and concentration on Faith's Phylogenetic Diversity Index 77

Figure 37 Non-Metric Multidimensional Scaling (NMDS) ordination analysis 78

Figure 38 Non-Metric Multidimensional Scaling with confidence ellipses and variance boxplots 79

Figure 39 Multivariate homogeneity of group dispersions (variances) analysis 81

Figure 40 Log2-fold-change of OTUs in response to xylan amendment 85

Figure 41 Differential abundant OTUs 86

Figure 42 Phylogenetic tree of dominant Pseudoalteromonas OTUs 87

Figure 43 Phylogenetic tree analysis of Pseudoalteromonas denovo OTUs 88

Figure 44 Phylogenetic tree analysis of Pseudoalteromonas denovo OTUs at each timepoint 89

Figure 45 Experimental Design 104

Figure 46 Regression of carbon dioxide and oxygen accumulation within xylan and lignin amended microcosms 105

Figure 47 Carbon dioxide production 106

Figure 48 Non-metric Multidimensional Scaling (NMDS) Bray Ordination of functional gene structure 108

Figure 49 Average log_2-fold change of differentially abundant functional categories between lignin and control microcosms 109

Figure 50 Number of detected functional genes in all metagenomes per SEED Subsystems category 110

Figure 51 Average log_2-fold change of differentially abundant carbohydrate catabolism related functions between lignin and control microcosms 111

Figure 52 Average log_2-fold change of differentially abundant aromatic catabolism related functions between lignin and control microcosms 112

Figure 53 Beta-diversity and Alpha-diversity 113

Figure 54 Taxa Bar plots of Archaea, Alphaproteobacteria, Gammaproteobacteria and Flavobacteria from the 16S rRNA gene amplicon sequencing 114

Figure 55 The relative abundances of taxonomic classes identified by 16S rRNA gene amplicon sequencing 115

Figure 56 The relative abundance of fungal taxa within the metagenomic reads 119

Figure 57 Average log_2-fold changes of phyla between lignin-adapted consortia and the controls 120

Figure 58 Taxonomic families from phyla that became higher in abundance in response to lignin 121

Figure 59 Average Indicator Values of taxonomic families for lignin amendment 122

Chapter 1 Introduction

Background

Lignin is the second most abundant biological polymer in the world. Lignin is a complex aromatic compound that provides structural support within the cell walls of terrestrial plants. It is formed by radical polymerization of three phenylpropanoids (paracoumaryl alcohol, coniferyl alcohol, and sinapyl alcohol). The use of radicals causes lignin to have a variety of carbon-to-carbon or carbon-to-oxygen linkages within a three-dimensional structure (Campbell and Sederoff, 1996). Lignin is known to be difficult and slow for microbes to degrade. However, lignin is not infallible. Aromatic compounds are known to breakdown in the environment through beta-ketoadipate pathways that produce intermediates for the citric acid cycle (Fuchs et al., 2011). These pathways contribute to carbon cycling, which must depend in part on microbes and their metabolic processes. Although the cycling of lignin may be slower than other simpler carbon compounds, mechanistic knowledge about the biological degradation processes would provide the means for industrial applications.

Like lignin, hemicellulose is also a heterogeneous component of the plant cell wall and contributes to biomass recalcitrance. Its structure varies between different feedstocks (Scheller and Ulvskov, 2010), but typically constitutes 16-33% of common bioenergy feedstocks like miscanthus, switchgrass, cornstover, poplar, eucalyptus, and pine (Ragauskas et al., 2014). An investigation into the enzymes specific for hemicellulose would complement the lignin degrading enzymes.

Interest in lignin and hemicellulose has increased since the US Energy Independence and Security Act of 2007 mandated increasing biofuel production. Lignin is a major underutilized waste stream. Despite the large supply chain costs associated with biomass (Ekşioğlu et al., 2009; Ajanovic and Haas, 2014), up to 40% of the initial material can be wasted because it is lignin (Ragauskas et al., 2014). Lignin must be removed for cellulosic ethanol because it is a physical barrier preventing access to the cellulose and occludes the action of cellulases (Ooshima et al., 1990). DOE reports that 12 to 25 billion dollars could be gained from conversion rather than incineration of 0.225 billion tons of lignin (Holladay et al., 2007). Environmental analysis has shown that lignin conversion to higher value chemicals will produce significantly less greenhouse gases than conversion to electricity (Davis, 2013). For example, carbon fiber production from lignin (Ragauskas et al., 2014) or the medium chain length polyhydroxyalkonoates that serve as plastic precursors (Linger et al., 2014) would both require lignin without contaminants like hemicellulose. Methods to separate lignin and hemicellulose are important for lignin valorization.

Few microbes are known to produce lignin-degrading enzymes besides fungi. White-rot fungi like *Phanerochaete chrysosporium* are frequently assumed to be the only lignin degrading microorganisms (Kirk and Farrell, 1987). Fungi rely heavily on expensive carbohydrates like glucose before they start producing the enzymes. As a result, fungal enzymes are expensive and can attribute up to 30 cents per gallon of ethanol produced (Klein-Marcuschamer et al., 2012). Enzymes tend to be inactivated by chemical reagents like the organic salt, ionic liquid (Turner et al., 2003). The rising popularity of biomass pretreatment methods using ionic liquid has caused a strong demand for ionic liquid tolerant enzymes.

Recent evidence show that bacteria play a larger role in lignin degradation than previously thought. The known bacterial lignin degraders so far come from phylogenetically diverse phyla of both gram-positive and gram-negative *Actinobacteria*, *Bacilli*, *Clostridia*, various *Proteobacteria*, *Bacteroidetes* and *Cyanobacteria* (Bugg et al., 2011b). Bacteria possess novel accessory enzymes like binding proteins that could aid lignin degradation (Brown and Chang, 2014). Within decomposing popular woodchip piles, more bacterial lignolytic oxidases than fungal were found using metagenomics (van der Lelie et al., 2012).

Compared to soil and compost environments, the ocean has not been well investigated for extracellular lignocellulolytic microbial enzymes. Lignocellulose is allochthonous to marine ecosystems, because it is a uniquely terrestrial organic carbon that can only enter marine systems through rivers or run off. However, terrestrial organic carbon including lignin is degraded in the marine environment, but the mechanism behind this phenomenon is unclear (Hedges et al., 1997). The estimated input of terrestrial organics far exceeds the amount of lignin buried in the sediment (Bianchi, 2011a). The missing fraction of terrestrial organic carbon is degraded and metabolized. An enzyme discovery project targeting the deep ocean would yield a new bounty of non-fungal microbial enzymes for possible commercialization. Marine fungi are rare (Richards et al., 2012). Artificially sunk wood logs are hotspots of biodiversity (Bienhold et al., 2013; McClain and Barry, 2014), which suggests a widespread ability among marine microbes to degrade allochthonous lignocellulosic material.

Next-generation sequencing can be an inexpensive tool to identify the lignin and hemicellulose degrading bacterial species. 16S rRNA gene amplicon and shotgun metagenome sequencing are now commonplace for environmental community analysis because of the high throughput and low cost. A recent paper by Strachan et. al. proposes 6 different functional gene classes responsible for lignin biodegradation in the environment (Strachan et al., 2014), however the genetic basis of bacterial lignin degradation is not completely understood yet (Bugg and Rahmanpour, 2015b). Sequencing can be a key method in identifying species and functional genes related to lignin and hemicellulose degradation.

The heterogeneity and complexity of the structure of lignin creates challenges in the characterization of degraded lignin. The problem becomes even more difficult when sediment and inorganics from environmental samples are present. There are many rapid spectroscopy methods to assess lignin (Lupoi et al., 2014) that may be high throughput methods to screen for degraded lignin in environmental samples. A particular method using ionic liquid extraction by Kline et. al. for FTIR analysis may provide some insight (Kline et al., 2010). Since lignin is fluorescent, UV-VIS spectroscopy could be used to ascertain if any changes are occurring with lignin content in the microcosms. If rapid methods fail, more intensive methods of lignin analysis in environmental matrices are available. For example, CuO oxidation phenol of lignin has been used on lignin in soils and seawater (Goñi and Montgomery, 2000). More work is needed on methods to assess lignin in environmental samples.

Dissertation Overview

Biological processes have long been associated with the rapid cycling of terrestrial organic carbon in the ocean. To my knowledge, there has not been a sequencing based survey of deep-ocean microbial diversity capable of metabolizing lignin and hemicellulose specifically. Therefore, the mechanistic understanding of lignin degradation by marine microbes is a knowledge gap. With the recent interest in lignin and hemicellulose degrading enzymes, marine microbes could be novel non-fungal sources of commercial enzymes. Enzyme discovery projects have not targeted deep ocean.

In chapter 2, the hypothesis was that sediment and seawater microbial communities of the Eastern Mediterranean would respond differently to lignin. Sediment may respond better due to being continually exposed to recalcitrant carbon in the deep ocean that would cause them to adapt to recalcitrant carbon utilization. Lignin degradation potential was compared between sediment and seawater microbial communities. The effect of phosphate on lignin degradation was also investigated.

In chapter 3, the hypothesis was that dominant populations of the microbial community subsisting on hemicellulose were microbial cheaters. The relevance of microbial cheaters in hemicellulose degradation was assessed by comparing seawater microbial communities enriched with the polymer hemicellulose, xylan, and monomer sugar, xylose. The xylose enriched microbial community was used to determine potential cheater taxa that may bloom quickly in response to available xylose.

In chapter 4, the hypothesis was that bacteria, rather than fungi, contribute to lignin degradation in the ocean. Marine fungi exist in the ocean where their role is largely unknown but we believe fungi would have a diminished role in lignin-degradation compared to bacteria. The relative abundance of fungi and bacteria in lignin-consortia and hemicellulose-adapted consortia were compared using metagenomics and 16S rRNA gene amplicon sequencing. The functional gene profiles were also compared using metagenomics.

Chapter 2 Comparing the lignin degrading potential of the deep ocean sediment and surface seawater microbial communities in the Eastern Mediterranean Sea

Hannah L. Woo[1], Jingming Tao[2], Jing Wang[2], Stephen M. Techtmann[1,3], Nicole Labbe[2], Terry C. Hazen[1,4,5]

Affiliations:

[1]University of Tennessee, Civil and Environmental Engineering

[2]University of Tennessee Institute of Agriculture, Center of Renewable Carbon

[3]Michigan Technological University, Biological Sciences

[4]University of Tennessee, Microbiology

[5]University of Tennessee, Earth and Planetary Science

Corresponding Author:

Terry C. Hazen

676 Dabney Hall
Knoxville, Tennessee 37996-1605
Phone: 865-974-7709
E-mail: tchazen@utk.edu

Author Contributions:

Conceived or designed experiments- HLW, TCH, NL

Collected samples & performed the experiments- HLW, JT, JW, SMT

Analyzed the data- JT, HLW

Wrote the paper- HLW

Abstract

Terrestrial organic matter, including lignin, enters the ocean through rivers where it is rapidly degraded. Only a fraction of the incoming terrestrial organic matter is ultimately buried in the deep ocean sediment. The microbial diversity contributing to lignin degradation in the ocean is unknown but their enzymes could be a key discovery for lignin valorization, the conversion of lignin into higher value products and chemicals. In our survey of marine lignin-degrading bacteria in the Eastern Mediterranean, we hypothesized that the microbial communities of the sediment would degrade more lignin than that of the surface seawater, since sediment heterotrophic microbes are more adapted to utilize the recalcitrant organic matter of the deep ocean. Organosolv lignin was amended to seawater and sediment microcosms along with phosphate to alleviate nutrient deficiencies. Lignin-amended seawater and sediment microcosms had higher respiration rates and oxidative enzyme activity in comparison to the unamended control after 2 weeks. Slightly higher enzyme activity was found in the sediment. Excitation and emission fluorescence spectroscopy showed differences in the colorimetric dissolved organic matter between sediment and seawater with lignin. UV-VIS estimation of the solubilized lignin showed a greater decrease in soluble lignin within the sediment than the seawater. Based on 16S rRNA gene amplicon sequencing, *Gammaproteobacteria* and *Alphaproteobacteria* dominated the lignin-amended microbial communities. *Halomonas* and *Sphingorhabdus* dominated in the lignin-amended sediment, while *Idiomarina* and *Thalassospira* dominated in the lignin-amended seawater. Our findings demonstrate the potential for deep ocean microbial communities to contribute to rapid terrestrial organic matter cycling and elucidates the microbial diversity of bacteria that may be able to produce lignin-degrading enzymes for lignin valorization.

Keywords: Lignin valorization, enzyme discovery, terrestrial organic carbon cycling, 16S rRNA gene amplicon sequencing, UV-VIS spectroscopy, Excitation and emission matrices

Introduction

The fate of terrestrial organic carbon is unclear after it enters the ocean through rivers (Hedges et al., 1997; Blair and Aller, 2012). Very little terrestrial organic carbon is detected in the global open oceans but only an estimated 30% of the input is found buried in the sediments (Bianchi, 2011b). The rapid remineralization of the "missing" terrestrial organic carbon in the ocean is sometimes called paradoxical because terrestrial organic carbon consists of plant-derived organics such as lignin and cellulose that are not easily degraded (Hedges et al., 1997). Lignin-derived phenolics are thermodynamically stable due to the resonance of its aromatic rings.

Many studies focused on the characterization of terrestrial organic matter in aquatic or marine systems posit the significance disappearance of terrestrial organic matter to biological remineralization (Schlünz and Schneider, 2000; Ward et al., 2013). However, microbial species contributing to the rapid turnover of terrestrial organic carbon in the ocean have not been well-investigated. We believe a survey of marine bacteria capable of degrading lignin would provide novel and effective enzymes for industry. The rise of cellulosic biofuels has sparked more interest in lignin valorization, which is the production of renewable products or chemicals from lignin (Zakzeski et al., 2010; Ragauskas et al., 2014). In attempt to make the lignin valorization profitable, more effort has been devoted to the discovery of more effective lignin-degrading enzymes and microbes (Ruiz-Dueñas and Martínez, 2009; Brown and Chang, 2014; Pollegioni et al., 2015). The biodiversity of lignin degrading microbial species is largely unknown aside from the white-rot fungi that have been well-studied for lignin degradation for decades (Kirk and Farrell, 1987).

Previous evidence suggests the importance of photooxidation on terrestrial carbon cycling in the ocean (Opsahl and Benner, 1998; Hernes and Benner, 2003). However, we hypothesized that microbial reactions will become more important in the deepest depths of the ocean where light cannot penetrate. In this study, we assessed the lignin degradation potential of seawater and sediment microbial communities of the Eastern Mediterranean Sea. We believe the sediment microbial communities may degrade more lignin than the seawater microbial communities because sediment heterotrophic bacteria have been continually exposed to recalcitrant carbon pools in the deep ocean and may be better adapted to utilizing recalcitrant carbon.

The Eastern Mediterranean Sea at the outlet of the Nile Delta may possess an exceptionally high amount of aerobic lignin-degrading species compared to other deep ocean environments due to its high dissolved oxygen content and warm temperatures. The fate of lignin has been correlated with mean average temperature in terrestrial environments (Thevenot et al., 2010). Lignin degradation can occur under anoxic conditions (Colberg and Young, 1985; Deangelis et al., 2011b; Hall et al., 2015), but is more typically studied under oxic conditions (Kirk and Farrell, 1987; Bugg et al., 2011b; Bugg and Rahmanpour, 2015a). Because of the high dissolved oxygen of the Eastern Mediterranean, we targeted aerobic microbial species with lignin degradation potential.

In this study, we added phosphate to alleviate the nutrient limitations when comparing the response of sediment and seawater to lignin. Phosphate limitation is a defining characteristic of the Eastern Mediterranean Sea (Krom et al., 2005; Krom et al., 2010) with the surface water having five times more phosphate than the lower depths (Techtmann et al., 2015).

We utilized a full factorial experimental design to assess the effect of lignin and phosphate amendment on sediment and seawater. We then characterized the differences in respiration rates, enzyme activity, solubilized lignin concentration, dissolved organic matter, and microbial community structure between lignin-amended sediment and seawater.

Material and Methods

Sample collection

Samples from 3 depths (near the surface, near the seafloor, sediment) were collected October 2012 from the oligotrophic, warm, and hypersaline Eastern Mediterranean Sea, near the outlet of the Egyptian Nile Delta. The latitude and longitude of the sampling were 31.852 and 29.9822. Water was sampled using Niskin bottles at 50m and 742m below the sea surface. Sediments were collected from the seafloor using a corer. The seafloor was 762m below the surface at the site. Samples were stored at 4°C until use for microcosms. The sampling site and geochemistry were described in depth by Techtmann et al (Techtmann et al., 2015)

Microcosm Enrichments and Respirometry

Microcosms of sediment slurry and seawater samples were amended with Organosolv lignin and phosphate in a full factorial experimental design: sediment alone (S), sediment with phosphate (S-P), sediment with lignin (S-OL), sediment with lignin and phosphate (S-OL-P), seawater alone (W), seawater with phosphate (S-P), seawater with lignin (W-OL), seawater with lignin and phosphate (W-OL-P). Each of the microcosms were prepared in duplicate for 16 microcosms total.

Lignin microcosms of seawater and sediment slurry were separately prepared in 60 ml mL volumes and amended with 0.3 g of insoluble Organosolv lignin extracted from switchgrass. The Organosolv lignin used was similar to the control lignin described by Tao et al. (Tao et al., 2016). Seawater was added directly to serum bottles while sediments were first made into a slurry consisting of 2.5 g sediment and 60 mL of near-bottom water before adding into the bottles. Sediments microcosms were more liquid than sediment (Figure 1). Phosphate is an extremely limited nutrient in the Eastern Mediterranean Sea with average concentrations being as low as 39µg/L (Techtmann et al., 2015). A 1.5mM phosphate sodium phosphate and potassium phosphate solution was added to phosphate amended microcosms to test their effect on the microbial community structure and respiration rates.

The Microoxymax respirometer (Columbus Instruments, Ohio, USA) was used to monitor the production of carbon dioxide in the microcosm bottles at 3 h intervals. All microcosms were continuously agitated on an orbital shaker at 100 rpm throughout the 2 wk incubation period. Microcosms were incubated at their *in situ* temperatures; seawater microcosms were incubated at 19°C while sediment microcosms were incubated at 14°C. After the 2 wks of incubation, each microcosm was harvested for downstream analysis after rigorous homogenization or filtration where required (Figure 2).

Cell counts

Direct subsamples from the microcosm were preserved for cell counting by adding formalin to a final concentration of 3.7% and then stored at 4°C. Lignin or sediment particulates within 1 ml mL of preserved sample were flocculated by adding 5ml each of calcium chloride (pH 11) and sodium pyrophosphate (pH 8), sonicating for 1 min, vortexing for 5 min, then centrifuging at 1000 rpm for 3 min to pellet the large flocs (Nakamura, 1961). A 10 µl of the supernatant was

then transferred to glass slide wells and then stained with acridine orange for counting under an epifluorescence microscope as described by Hazen et al. (Hazen et al., 2010). Samples with less than 3 cells per field of view on average were not considered above reporting limits.

Phenol oxidase and peroxidase enzyme activity assays

Extracellular lignin-degrading enzymes were measured by a colorimetric assay with the model lignin substrate, L-3,4-dihydroxyphenylalanine (L-Dopa) (Sinsabaugh, 2010; Bach et al., 2013). Enzyme activity was tested with and without the addition of the electron acceptor, hydrogen peroxide. Phenol oxidase activity is tested without hydrogen peroxide, while peroxidase activity is tested with hydrogen peroxide (Bach et al., 2013). The enzyme activity assay followed methods previously described using 10 mM L-Dopa in 50mM Tris-HCl pH 8.0 and 0.3% hydrogen peroxide (Woo et al., 2014). In brief, filtrate from the microcosms that passed through a 0.22µm filter were combined with the L-Dopa solution in a 1:5 ratio, incubated in the dark for 1 h, and then measured for absorbance at 460 nm using a Synergy HT plate reader (Biotek Winnoski, VT). The rate of each microcosm was calculated by the difference between the final and initial absorbance minus the difference between the final and initial absorbance of a control consisting of just L-Dopa alone in buffer.

Carbon and nitrogen measurements

Total organic carbon of microcosm filtrates were measured using a Shimadzu TOC-L Series (Shimadzu Kyoto, Japan), 680 °C Combustion Catalytic Oxidation Method at the University of Tennessee Institute of Agriculture Water Quality Laboratory.

UV-Vis spectroscopy

UV-Vis spectroscopy is a common technique to characterize lignin since lignin absorbs certain wavelengths of the electromagnetic spectrum (Hatfield and Fukushima, 2005; Kline et al., 2010; Lee et al., 2013b). Filtrate from the microcosms that passed through a 0.22µm filter were measured for absorbance over a broad range using a Thermo Scientific Evolution 200 series spectrophotometer (Thermo Scientific Waltham, MA). The absorbance at 286 nm was used as a proxy for lignin concentration. The Organosolv lignin used in this study had an absorbance maximum at 286nm (Figure 3), which is similar to previously found absorption maxima for lignin model compounds at 280 and 270 nm (Fergus and Goring, 1970). A standard curve was generated by measuring 7 dilutions of Organosolv lignin in artificial seawater medium (ONR7a (Atlas, 2010)). Absorbance at 286nm and the concentration of Organosolv lignin were linearly correlated with R^2=0.99 and linear fit equation of $y = 4.0496\ x + 0.065$ (Figure 4).

For sediment and seawater microcosms with lignin, additional UV-VIS spectra were collected from the formalin preserved microcosm sample by solubilizing the Organosolv lignin particulates using NaOH and then filtering the sample to remove precipitates and sediment. We found NaOH and DMSO were effective solvents to solubilize the Organosolv lignin. Ethanol was only slightly effective. HCl did not solubilize the lignin. A 10 ml mL of 0.1M NaOH was added to 0.2 ml mL of microcosm sample, which was then allowed to dissolve and equilibrate in the dark at room temperature for several hours. Any precipitates or sediment was then removed using a 0.22 µm filter. Filters were GD/X disposable nylon filters with polypropylene housing.

Filters were rinsed with MilliQ ultrapure water and dried completely before filtering. The first ml of sample eluted from the filter was disposed so that the last 3ml was filtered directly into cuvettes for UV-Vis spectroscopy.

Excitation and emission (EEM) fluorescence

Colorimetric dissolved organic matter was characterized using excitation and emission matrices (EEM). Filtrate from the microcosms that passed through a 0.22 µm filter was analyzed by a Horiba Scientific Fluoromax4 spectrofluorometer (Horiba Kyoto, Japan) with a Xenon lamp following the method previously described by Brannen-Donnelly et al (Brannen-Donnelly and Engel, 2015). Excitation wavelengths ranged from 240 nm and 440 nm in 1nm increments. Emission wavelengths ranged from 250 nm and 550 nm in 1nm increments. Fluorescence Index (FI), Humification Index (HIX), and Biological Index (BIX) were calculated using methods from Birdwell et al (Birdwell and Engel, 2010).

DNA extraction and 16S rRNA gene amplicon sequencing

Microbial biomass was harvested from microcosms by filtering onto a MoBio 0.22 µm water filter (MoBio Carlsbad, CA). The Organosolv lignin interfered with DNA extraction methods using organic solvents (Brodie et al., 2002; DeAngelis et al., 2011a)(Figure 5). The Organosolv lignin produced a viscous brown organic phase and a thick white interface when the phenol/chloroform/isoamyl alcohol solvent was added. To avoid organic solvents, the MoBio Powerwater DNA isolation kit (MoBio Carlsbad, CA) was used.

Amplicon libraries for the V4 region of the16S rRNA gene were prepared using the methods described by Techtmann et. al. (Techtmann et al., 2015). In brief, DNA extracts were cleaned using the Genomic DNA Clean and Concentrator™ (Zymo Research Irvine, CA) before PCR amplification with barcoded primers. Barcoded PCR products were first purified using the Agencourt AMPure beads (Beckman Coulter Indianapolis, IN). Pools of products were then analyzed for length using the Bioanalzyer (Agilent Santa Clara, CA). The Wizard SV Gel purification kit (Promega Madison, WI) was then used to further purify products. Final pooled libraries were quantified using qPCR (KAPA Biosystems Wilmington, MA) before loading onto an Illumina MiSeq platform with the v3 2x300 kit.

Forward reads were checked for quality using FastQC (Babraham Bioinformatics, Cambridge, UK). Reads were demultiplexed and checked for chimeras using QIIME (Caporaso et al., 2010). After chimeric sequences were removed, the open OTU picking strategy was used to assign Greengenes taxonomy (May 2013 version) (DeSantis et al., 2006) to OTU clusters of 97% sequence similarity.

Alpha diversity indices, Chao1 richness, Shannon's diversity and Faith's phylogenetic diversity, were calculated with the rarefied OTU table using R packages phyloseq (McMurdie and Holmes, 2013) and picante (Kembel et al., 2010). Beta diversity analysis, specifically the Non-metric Multidimensional Scaling (NMDS) ordination with Unifrac distance, was conducted using the R packages phyloseq (McMurdie and Holmes, 2013) and vegan (Dixon and Palmer, 2003). Before ordination, the OTU table was normalized by transforming sample counts to relative abundance

multiplied by the median sequencing depth. OTUs of low variance were filtered by using a threshold of coefficient of variation of at least 2.

ADONIS analysis, a statistical analysis on microbial community dissimilarities, was done using the online tool, Calypso (Zakrzewski et al., 2016). ADONIS was used to compare microbial communities between experimental factors—sample type, lignin amendment and phosphate amendment. ADONIS was repeated at different levels of resolution: OTU, species, genus, and family level. Bray-Curtis distance was used for all ADONIS tests. OTU data was filtered and normalized using default settings on Calypso.

Results

Insoluble Organosolv lignin was aerobically incubated with Eastern Mediterranean seawater and sediment for 2 weeks. After two weeks, the insoluble Organosolv lignin substrate appeared to partially solubilize within the seawater microcosms. The seawater microcosms were more brown in color at the end of the experiment (Figure 1). In contrast, the aqueous fraction of the lignin-amended sediment microcosms remained colorless.

Respirometry

Lignin increased the production of carbon dioxide in both the sediment and seawater (Figure 6). Similar amounts of carbon dioxide were produced by seawater and sediment microcosms in response to lignin. The sediment microcosms amended with lignin including the ones amended with phosphate (n=4) produced significantly higher amounts of carbon dioxide than the other sediment microcosms without lignin (n=4) (T-TEST p-value=0.00033). The lignin-amended sediment microcosms produced on average 3572 µg of carbon dioxide which is 6 times higher than the unamended sediment. Seawater amended with lignin (n=4) also produced significantly more carbon dioxide than unamended seawater (n=4) (T-TEST p-value=0.0034). After the 2 weeks of incubation, the rate of carbon dioxide production was still high and oxygen was still being utilized (Figure 7). The rate of production within lignin-amended microcosms at the final timepoint were on average 5.86 µg of carbon dioxide per hour while the unamended microcosms were only 0.55 µg of carbon dioxide per hour.

Phosphate did not significantly increase production of carbon dioxide within lignin-amended microcosms. It did, however, boost production of carbon dioxide within sediment and seawater microcosms without lignin. Phosphate increased the accumulation of carbon dioxide in sediment and seawater over 5-fold. However, within lignin amended microcosms, phosphate did not significantly increase the amount of carbon dioxide accumulation.

The pH of the microcosms did not change after incubation and remained at pH 8. Total inorganic carbon measurement did not correlate well with respiration levels, which preclude possibility of carbonate and bicarbonate of the seawater turning into carbon dioxide gas abiotically (Figure 8).

Cell Counts

Cell counts between microcosms varied only slightly ranging from 10^6 to 10^7 cells per ml (Figure 9). Lignin did not significantly change the cell counts in sediment microcosms (T-TEST p-value>0.05). The cell counts of most lignin-amended seawater microcosms were below detectable limits. Phosphate had a slightly negative effect of cell numbers (T-TEST p-value=0.023). Phosphate-amended microcosms had 3.0×10^6 cells per ml on average while microcosms without phosphate were twice as high at 7.6×10^6 cells per ml.

Enzyme Activity

Extracellular enzyme activities, phenol oxidase and peroxidase, on model lignin L-Dopa were higher in lignin-amended microcosms (Figure 10a and 10b). The lignin-amended sediment

microcosms had significant higher phenol oxidase (T-TEST p-value=0.0009) and peroxidase activity than the unamended sediment (T-TEST p-value= 7.01763E-06). Within seawater microcosms, only the peroxidase activity was significantly higher in the lignin-amended microcosms (T-TEST p-value= 0.009).

Among the lignin-amended microcosms, sediment microcosms had more phenol oxidase and peroxidase activity than seawater microcosms. Phenol oxidase activity within the sediment microcosms were 12% higher than the seawater. Peroxidase activity was 3.5 times higher in sediment than seawater.

In general, all microcosms had less peroxidase than phenol oxidase activity. Hydrogen peroxide may have suppressed enzyme activity. The addition of phosphate did not seem to have any significant effect on enzyme activity.

Total Carbon Measurements

Total organic carbon (TOC) represented dissolved carbon within the microcosms. Microbial biomass, particulate lignin, and sediment greater than 0. 0.22 µm were removed prior to analysis by filtration.

All microcosms had less dissolved organic carbon (DOC) than the un-degraded 0.5% Organosolv lignin standard (Figure 11). The DOC from the un-degraded Organosolv lignin standard was 4.1 ppm, indicating that Organosolv lignin is slightly soluble in seawater. The DOC of seawater microcosms ranged from 0.258-0.408 ppm (Table 1), which is an order of magnitude less than the un-degraded lignin standard and only slightly higher than the total organic carbon of MilliQ ultrapure water. In contrast, all sediment microcosms did not have detectable amounts of DOC.

UV-Vis

The colorimetric fraction of the DOC (CDOC) was characterized using UV-Vis. The un-degraded Organosolv lignin standard showed an absorbance maximum at 286nm, which was used as a proxy for lignin concentration.

Based on the absorbance at 286 nm, sediment microcosms amended with lignin had less residual lignin than the seawater microcosms with lignin after 2 weeks (T-TEST p-value=0.0005) (Figure 12a). Sediment microcosms with lignin had 33% less lignin than the seawater microcosms. In comparison to the un-degraded Organosolv lignin standard, the sediment had 31% less fluorescence at 286 nm. Phosphate did not affect the amount of residual lignin significantly.

Dissolved organic carbon can possibly adsorb to particulate Organosolv lignin or sediment particulates. To test if adsorption influenced the UV-Vis results within the sediment, we also solubilized the particulate lignin by adding NaOH. The filtrate was then analyzed for absorbance at 286 nm. The solubilized lignin UV-Vis corroborated the finding that significantly less residual lignin in the sediment microcosms after 2 weeks (T-TEST p-value=0.03) (Figure 12b). The sediment had 30% percent less residual lignin than the seawater microcosms. In contrast, the

seawater did not have significantly less lignin after 2 weeks of incubation (T-TEST p-value=0.27).

Excitation and Emission Matrices

The colorimetric fraction of the DOC (CDOC) was further characterized using EEM fluorescence spectroscopy. Several commonly used EEM indices, FI, HIX, and BIX, were calculated from the EEM data (Figure 13a). The FI and HIX of the seawater microcosms with lignin were significantly higher than the sediment microcosms with lignin (FI T-TEST pvalue=0.004, HIX T-TEST p-value=0.0011).

Based on the EEM profiles, the sediment and seawater microcosms possess different CDOC pools. The EEMs were one of three patterns of peaks (Figure 13b). For the sediment and seawater with lignin, their EEMs had two high peaks centered approximately at Ex/Em 300/425 and Ex/Em 425/310. The sediment without lignin had a high peak at Ex/Em 245/425 and a lower peak at Ex/Em 340/425. Lastly, the seawater without lignin had one peak at Ex/Em 280/350.

16S rRNA gene amplicon sequencing

The microbial communities of sediment and seawater were different in composition at the species level despite *Proteobacteria* being the ubiquitous dominant phylum in all microcosms. Because the microbial communities were so different, sediment and seawater had different bacterial OTUs responding to the lignin amendment. Phosphate amendment affected the microbial community structure of both the sediment and seawater but its effect was muted when co-amended with lignin.

Microbial communities between sediment and seawater were different in terms of richness and level of diversity. Richness and diversity was evaluated using three common alpha diversity indices: Chao1 richness, Shannon Diversity and Faith's Phylogenetic Diversity. Compared to the unamended seawater and sediment, lignin-amended microcosms had less species richness and diversity (Figure 14, 15, and 16). The lignin-amended sediment microcosms were more complex than the lignin-amended seawater microcosms.

At both the phylum and class level of taxonomy, lignin-amended microcosms appeared similar to their unamended counterparts (Figure 17 and 18). S, S-OL, and S-OL-P were very similar in that they all had large population of the class *Alphaproteobacteria* and class *Gammaproteobacteria*. Likewise, W, W-OL, and W-OL-P all had a dominant population of *Alphaproteobacteria* and *Gammaproteobacteria*. Among the seawater microcosms, the *Gammaproteobacteria* were more abundant than the *Alphaproteobacteria*. The unamended seawater had more *Flavobacteria* and *Betaproteobacteria* than other seawater microcosms.

When comparing communities at greater level of resolution at the family level of taxonomy, seawater and sediment microcosms appeared more distinct (Figure 19). Within sediment microcosms with lignin, the most common bacterial OTUs were closely related to the family *Alcanivoraceae* and *Halomonadaceae* (Phylum *Proteobacteria*, Order *Gammaproteobacteria*, Class *Alteromonadales*). Sediment microcosm had a large amount of *Sphigomonadales* that

could not be identified using the Greengenes database at a greater level of resolution. We found that the representative sequence of that OTU cluster closely matched the genus *Sphingorhabdus* in a BLAST search against the NCBI database. Meanwhile, the most common OTU within seawater microcosms with lignin was closely related to the *Gammaproteobacteria* taxonomic family *Idiomarinacaeae* (Phylum *Proteobacteria*, Order *Gammaproteobacteria*, Class *Alteromonadales*).

Beta-diversity analysis using Non-metric Multidimensional Scaling (NMDS) ordination with Unifrac distance corroborated the large differences observed between sediment and seawater (Figure 20a). The dissimilarities between sediment and seawater was statistically significant with Bray-Curtis distance at the species level (ADONIS p-value=0.032) (Figure 20b). Lignin amended microcosms were also significantly different from their non-lignin counterparts (ADONIS p-value=0.0473).

Phosphate amendment affected the microbial community to lesser degree than lignin (Figure 20b). S-P and W-P, the sediment and seawater microcosms with phosphate, had a large abundance of the phylum *Firmicutes*, particularly the class *Bacilli*, that distinguished them from the other microcosms. The most common OTU in phosphate-amended microcosms was closely related to *Lactobacillaceae* (Phylum *Firmicutes*, Order *Bacilli*, Class *Lactobacillales).* However, when phosphate was added along with lignin, *Lactobacillaceae* were rare. Phosphate-amended microcosms, however, were not significantly different from the non-phosphate (ADONIS p-value=0.748).

The seawater microcosm with lignin and phosphate was further enriched on lignin as part of another study. The resulting lignin seawater microcosm was characterized using 16S rRNA gene amplicon sequencing. Several bacterial taxonomic families were ranked for their relevance in lignin degradation (Figure 21). We found that *Idiomarinacaeae* was also highly dominant in the lignin amended microcosms. The sediment did not have many taxa in common with the lignin-amended seawater.

Conclusions

Our main finding was that the addition of high-purity Organosolv lignin significantly increased microbial activity in both sediment and seawater samples from the Eastern Mediterranean. The additional lignin boosted respiration rates and enzyme activity of the microbes. The positive effect of lignin on microbial activity demonstrates the potential impact of microbial activity on terrestrial organic carbon cycling.

We hypothesized that sediment microbial communities would degrade lignin better than the seawater. UV-Vis showed a larger decrease in soluble Organosolv lignin within sediment microcosms than seawater. The CDOC characterized within the lignin-amended sediment and seawater microcosms by EEMs were slightly different. The differences could indicate that the microbes had utilized different pools of organic carbon or that the microbe had produced different breakdown products.

However, respiration rates, cell counts, and phenol oxidase enzyme activities were similar between the two depths when amended with lignin. Respiration rates below the photic zone in the ocean is complicated (Andersson et al., 2004), but oxic respiration is thought to be correlated with water depth and the overlying water productivity (Smith Jr. and Hinga, 1983). Since the surface water and the seafloor are less than 800m apart and the Eastern Mediterranean is known for low productivity, the lack of variation between the surface and sediment may be reasonable.

Phosphate was added to alleviate nutrient constraints in our comparison between sediment and seawater. We found that phosphate was not critical limiting factor for the mineralization of lignin. The amendment of phosphate did not influence the functional activity or microbial community significantly when lignin was present. The extreme oligotrophy of the Eastern Mediterranean may have selected for K-species that are able to survive on limited resources (Pianka, 1970).

Despite how similar the response was to lignin, we found that the lignin-associated microbial species in seawater and sediment were very different. The differences based on depth were expected as water masses of the Eastern Mediterranean have distinct microbial communities (Techtmann et al., 2015). Overall, *Proteobacteria* dominated the seawater and sediment microbial communities but distinct Proteobacteria species were found in each sample type. We found *Idiomarinaceae* OTUs were in higher abundance within the seawater microcosms. Meanwhile, *Sphingorhabdus* OTUs and *Halomonadaceae* were found in higher abundance in the sediment. The differences in microbial communities but similar performance on lignin suggests functional redundancy between multiple species of microbes.

Little is known about lignin degradation by marine microbes. *Idiomarina* and *Halomonas* spp. have been previously found associated with lignocellulose in marine environments (Sánchez-Porro et al., 2003; Ohta et al., 2012; Fernandez-Gomez et al., 2013; Dalmaso et al., 2015; Mathews et al., 2015; O'Dell et al., 2015). *Halomonas* is also a species that responds well to nutrient amendment in sediment (Ponce-Soto et al., 2015). However, *Sphingorhabdus* is not well characterized nor is it well represented in databases. It was first isolated from oligotrophic environments (Jogler et al., 2013). Sediment has a more complex microbial diversity responding to lignin that may be worthy to pursue with more enrichment.

The rapid disappearance of terrestrial organic carbon in the ocean has been attributed to biological remineralization using geochemical evidence. We provide the microbial activity and microbial ecology data that supports the potential of bacteria to contribute to terrestrial organic carbon degradation in the ocean. The amendment of an allochthonous organic carbon, lignin, stimulated microbial activity in both the surface seawater and sediment, indicating that a widespread ability to degrade recalcitrant carbon within the oligotrophic, warm and oxic Eastern Mediterranean water column. We found different populations of bacteria associated with lignin within the sediment and seawater. With future research, the bacteria may be developed into sources of lignin-degrading enzymes for lignin valorization in industry.

Acknowledgements

This material is based upon work supported by the National Science Foundation Graduate Research Fellowship Program under grant no. DGE-1452154. The authors thank Kathleen Brannen-Donnelly and Annette Engel for use of their lab equipment and training. We would also like to thank Julian Fortney, Andrew Griffith, Andrew Matheson and the Captain and crew of the MV Fugro Navigator for assistance in collection of samples. We would also like to thank Oceanlab in Aberdeen, UK for use of the SAPS pump. We would also like to acknowledge Arden Ahnell, Maarten Kuijper, Sam Walker and Anne Walls for enabling this work. This work was supported in part through contract A13-0119 between BP America and The University of Tennessee.

Appendix A: Figures and Tables

Figure 1 Photo of microcosms after 2 wk of incubation

Photos show microcosms of seawater only (top left), seawater and lignin (top right), sediment only (bottom left), sediment and lignin (bottom right).

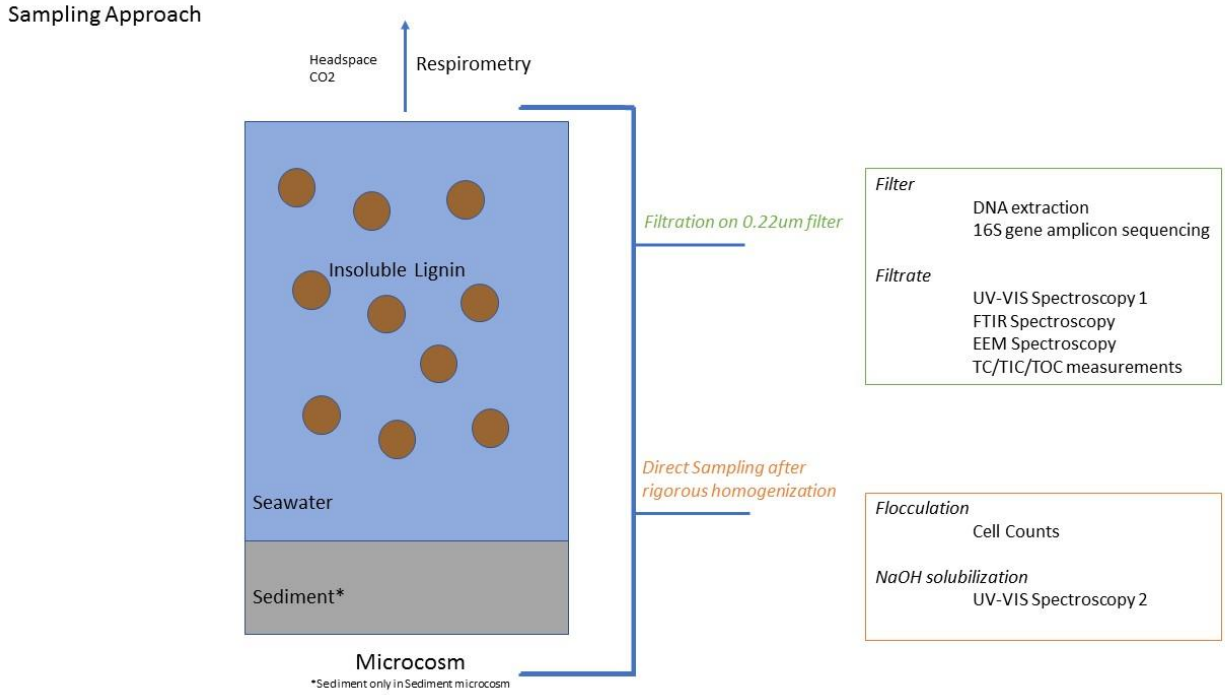

Figure 2 Sampling Approach

The conceptual diagram describes the sampling approach for all analyses.

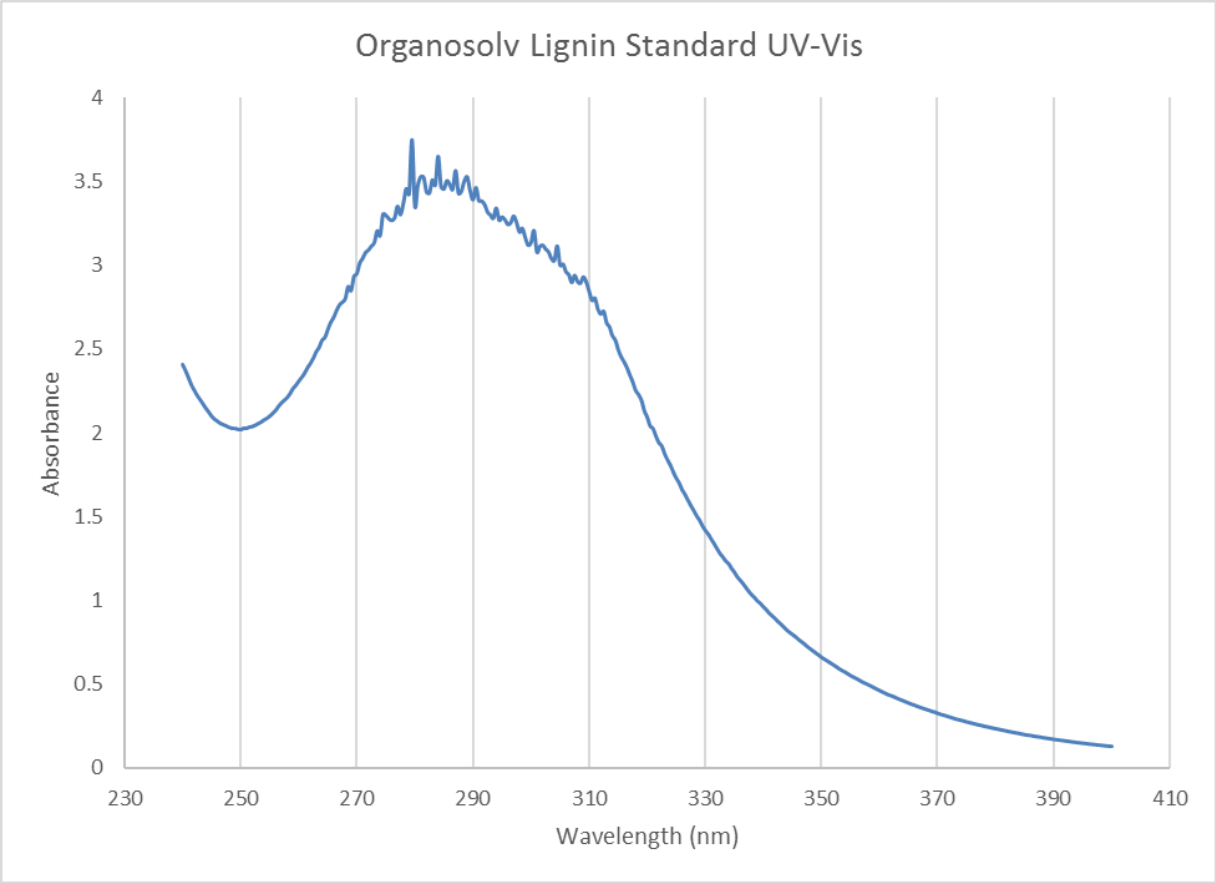

Figure 3 Organosolv lignin UV-VIS spectrum

UV-VIS spectrum was collected from the filtrate of a 1% Organosolv lignin standard in artificial seawater medium that had passed through a 0.22 um filter. From the UV-VIS spectra, we determined the Organosolv lignin has an absoption maximum at 286 nm.

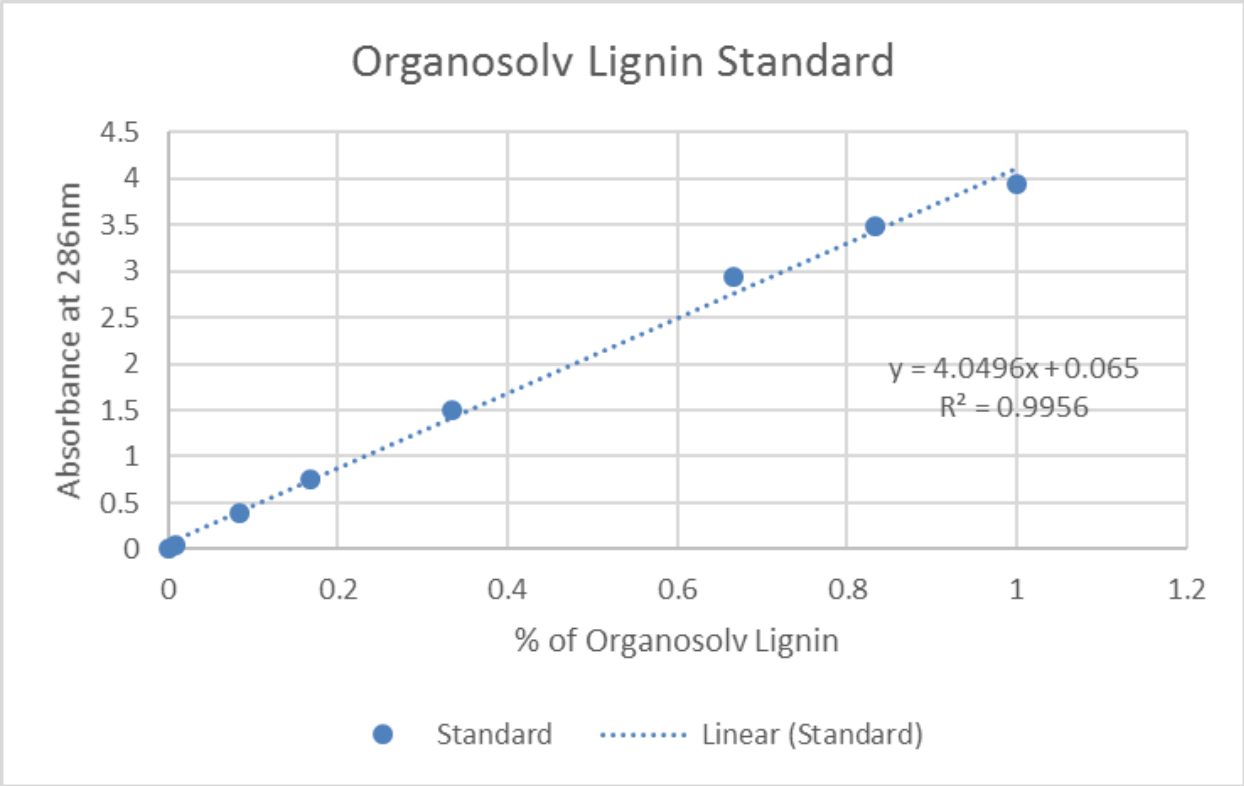

Figure 4 Beer's Law of Organosolv lignin dilution series

The UV-VIS spectrum of various dilution of the Organosolv lignin standard were measured. The absorbance at the absorption maximum at 286 nm was linearly correlated with the dilution factor (R-squared=0.99). The high correlation suggested that the absorbance could be used as a proxy for concentration.

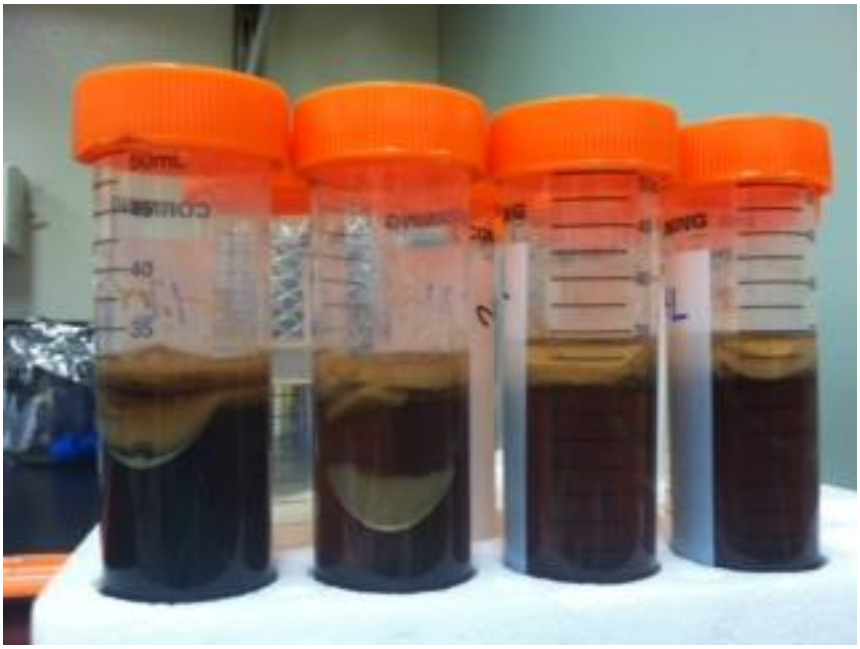

Figure 5 Photo of DNA extraction of mock samples with Organosolv lignin

DNA extraction protocols that utilize organic solvents such as phenol and chloroform did not work with samples amended with Organosolv lignin. As a test, pure bacterial cell cultures were spiked with lignin before extraction. After the addition of phenol:chloroform:isoamyl alcohol, the aqueous layer could not be recovered. The organic layer and the interface were viscous.

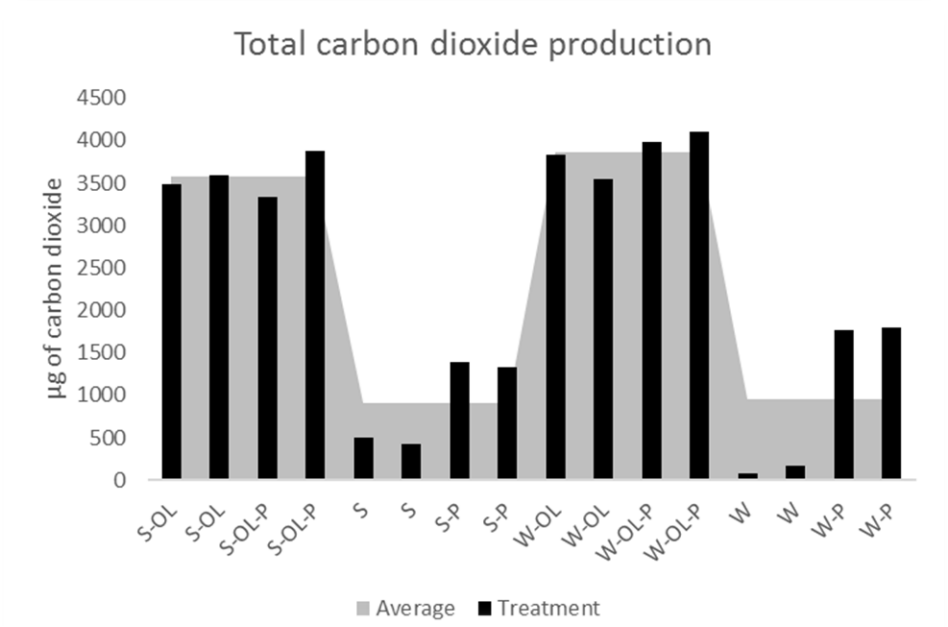

Figure 6 Total carbon dioxide production

Each microcosm was monitored for carbon dioxide production for 2 wks. Microcosms are indicated by the sample type and their amendments: S is for sediment microcosm, W for water microcosm, P for phosphate amendment, OL for Organosolv lignin amendment. Black bars are superimposed over a gray area graph which is the average of the 4 sediment samples with lignin, 4 sediment without lignin, 4 water samples with lignin, and 4 water samples without lignin.

A

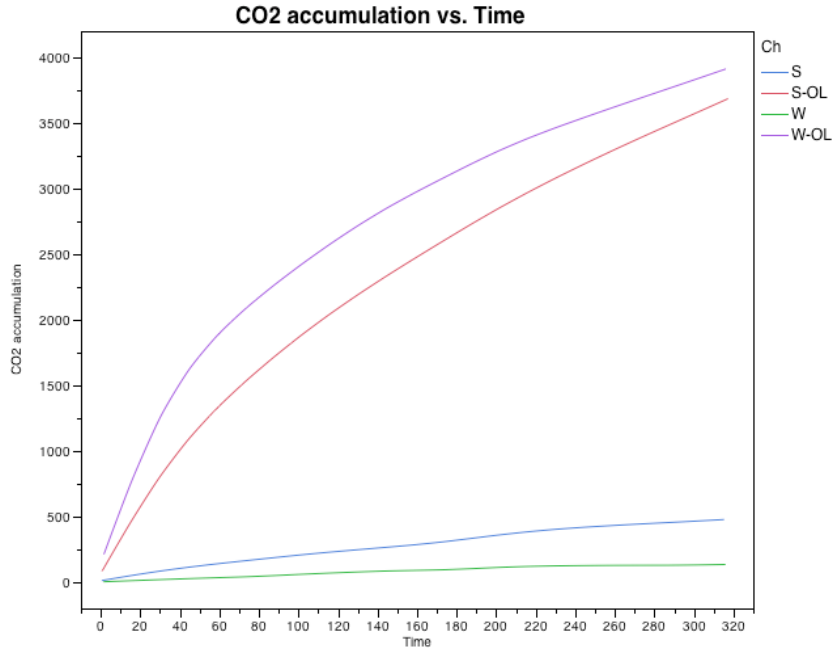

B

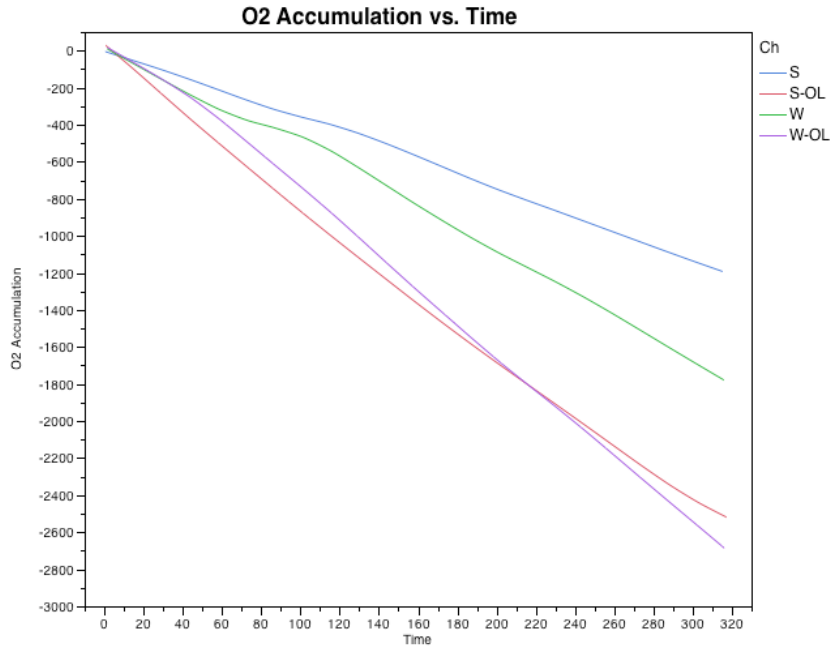

Figure 7 Respiration curves

A) Carbon dioxide production over time B) Oxygen utilization over time Curves are the average of duplicate microcosms.

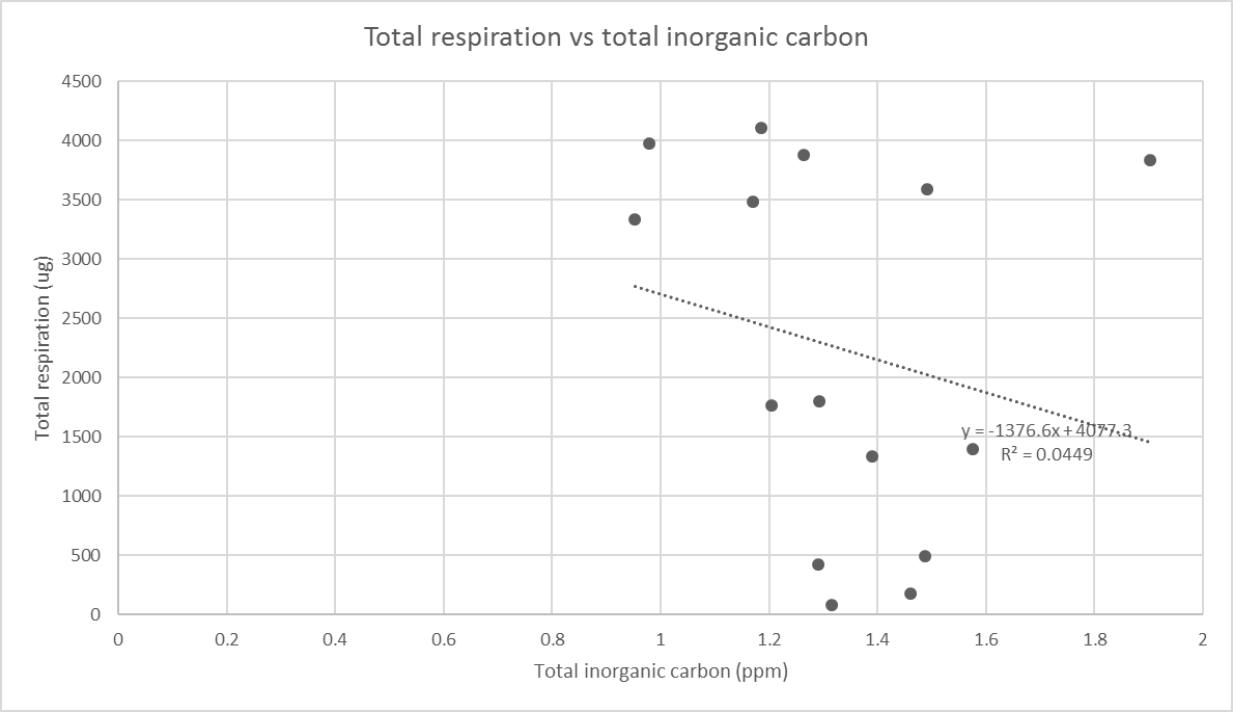

Figure 8 Total carbon dioxide production and total inorganic carbon

Scatterplot of total carbon dioxide produced in each microcosm and the microcosm's TIC showed no linear trend. Total carbon dioxide is unlikely to be correlated to losses in TIC.

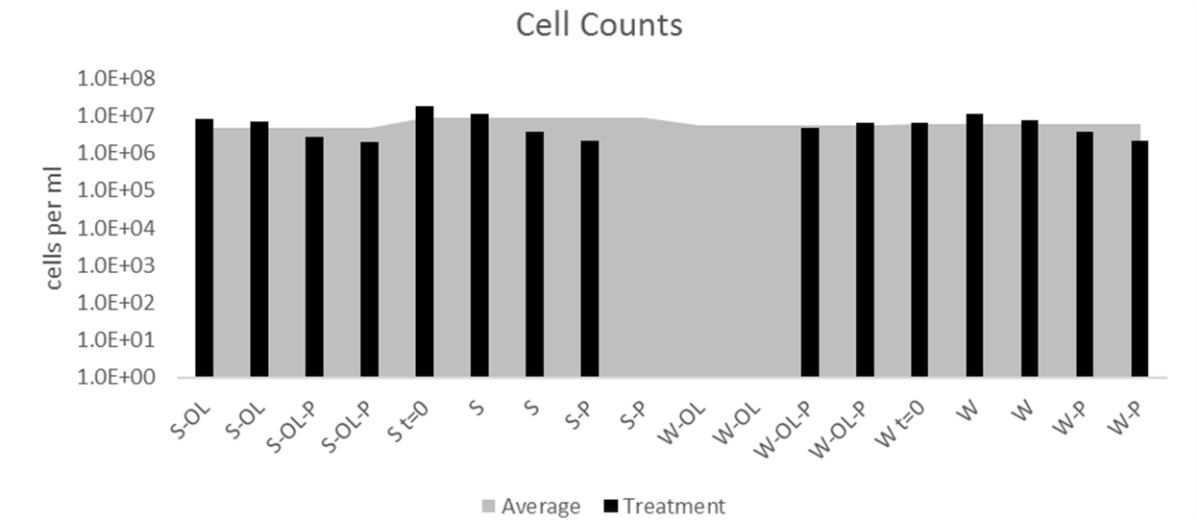

Figure 9 Cell counts

Microcosms without any bars were below reporting limits (see methods for definition of reporting limits). Initial sediment and seawater samples are included as S t=0 and W t=0. Black bars are superimposed over a gray area graph which is the average of the 4 sediment samples with lignin, 4 sediment without lignin, 4 water samples with lignin, and 4 water samples without lignin.

A

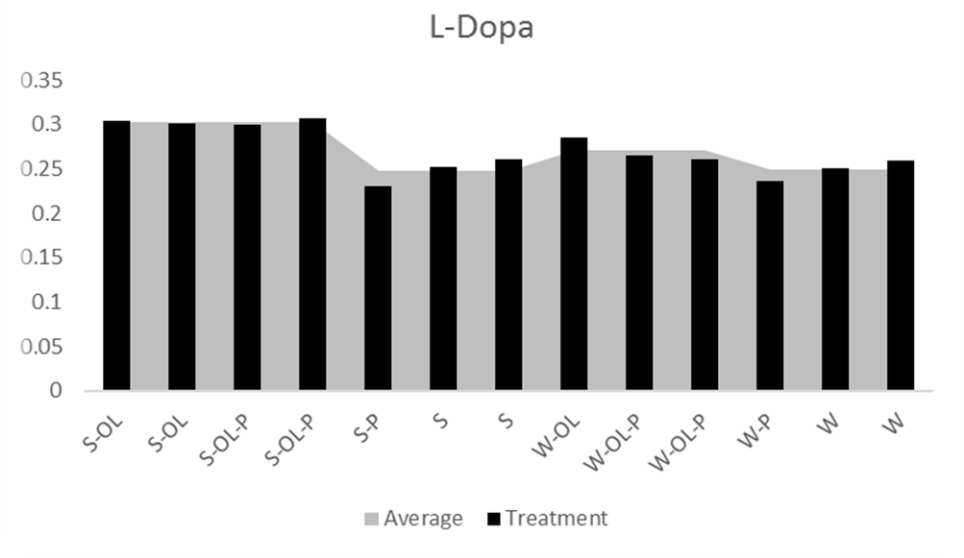

B

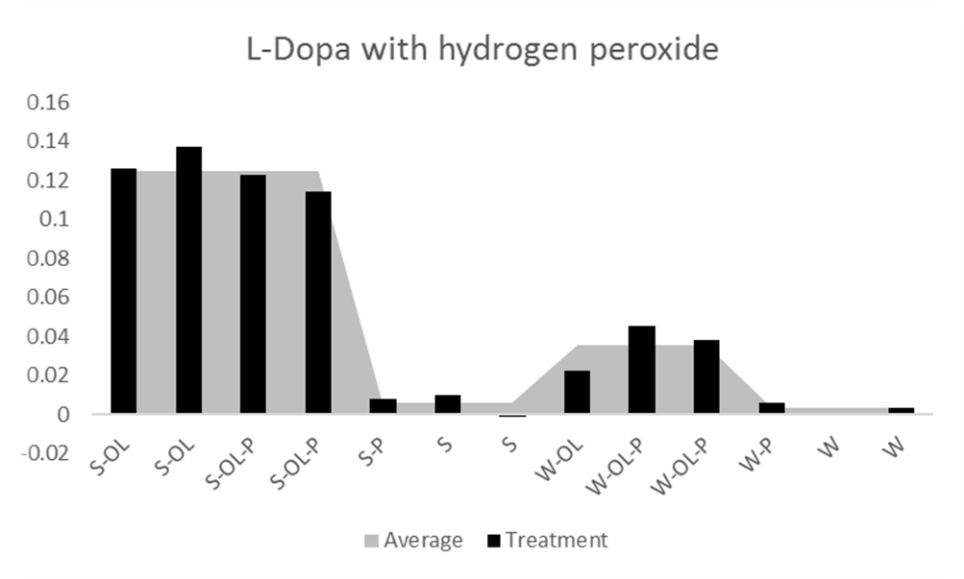

Figure 10 Enzyme activity on model lignin L-Dopa

A) L-Dopa alone B) L-Dopa with hydrogen peroxide Extracellular Enzyme activity for model lignin was tested using L-dopa with and without addition of hydrogen peroxide as an electron donor. Black bars are superimposed over a gray area graph which is the average of the 4 sediment samples with lignin, 4 sediment without lignin, 4 water samples with lignin, and 4 water samples without lignin.

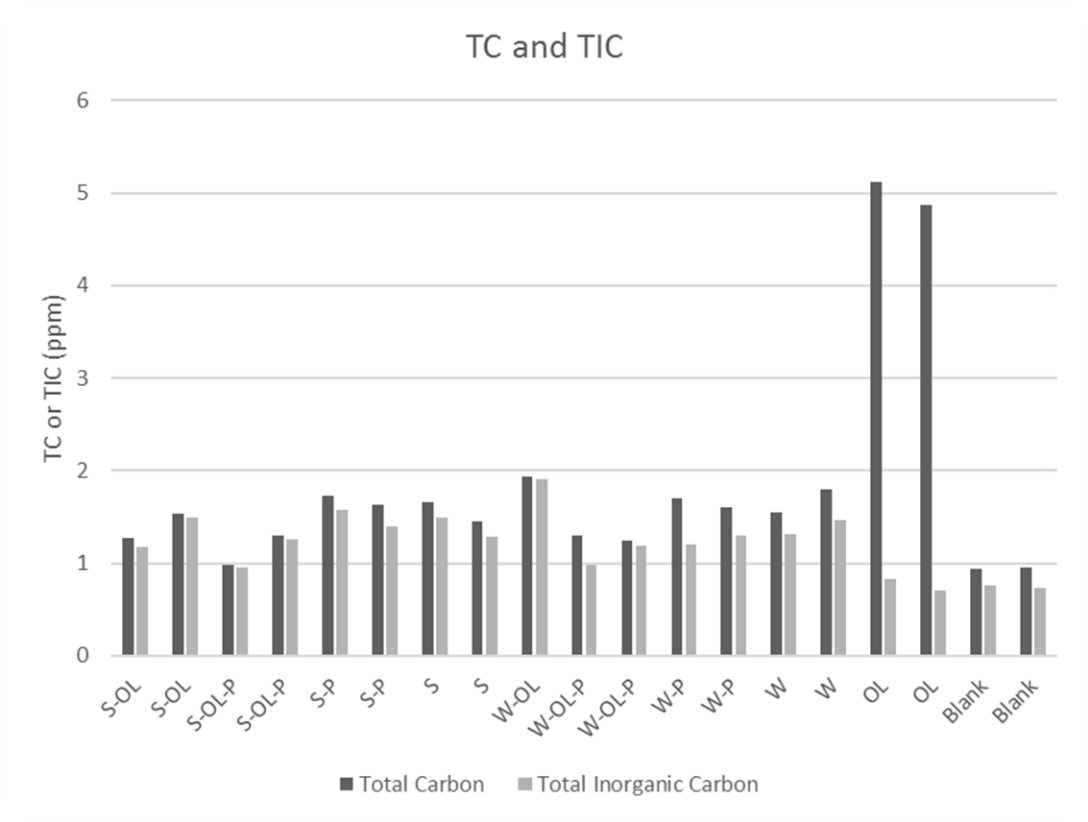

Figure 11 Total Carbon (TC) and Total Inorganic Carbon (TIC) Measurements

Microcosm filtrate were measured for their total carbon and total inorganic carbon content. Blank samples were ultrapure MilliQ water.

Table 1 Total Organic Carbon measurements

Total organic carbon was measured simultaneously as total nitrogen. N/D indicates sample TOC was not detectable. BDL indicates sample TOC was below the water blank's TOC and therefore unreliable.

	TOC
S-OL	BDL
S-OL	BDL
S-OL-P	N/D
S-OL-P	N/D
S-P	N/D
S-P	N/D
S	N/D
S	N/D
W-OL	N/D
W-OL-P	0.302
W-OL-P	N/D
W-P	0.408
W-P	0.311
W	0.258
W	0.304
OL	4.108
OL	4.119
Blank	N/D
Blank	0.204

A

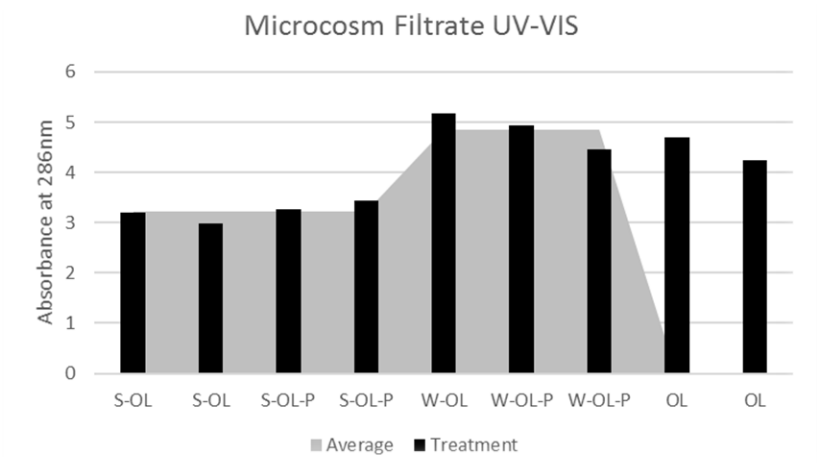

B

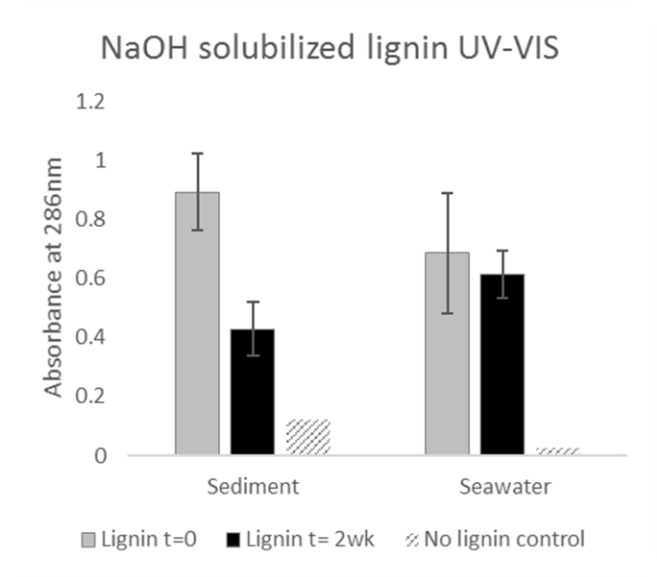

Figure 12 UV-Vis Spectroscopy

A) Microcosm Filtrate B) NaOH soluble lignin Microcosm filtrate represents the dissolved fraction of the microcosm sample that passed through a 0.22 um filter. NaOH soluble lignin was the microcosm sample amended with NaOH to solubilize the lignin and passed through a 0.22 um filter. For both sample preparations, the absorption at the determined absorption maximum of Organosolv lignin, 286 nm, was used as a proxy for lignin concentration. OL samples are un-degraded controls of original Organosolv lignin in an artificial seawater medium. The gray area graph in part A represents the average of the 4 sediment samples with lignin and the 4 seawater samples with lignin. Part B shows the average absorbance and standard deviation from 3 replicates of lignin samples before and after incubation. The control was the sediment or seawater without lignin.

A

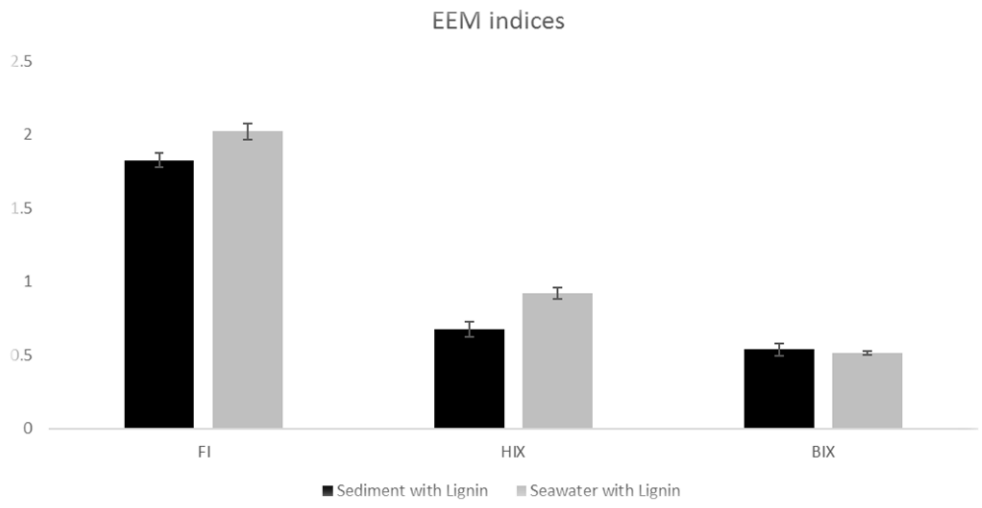

B

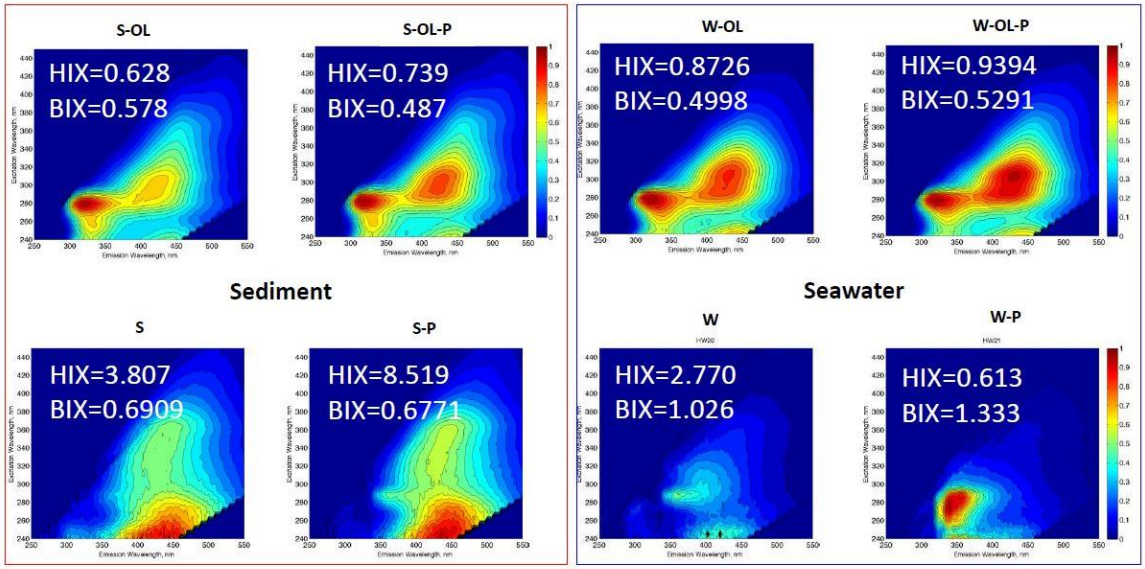

Figure 13 Excitation-emission matrix (EEM) spectroscopy

A) Indices Average FI, HIX and BIX of all seawater and sediment microcosms with lignin are shown with the standard deviation. Sediment microcosms are the 2 microcosms with lignin and the 2 microcosms with lignin and phosphate for n=4. Seawater microcosms are 2 microcosms with lignin and phosphate and only 1 microcosms with lignin for n=3. **B) EEMs** An EEM of each treatment in the full factorial experiment is shown with their humification index (HIX) and biological index (BIX).

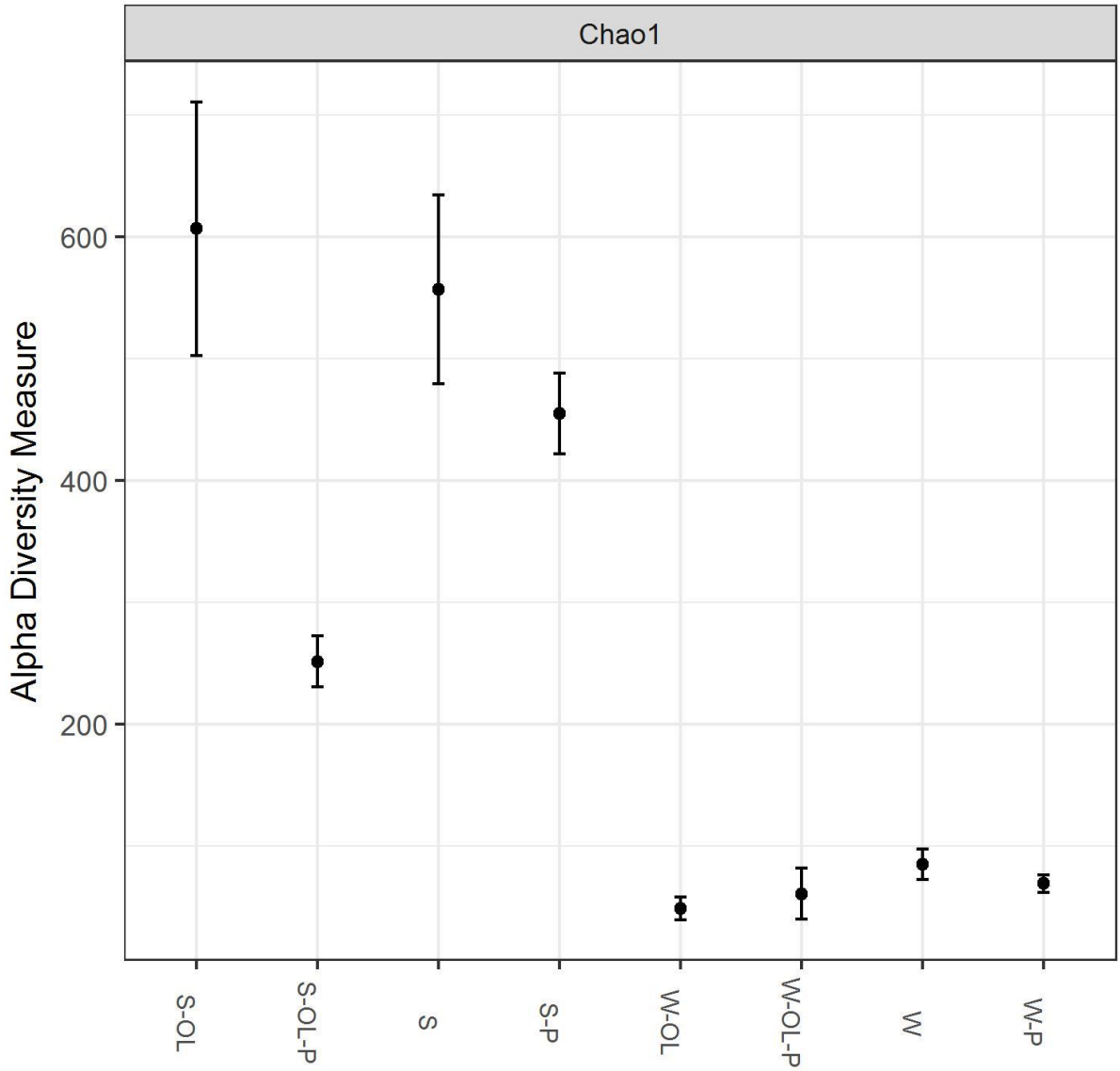

Figure 14. Chao1 Richness

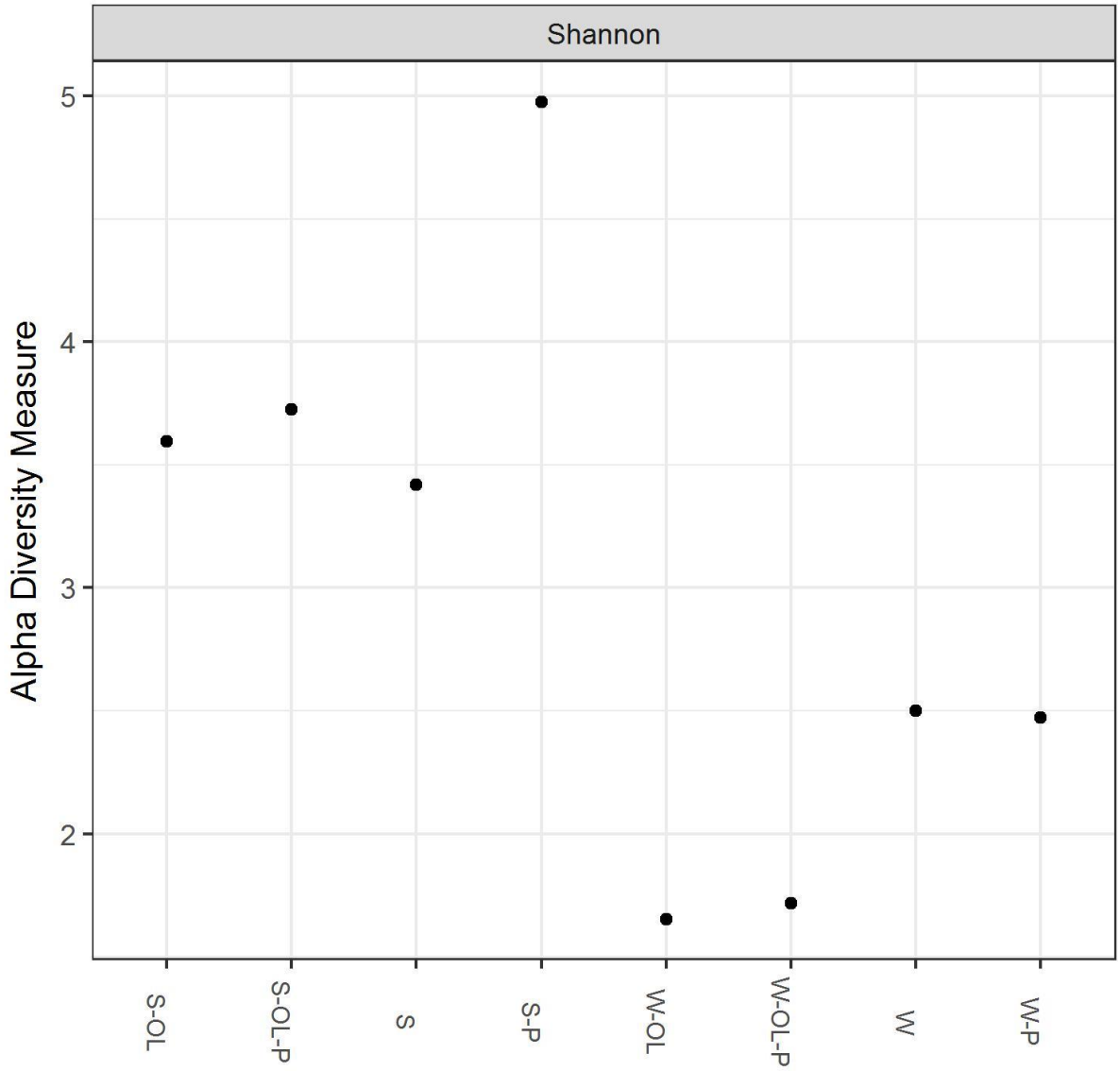

Figure 15 Shannon's Diversity

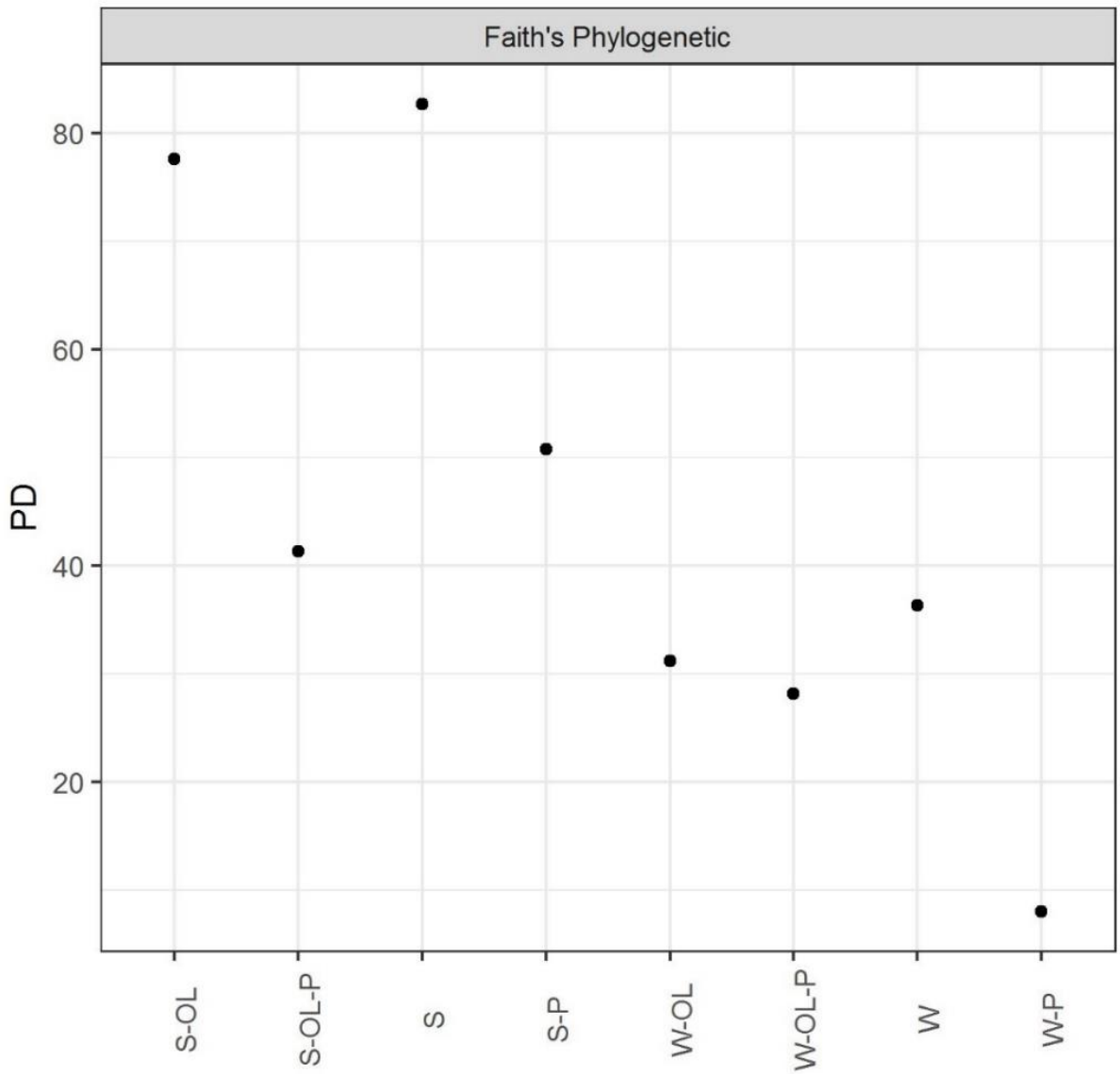

Figure 16 Faith's Phylogenetic Diversity

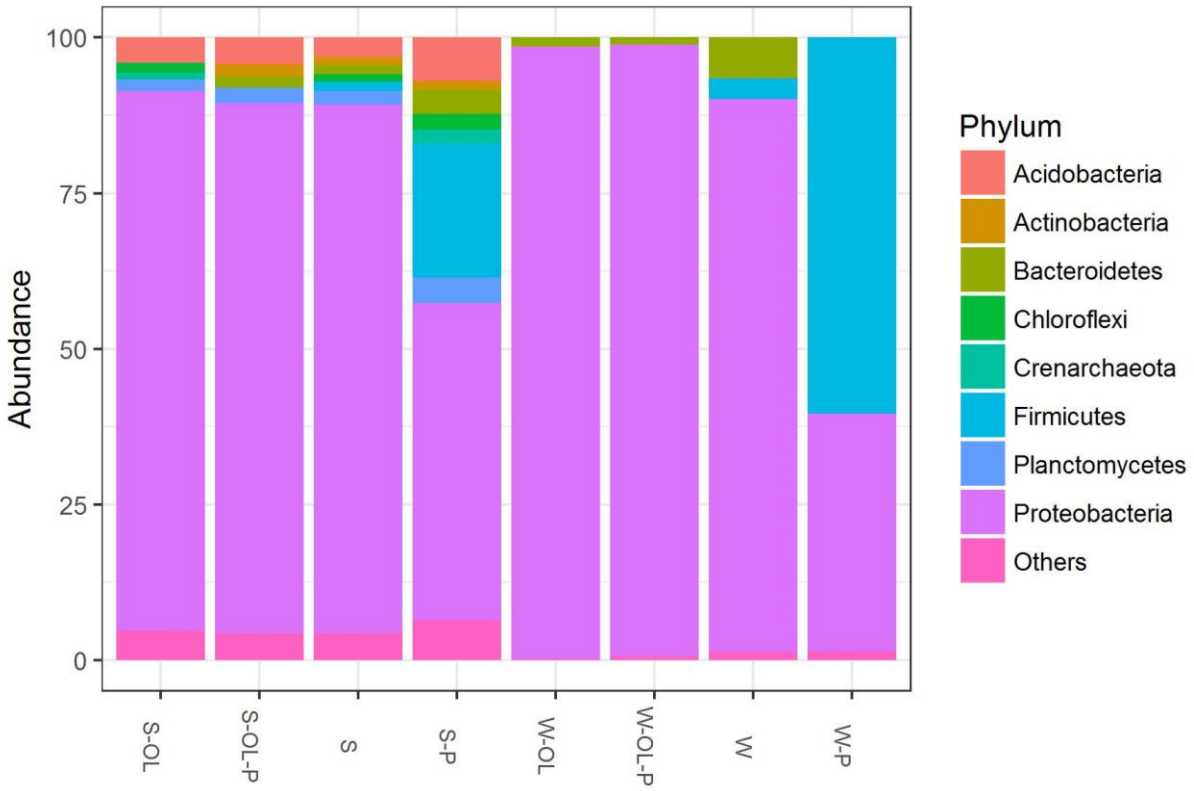

Figure 17 Phylum level taxonomy

Phyla less than 1% were aggregated as others.

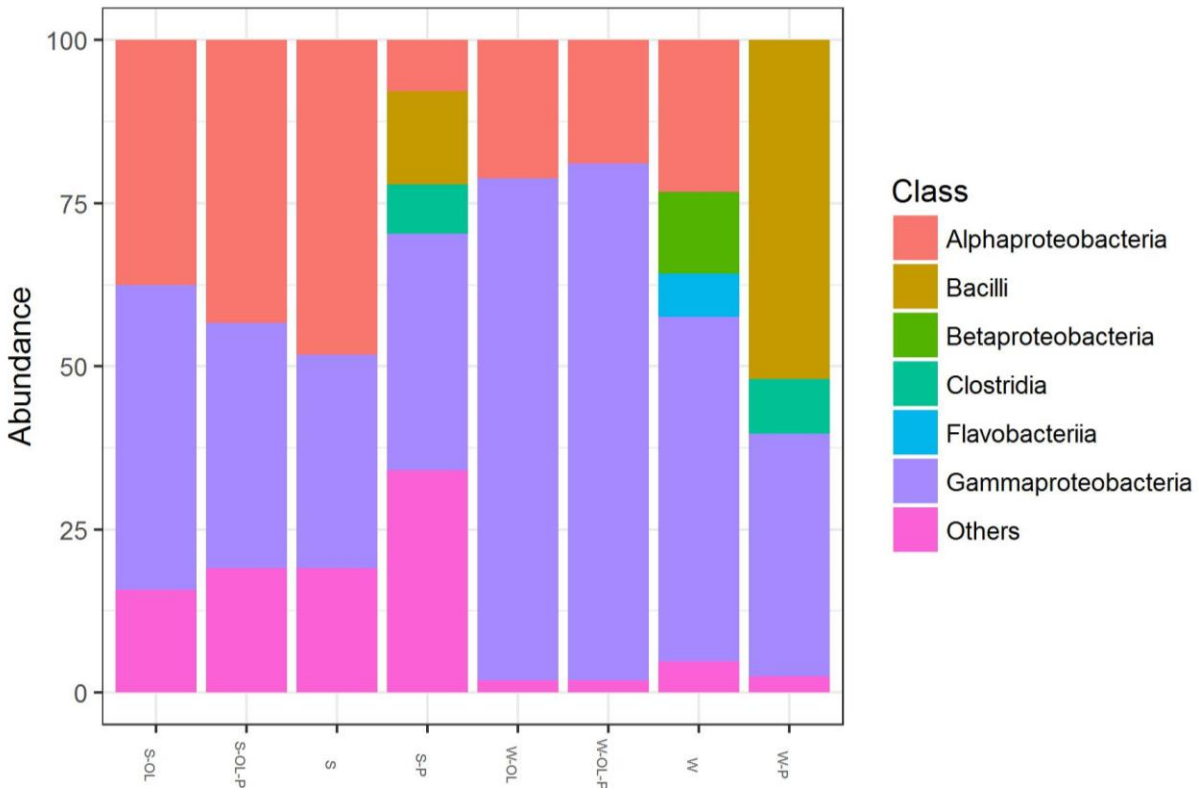

Figure 18 Class level taxonomy

Classes less than 5% were aggregated as others.

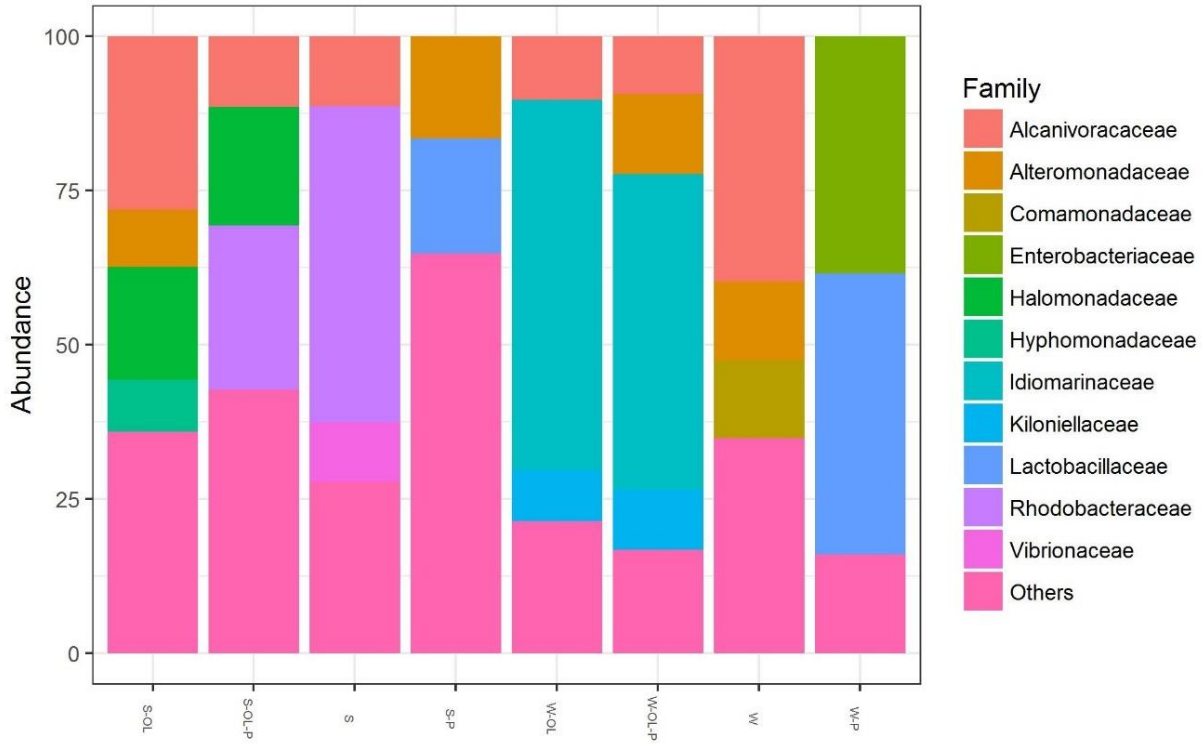

Figure 19 Family level taxonomy

Families less than 10% were aggregated as others.

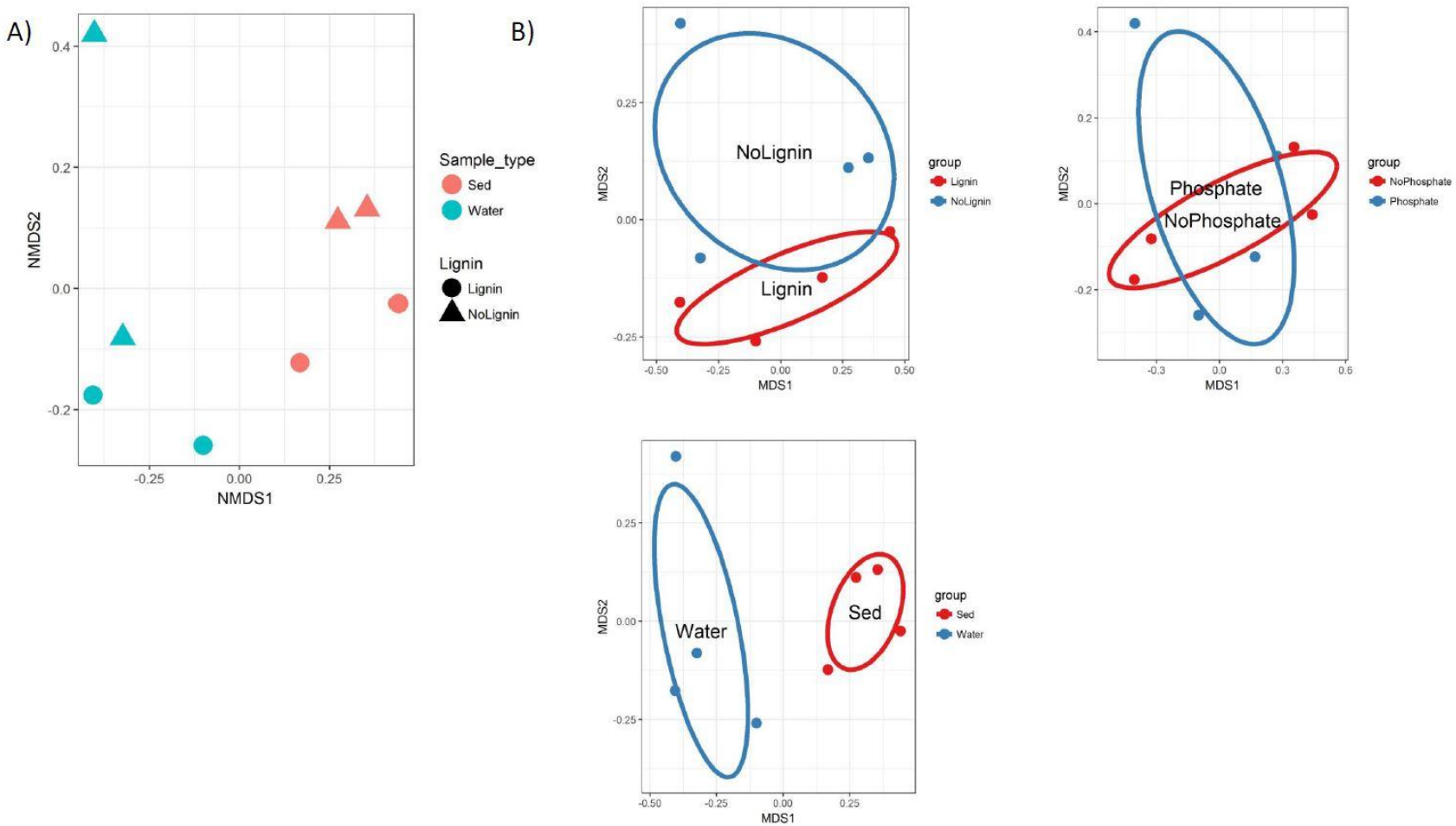

Figure 20 Beta Diversity

A) Non-metric dimensional scaling (NMDS)-Unifrac distance ordination of all microcosm treatments B) NMDS-Unifrac ordination of all microcosms with 95% confidence ellipses for lignin amendment, sample type and phosphate amendment
Stress of the NMDS-Unifrac ordination was .0286

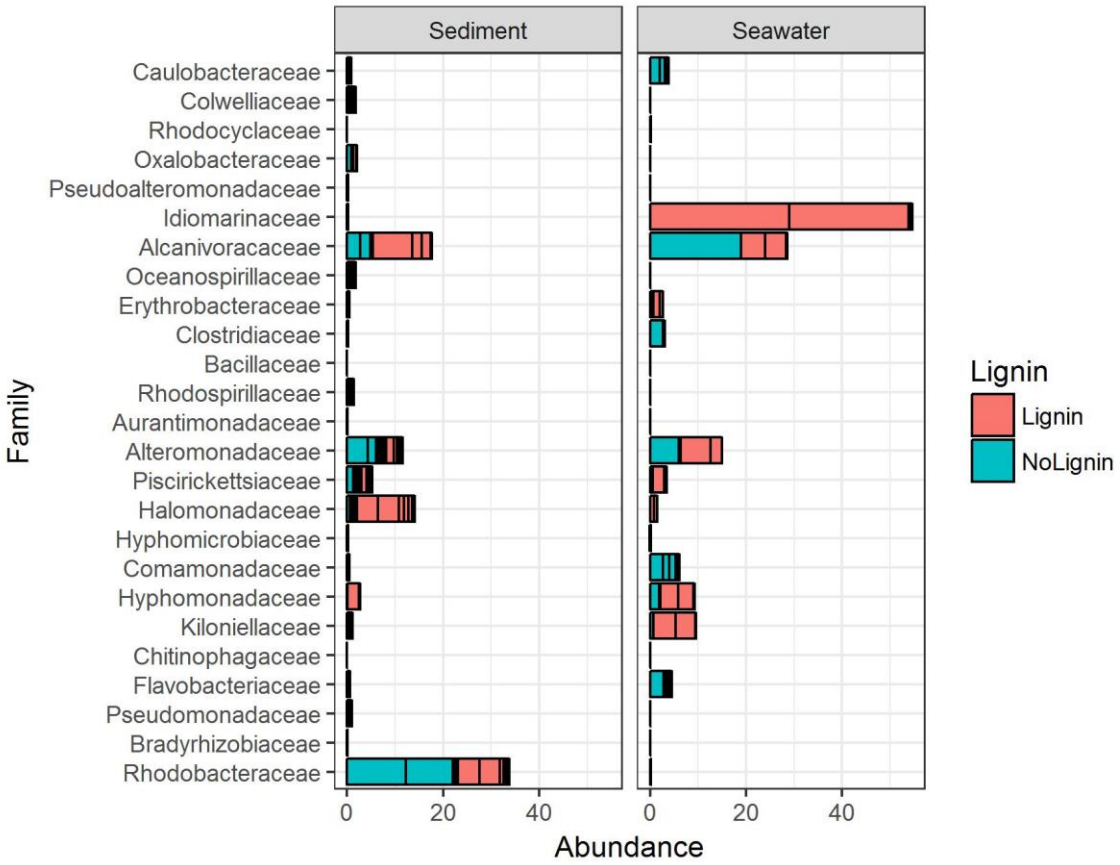

Figure 21 Relative abundance of lignin-associated species identified in previous Eastern Mediterranean Study

The following taxonomic families were identified in a previous study that enriched Eastern Mediterranean seawater with Organosolv lignin. Families are ordered from top to bottom in decreasing indicator species value for lignin as reported in that paper.

Chapter 3 Distinguishing keystone species and "cheaters" in the biodegradation of recalcitrant hemicellulose using polysaccharide xylan and monosaccharide xylose in enrichment microcosms

Authors: Hannah L. Woo[1], Anthony Rossi[2], Jing Wang[3], Nicole Labbe[3], and Terry C. Hazen[1,4,5]

Affiliations:

[1]University of Tennessee, Civil and Environmental Engineering

[2]University of Birmingham-Southern College, Microbiology

[3]University of Tennessee Institute of Agriculture, Center of Renewable Carbon

[4]University of Tennessee, Microbiology

[5]University of Tennessee, Earth and Planetary Science

Corresponding Author:

Terry C. Hazen

676 Dabney Hall
Knoxville, Tennessee 37996-1605
Phone: 865-974-7709
E-mail: tchazen@utk.edu

Author Contributions:

Conceived or designed experiments- HLW, NL, TCH

Performed the experiments- HLW, AR, JW

Analyzed the data- HLW, AR

Wrote the paper- HLW

Submitted to ISMEJ

Abstract

Substrate-amended microcosms and 16S rRNA gene amplicon sequencing are common approaches to study the biodiversity of microbes associated with high molecular weight organic polysaccharide degradation such as hemicellulose xylan. Distinguishing keystone species of the active microbial community is difficult because "cheater" taxa may outcompete and outnumber keystone species by utilizing the released low molecular weight organic monosaccharides more quickly. Hemicellulose is a particularly important polysaccharide due to its relevance in carbon cycling in marine ecosystems and lignocellulosic biofuels. The full biodiversity of microbes capable of producing hemicellulose-degrading enzyme is unknown. We separately amended the polysaccharide hemicellulose, xylan, and its constituent monosaccharide, xylose, to marine microbial consortia from the Great Australian Bight to understand the extent of cheating behavior in hemicellulose degradation. Microcosms amended with 0.05% weight to volume of xylan had positive microbial activity by the second week of incubation as assessed by respirometry, 16S rRNA gene copy number, and optical density. Using 16S rRNA gene amplicon sequencing at three timepoints, we found that the microbial communities between xylan and xylose were significantly different. The difference suggested that the xylan microbial consortia will have significant amounts of "cheater" taxa that could respond rapidly to xylose and dominate the microbial community. We used differential abundance analysis to compare taxa within the active xylan microcosms against the xylose "cheater" and unamended control to determine potential keystones species. *Muricauda* and *Pseudoalteromonas* were some dominant taxa that seemed to be candidate keystone species. Because of the "cheaters", we found that the interpretation of dominance must be conservative to prevent false positives of keystones species.

Keywords: keystone species, microbial cheaters, hemicellulose degradation, 16S rRNA gene amplicon sequencing, extracellular enzymes

Graphical Abstract

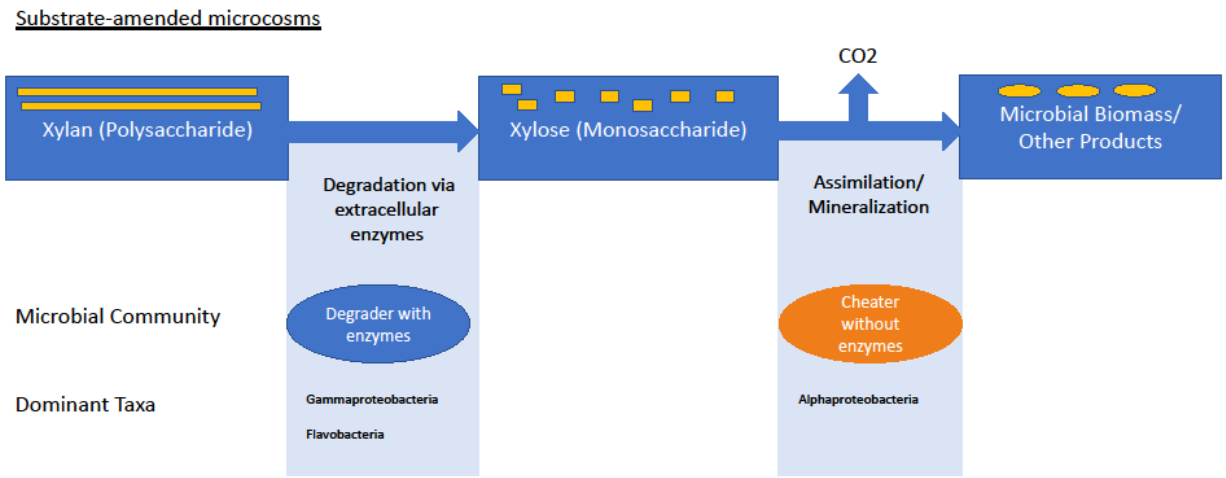

Introduction

Substrate-amended microcosms are a common method to study recalcitrant organic carbon compound degradation by microbes, particularly complex high molecular weight organics like lignocellulose (Haruta et al., 2002; Allgaier et al., 2010; Wang et al., 2011; DeAngelis et al., 2012; Eichorst et al., 2013; Eichorst et al., 2014) . Next-generation DNA sequencing is also commonly used to study the lignocellulolytic microbial diversity and functional genes encoding enzymes from the enriched microbial community (DeAngelis et al., 2010; Hess et al., 2011; Scully et al., 2013; Xia et al., 2013). However, it is difficult to distinguish the keystone microbes responsible for the enzymatic degradation of substrate from those that are cross-feeding and benefiting from the released breakdown products (van der Lelie et al., 2012; Lee et al., 2013a; Jimenez et al., 2014). The microbes that take advantage of the released breakdown products but do not produce any enzymes on their own are known as microbial "cheaters" (Velicer, 2003). Another confound in distinguishing keystones species may be that microbes that produce efficient extracellular enzymes for biodegradation of high molecular weight organics do not benefit from the breakdown product. For example, *Clostridium thermocellum* produces effective cellulose degrading enzymes but does not utilize the released glucose very well (Lynd et al., 2002).

Hemicellulose is an important carbon substrate to study in marine environments for enzyme discovery. Hemicellulose is a high molecular weight organic polysaccharide found in the algal extracellular matrix (Domozych, 2016) as well as terrestrial plants (Scheller and Ulvskov, 2010). This compound along with cellulose and lignin is being targeted for use in next-generation lignocellulosic biofuel production (Dodd and Cann, 2009) but must first be depolymerized using extracellular microbial enzymes. Relatively little is known about marine hemicellulases compared to terrestrial ones; full biodiversity of hemicellulolytic microbes is still unknown (Prasad and Sethi, 2013). Since marine microbial enzymes are crucial in carbon cycling in the ocean (Arnosti, 2011), marine microbes must have effective hydrolytic enzymes for high molecular weight organics. Hemicellulose like xylan are readily degraded by enzymes compared to cellulose or lignin (Bayer et al., 1994), but current research is focused on finding more stress and salt tolerant enzymes that can better withstand high ionic strength conditions found in industrial processes (Ilmberger et al., 2012; Khudyakov et al., 2012; Park et al., 2012)

The impact of "cheaters" in substrate-amended microcosms is rarely addressed directly. Even with the use of ^{13}C-labelled hemicellulose, microbes cannot be distinguished as "cheaters" due to limitations in the stable isotope probing methodology (Leung et al., 2016). To enrich for keystone species and "cheaters" separately, we used hemicellulose xylan from beechwood and its monomer xylose, as substrates in separate microcosms. We hypothesized that xylan and xylose amendment enrich for different population of microbes, where the xylose microcosm consists of "cheaters" capable of responding rapidly and blooming in the presence of labile carbon. We compared the microcosms over 3 timepoints spanning a month's period to determine if succession of microbial communities occurred. We tested multiple concentrations of xylan in a modified "dilution to extinction" experimental design (Lee et al., 2013a), but the substrate was diluted instead of the cells. This allowed a comparison between active and non-active xylanolytic microbial communities.

Of the 3 different concentrations of xylan tested, microbes only showed significant activity on the highest tested concentration. In an ad-hoc experiment, we performed a microbial swap experiment where the active xylan degrading community of the highest concentration of xylan (0.05%) was transferred to a lower concentration of fresh xylan (0.01%). We believed the well-adapted xylan consortia would be robust enough to utilize the lower concentration of substrate.

Material and Methods

Initial enrichment of Great Australian Bight seawater on xylan

The initial enrichment microcosms consisted of 60 ml mL of seawater and 0.30 g of Sigma xylan from beechwood (Sigma-Aldrich). The seawater was collected from the Great Australian Bight at 1500 m below the surface and 66 m above the seafloor at Sampling Station 2 (35 20.112S 134 03.534E), which was near the seafloor. The enrichment was incubated for 200 hours in the dark and at the *in situ* temperature of the sampling site, i.e. 3°C. Carbon dioxide accumulation in the microcosm headspace was measured by a MicroOxyMax respirometer (Columbus Instruments Columbus, Ohio) every 3 hours. A separate 60 mL microcosm of unamended seawater was also incubated and monitored as the control. After the incubation, 30 mL of the initial xylan-amended Australian Bight seawater were filtered onto a MoBio 0.2μm water filter (MoBio Carlsbad, CA) for DNA extraction and 16S rRNA gene amplicon sequencing. Approximately 0.5 mL of the microcosm was frozen with 0.5 mL glycerol and stored at -80°C for future use as an inoculum.

Respirometry of xylan-amended microcosms, xylose-amended microcosms, and control microcosms and respirometry data analysis

The frozen stock was thawed to room temperature and resuspended in 50 mL of modified artificial seawater medium, ONR7a Medium pH 8.2 (Atlas, 2010) without bactopeptone, vitamins or trace elements. One mL of cell suspension was transferred to 200 mL microcosms with xylan or xylose as a sole carbon source in ONR7a. Xylan or xylose was amended in 3 different concentrations, 0.002%, 0.01%, and 0.05% (weight to volume), respectively referenced as “low”, “medium” and “high” within this study. Each concentration of substrate was prepared in triplicate. The xylan was not sterilized or autoclaved to avoid altering its structure by heat or pressure. Xylose was prepared as a 1M solution and autoclaved before use.

Carbon dioxide production was monitored using the MicroOxyMax respirometer over a month’s time at ambient room temperature in the dark. The MicroOxyMax was stopped at 3 timepoints to allow subsampling of the microcosms for DNA extraction and Optical Density measurements. Microcosms were immediately returned to the respirometer after subsampling which was completed in less than 4 hours.

Multiple controls were used to ensure that microbial degradation of xylan or xylose was the main source of carbon dioxide and significant microbial contamination was not introduced from nonsterile xylan. Six control conditions were prepared in triplicate: sterile media control, low xylan abiotic control, medium xylan abiotic control, high xylan abiotic control, killed high xylan control, and unamended control. The sterile media control was sterile ONR7a alone. The low, medium and high xylan abiotic controls were the respective concentration of xylan in ONR7a without cell inoculum. The killed high xylan control was the high concentration of xylan with cell inoculum and sodium azide to inhibit respiration. The unamended control was the cell inoculum in ONR7a without any substrate.

The three concentrations of xylose and the high xylan treatment had positive total accumulation of carbon dioxide. Other treatments and controls had negative total accumulation of carbon

dioxide, indicating that there was less carbon dioxide in the headspace at the final timepoint than at the initial. MicroOxyMax reports negative carbon dioxide production rates if microcosms have very small amounts of dissolved carbon dioxide and carbon dioxide dissolves into the solution to reach equilibrium (International, 2010). The freshly autoclaved ONR7a media was not sparged with air to allow equilibration with atmospheric carbon dioxide concentration before the start of the experiment due to concerns of microbial contamination. The sterile media control produced the least amount of carbon dioxide, -5039.43 μg (Table 2). All respirometry data reported are relative to the sterile media control. The total amount of carbon dioxide produced by all microcosms were was adjusted by adding 5039.43 μg so the sterile media control was exactly 0.00 μg.

Optical Density at 600nm (OD 600nm)

When subsampling the microcosms at each timepoint, the absorbance at 600 nm of the microcosms was measured using a Synergy HT plate reader (Biotek Winnoski, VT). Because of the insolubility of the xylan substrate, each of the 3 microcosm replicates was measured 3 times for a total of 9 replicates per treatment.

Real-Time qPCR quantification of bacterial 16S gene copy number

Bacterial 16S rRNA gene copy numbers within the xylan-amended and unamended control microcosms were quantified by qPCR using bacterial-specific primers, bac341f (5′-CCTACGGGWGGCWGCA-3′) (Ishii and Fukui, 2001) and the prokaryotic 519r (5′-TTACCGCGGCKGCTG-3′) (Ovreås et al., 1997). Standard curve was generated using a dilution series of cloned *Alcanivorax* from 20 to 2x10-3 pmol/ul. The linear fit of the standard curve was y = -3.1189 x - 15.826, with $R^2 = 0.81$. PCR amplification efficiency was 109%. The thermal cycle program was 15 min at 95°C, 35 cycles of 95°C for 15s, 58°C for 30s, and 72°C for 30s. (Jorgensen et al., 2012). Samples were quantified using triplicate measurements of two different dilutions of input DNA, a 1:10 dilution and 1:100 dilution for a total of 6 replicates per sample. Copy number was normalized by ng of input DNA.

High performance liquid chromatography (HPLC) measurement of xylose sugars

The amount of free soluble xylose in the active high xylan microcosm was measured at timepoint 1, 2, and 3. Samples taken from the aqueous fraction of the microcosm were analyzed by high performance liquid chromatography with a refractive index detector equipped with a Bio-Rad Aminex HPX-87P carbohydrate analysis column (Richmond, CA) with deashing guard column (Biorad, Hercules, CA) at 85 °C, and water as the mobile phase at a flow rate of 0.25 mL/min. The concentration of xylose was below detectable limits of 0.05mg/mL.

Ad-hoc Swapped Microcosm Community Test

To determine if the microbial community from the high xylan could utilize the lower concentrations of xylan, we inoculated fresh 0.01% of xylan in media with cells from the high xylan. Ten mL of each of high xylan were pelleted by centrifugation and residual media was decanted. The pellet was resuspended in fresh media and a medium 0.01% concentration of xylan for the “xylan to xylan” treatment. The 3 replicate microcosms were monitored using

respirometry for 1 week. Following the same methods, a "xylose to xylan" treatment was also established simultaneously using a pellet from the high xylose microcosm transferred to fresh media and 0.01% xylan.

Statistical Analysis

Statistical analysis of the total respiration data, qPCR copy numbers, OD 600nm, and alpha diversity measures was performed in JMP®, Version *Pro 12* (SAS Institute Inc., Cary, NC, 1989-2007). One-way ANOVA analysis was used to determine if the data varied between three factors: amended substrate, concentration of amended substrate, and timepoint of enrichment sampling. As a factor, substrate had 3 levels: unamended, xylan, and xylose. Concentration of the amended substrate had 4 levels: none, low, medium, high. Timepoint of sampling had 3 levels: t1, t2, t3. Student's t-test was used to compare model effects pairwise at $\alpha = 0.050$.

16S rRNA gene amplicon sequencing using the Illumina MiSeq and QIIME analysis

Thirty mL subsamples were taken from the microcosms at 3 timepoints: 6, 21, and 27 days. Subsamples from each replicate of a treatment were combined to reach a total volume of 90 mL and then filtered using a MoBio water 0.2μm filter (MoBio Carlsbad, CA). DNA from the filters was extracted using the MoBio PowerWater kit (MoBio Carlsbad, CA). The amplicon libraries for the V4 region of the16S rRNA gene were prepared using the methods described by Techtmann et. al. (Techtmann et al., 2015) with the exception that DNA extracts were further purified before library preparation using the OneStep™ PCR inhibitor removal kit (Zymo Research Irvine, CA) and Genomic DNA Clean and Concentrator™ (Zymo Research Irvine, CA). Purified DNA concentrations were determined using Qubit (ThermoFisher Scientific Waltham, MA). Final pooled libraries were quantified using qPCR (KAPA Biosystems Wilmington, MA). Sequencing was performed using an Illumina MiSeq platform and a v2 2x150 Nanokit. Forward and reverse reads were joined using a quality score minimum threshold of 19, demultiplexed, and checked for chimeras using QIIME (Caporaso et al., 2010). The open OTU picking strategy was used to assign Greengenes taxonomy (DeSantis et al., 2006) to OTU clusters of 97% sequence similarity. The final OTU table was filtered so that all OTUs were at least 0.005% relative abundance.

Alpha diversity, Beta Diversity, and Differential Abundance analysis using various R packages

Alpha diversity was calculated using the non-rarefied OTU table (McMurdie and Holmes, 2014). Chao1 richness, Simpson diversity, was calculated using the phyloseq R package (McMurdie and Holmes, 2013). Faith's phylogenetic diversity was calculated using the picante R package (Kembel et al., 2010). For beta diversity analysis, data were rarefied using the *rarefy_even_depths* function in phyloseq (McMurdie and Holmes, 2013). Dissimilarities between samples were estimated using weighted Unifrac distance (Lozupone and Knight, 2005). Ordination was performed using Non-Metric Multidimensional Scaling (NMDS). 95% confidence interval ellipses were drawn using the vegan R package *ordiellipse* function (Dixon and Palmer, 2003).

Statistical testing of microbial beta diversity between treatments was conducted in R using the vegan R package ADONIS function with the default 999 permutations. The *betadisper* function

from the vegan R package was used to analyze variance between groups. Differential abundance analysis of the OTUs in microcosms of different treatments was performed using the DESeq2 R package. The DESeq2 generated the log fold change values, normalized relative abundances ("basemean"), and p-values from the Wald test with local fitting.

Phylogenetic Tree analysis of Pseudoalteromonas OTUs

Pseudoalteromonas sp. OTU clusters of 97% similarity were reanalyzed in QIIME to produce OTUs of higher similarity at 99.8%. Sequences clustered within OTUs that were classified as genus *Pseudoalteromonas* were re-clustered using the QIIME *pick_otus* function at a higher 99.8% similarity threshold. Representative sequences of the high similarity OTUs were assigned using QIIME *pick_rep_set* for phylogenetic tree analysis. Phylogenetic tree analysis was used to compare *Pseudoalteromonas* sp. OTUs from the microcosms and type strain *Pseudoalteromonas* sp. 16S rRNA genes from Ribosomal Data Project (RDP) (Cole et al., 2014). Sequences were aligned using the default gap cost settings and the fast alignment within CLCBio (https://www.qiagenbioinformatics.com/) (Qiagen Redwood City, CA). The alignment was used to create a neighbor-joining tree with Jukes-Cantor nucleotide distance.

Results

The initial xylan enrichment of Australian Bight seawater produced a significant amount of carbon dioxide during the short 8 days of incubation. *Gammaproteobacteria* dominated the microbial community. The enrichment produced 1500 µg of carbon dioxide after 200 hours, while the unamended seawater control did not produce significant amounts of carbon dioxide (Figure 22). After the 200 hours of incubation, the respiration rate had decreased substantially (Figure 22). At that time, the enrichments were harvested for DNA extraction and 16S rRNA gene amplicon sequencing. Based on the 16S rRNA gene amplicon sequencing, 90% of the microbial community closely matched taxonomic families within the bacterial phylum *Gammaproteobacteria* such as *Colwelliaceae*, *Moritellaceae*, *Oceanospirallaceae*, and *Pseudoalteromonadaceae* (Figure 23). OTUs within *Colwelliaceae* alone were 50% of the overall community. *Pseudoalteromonas*, *Moritella* and *Marinomonas* were genera in high abundance.

The revived microbial community from the frozen glycerol stock mineralized xylan only at the highest tested concentration of 0.05%. The high xylan microcosms produced an average of 8 mg of CO_2 after the 27 days of incubation (Figure 24). It produced statistically more than the other lower concentration of xylan microcosms and the controls. Control microcosms with varying concentrations of xylan without cells produced an order of magnitude less carbon dioxide than any of the xylan microcosms inoculated with cells. By the second week of the experiment, the high xylan microcosm was accumulating carbon dioxide linearly with time (Figure 25).

Real-time qPCR measurement of bacterial 16S rRNA gene copy number and the optical density at 600 nm (OD 600nm) support a microbial response only in the highest concentration of xylan. The sum of bacterial 16S rRNA gene copy from each timepoint was significantly higher in high xylan than the lower concentration of xylan and the unamended control (Figure 26). OD 600 nm of the microcosms between each xylan amended microcosms and xylan amended abiotic control were compared at each timepoint. Only the high xylan microcosm increased in OD 600nm enough to be statistically higher than its respective concentration of xylan abiotic control (Figure 27). High xylan had a higher optical density than other concentrations of xylan and the unamended control.

When the microbial community from the high xylan microcosm was transferred to fresh media and less xylan, carbon dioxide production decreased to undetectable levels. Although the high xylan microbial community was active, it failed to produce positive carbon dioxide rates within 1 week on the lower concentration of xylan (Figure 28). The high xylose microcosm's microbial community was also transferred to xylan for a comparison, where it also failed to produce carbon dioxide after 1 week (Figure 28). Since we did not see any respiration after a week, the 0.01% xylan may be too dilute to sustain microbial growth.

Xylose-amended microcosms produced significantly more carbon dioxide than the xylan-amended microcosm. Xylose-amended microcosms peaked in production rates faster than the xylan-amended microcosms. During the first 6 days of incubation, only the high xylose microcosms produced detectable amount of carbon dioxide (Figure 25 and 29). The high xylose microcosms produced the highest amount of carbon dioxide with an average at 72.8 mg (Figure 24). Both the highest and medium xylose produced significantly higher amount of carbon

dioxide than the controls (t-test p-value<0.05). The medium and high concentration may be in the substrate-limited range of growth as we saw a 4.2 fold difference by adding 5 times more substrate between the medium and high concentration. The rate of carbon dioxide production within the high xylose increased rapidly during the first week of incubation, but appeared to slow down during the later timepoints (Figure 29).

All concentrations of xylan-amended and xylose-amended microcosms and the unamended were sequenced at 3 timepoints for their microbial community structure using 16S rRNA gene amplicon sequencing. Replicates were pooled so that one composite sample represented the treatment. The sequencing depth ranged from a minimum of 4986 sequences per sample to a maximum of 18004 (Table 3). The dominant species of all the enrichments belonged to 3 taxonomic classes: *Alphaproteobacteria*, *Gammaproteobacteria*, and *Flavobacteria* (Figure 30). The most abundant genera were *Alteromonas, Anaerospora, Glaciecola, Loktanella, Marinobacter, Muricauda, Phaeobacter, Pseudoalteromonas,* and *Thalassospira*. The most abundant species in the high xylan microcosm was the *Gammaproteobacteria* genus, *Pseudoalteromonas*, which was over 40% of the overall community. *Pseudoalteromonas* was also one of the dominant species in the medium xylan microcosms but to a lesser degree. The medium xylan microcosm also had a large abundance of the *Gammaproteobacteria* genus, *Marinobacter*. High xylose microcosms had more *Alphaproteobacteria* taxa such as the genus *Thalassospira* and *Loktanella*. All treatments were sequenced at 3 timepoints, where the identity of the dominant species remained very stable over time. The xylan and xylose microcosms had different dominant taxa than the initial enrichment. The only dominant taxa that was revived was the *Pseudoalteromonas*.

The alpha diversity ("within-sample diversity") of our microcosms was estimated by Chao1 richness, Simpson diversity, and Faith's phylogenetic diversity (Figure 31, 32, 33). All three diversity indices were not significantly different between xylan and xylose amended microcosms.

However, indices were slightly different by timepoint and concentration. We observed near significant differences in Chao1 species richness based on timepoint [$F(2,18)=2.98$, $p=0.0761$] (Figure 34). The Chao1 at the second timepoint was less than the first or third timepoint, indicating a temporary decrease in species richness at the second timepoint. There were near significant differences in Simpson diversity based on timepoint [$F(2,18)=3.162$, $p=0.068$] (Figure 35) and concentration [$F(3,17)=3.14$, $p=0.0525$] (Figure 36). Simpson diversity increased after the first timepoint and for the medium concentration of substrate. Unlike Simpson diversity, Faith's phylogenetic diversity assesses species diversity using phylogeny of the OTUs. Faith's phylogenetic diversity significantly decreased after the first timepoint [$F(2,18)=4.102$,$p=0.0340$] (Figure 36).

Despite their similar degree of species richness and alpha diversity, the xylan and xylose amended microcosms differed significantly in their microbial community taxonomic structure. In an NMDS ordination analysis, the microbial communities appeared to be distinct groupings of the microbial community based on xylan, xylose, or unamended (Figure 37). The 95% confidence intervals on the NMDS in ellipses separated samples more distinctly by substrate than concentration or timepoint (Figure 38a, 38b, 38c). An ADONIS test, the ecological equivalent of a multivariate analysis of variance test, supported significantly different microbial

communities by substrate at $\alpha = 0.05$ (Table 4). Betadisper analysis, an ecological equivalent of Levene's test of homogeneity, showed similar variance between xylose and xylan amended samples, indicating that the significant ADONIS result was due to differences in community structure and not simply from differences in variance. (Figure 38a and 39).

A significant statistical interaction between substrate and concentration ($p = 0.001$) and a near significant interaction between substrate and timepoint ($p = 0.07$) suggests that the effect of substrate on the microbial community may be dependent on concentration and timepoint (Table 5). Microbial communities of xylan were significantly different based on concentration (Table 6). The high concentration of substrate had more variance than the lower concentrations, which may have caused a significant ADONIS result (Figure 39).

Microcosm that produced significant respiration had different microbial communities and alpha diversity indices than those without detectable levels of respiration. Samples with significant respiration, the high xylose, medium xylose and high xylan, are the "respiration" group. The other lower concentrations of substrates and unamended control did not have significant respiration and are grouped as below detectable limit respiration (BDLrespiration). The taxonomic structure was different as seen by NMDS analysis and ADONIS testing (Figure 38d). Chao1, Simpson and Faith's diversity was calculated between the two groups (Table 7) where a significant amount of difference was observed in Simpson and Faith's diversity after the final timepoint. Simpson diversity was higher while the phylogeny based Faith's diversity was lower in the respiration group .

Using differential abundance analysis, we wanted to identify species that increased only in response to xylan and not xylose or the unamended control. In this manner, we hoped to specifically identify species associated with the breakdown of high molecular weight xylan and eliminate species that may be only be scavenging the released xylose. Over the span of all three timepoints, only several OTUs consistently increased in response to xylan: *Pseudoalteromonas*, *Prosthecobacter*, Candidate *Xiphinematobacter*, *Muricauda*, and *Alteromonas* (Figure 40). *Muricauda* was exclusively found in the highest concentration of xylan (Figure 41).

Since *Pseudoalteromonas* was present in all concentrations of xylan (Figure 41), we re-classified the *Pseudoalteromonas* sequences at a higher level of similarity, 99.8%, to identify any trends at a higher level of resolution. Some of the 99.8% similarity OTUs were more frequently found in the xylan-amended microcosms while others were more ubiquitous (Figure 42, 43, 44). When compared to type strain 16S rRNA gene sequences, we found a cluster of OTUs possessed several xylan-associated OTUs.

Conclusions

Our main result was that the high molecular weight hemicellulosic xylan and its monosaccharide monomer xylose enriched different microbial consortia from the Australian Bight seawater microbial community. The difference in microbial consortia provides evidence to reject the null hypothesis that a single microbial consortium degrades xylan and then utilizes the released xylose. We conclude that it is more likely that a subpopulation of microbes degrades the high molecular weight xylan while a different subpopulation, including "cheater" microbes, utilizes the released low molecular weight xylose oligomers and monomers. A similar study comparing microbial communities growing on polysaccharide cellulose and its shorter oligosaccharide and monosaccharide, cellobiose and glucose, also found differences in microbial community structure (Schellenberger et al., 2010). The microbial community within our xylose-amended microcosms likely consists of taxa that quickly respond and bloom in response to available xylose and therefore might be involved in "cheating" behavior if they cannot produce extracellular hemicellulolytic enzymes.

Since we established xylose "cheaters" were likely present in our xylan microcosms, we interpreted the role of dominant taxa in our xylan amended microcosms with some degree of caution. To reduce false positives, we limited the definition of keystone species as species that were dominant in the only concentration of xylan with detectable microbial activity, the high xylan microcosm, and rare in the xylose microcosms. In this manner, we precluded the "cheater" taxa of xylose as potential keystone species.

Members of genus *Muricauda* within the bacterial family Flavobacteriaceae of the phylum 'Cytophaga-Flavobacterium-*Bacteroidetes'* increased in response to the high xylan amendment after the second timepoint. *Bacteroidetes* in marine ecosystems have been long-associated with the degradation of high molecular weight organic matter, especially particulate organics (Fernandez-Gomez et al., 2013). Since xylan was insoluble in the medium, *Bacteroidetes* such as *Muricauda* may have had the advantage to attach. In fact, characterization of the M. *ruestringensis* B1 shows it prefers to live on surfaces rather than freely in the medium (Bruns et al., 2001b). M. *ruestringensis* B1 also grew in a wide temperature range which could be why it revived well at room temperature despite the original Australian Bight being cold at 4°C (Bruns et al., 2001a). *Muricauda* is unlikely to be a "cheater" because it was absent in all concentrations of xylose microcosms. We do not have evidence to interpret the absence of *Muricauda* in the xylose microcosms as the inability to utilize xylose. Its absence from the xylose microcosms could suggest it does not utilize xylose very well. Previous evidence shows members of the phylum *Bacteroidetes* prefer polymers rather than monomers (Cottrell and Kirchman, 2000).

Muricauda has not been well characterized as a bacterial species. There are only two publicly available genome sequences from *Muricauda* isolates (Huntemann et al., 2012; Oh et al., 2015). Based on their annotation from the UniProt protein database (2014), the *Muricauda* possesses genes encoding various xylose isomerases, endoxylanases, and xylosidases. The CaZY database of carbohydrate-active enzymes (http://www.cazy.org/) predicted 2 glycosyl hydrolase (GH) family 43 xylanases, one of the lesser studied xylanase families (Collins et al., 2005), in the *Muricauda ruestringensis* DSM 13258 genome (Cantarel et al., 2009).

Pseudoalteromonas, a *Gammaproteobacteria* genus, was also a likely keystone species candidate. It was the most dominant bacterial taxa in the high xylan microcosm at all timepoints by a large margin while being very rare in the xylose microcosms. *Pseudoalteromonas* has been found to produce extracellular agarlytic enzymes (Vera et al., 1998; Skovhus et al., 2007). Of the 12 *Pseudoalteromonas* genomes annotated within the CAZY database of enzymes (Cantarel et al., 2009), 8 species have at least 1 predicted xylanase of the identified GH families with xylanases, which are GH 5, 7, 8, 10, 11, and 43 (Collins et al., 2005). *Pseudoalteromonas* was more ubiquitous than *Muricauda* in that it was present in both xylan and xylose. With 99.8% similarity clustering of the *Pseudoalteromonas* sequences into OTUs, we have some preliminary evidence that the *Pseudoalteromonas* found in xylan and xylose treatments may not have been the same. Future work is required to explore the differences in *Pseudoalteromonas* at a higher resolution. This future work would align with the increasing number of 16S rRNA gene based microbial surveys that have been questioning the threshold of 97% clustering for OTU clustering (Nguyen et al., 2016).

Substrate-amended microcosms are usually sequenced at multiple timepoints to look for trends of succession. Incubation usually reduces microbial diversity and species richness so that sequencing based approaches can readily detect important changes (DeAngelis et al., 2010) . However, microbial communities only slightly differed between timepoint. Most of the dominant taxa had already become established by the first week of incubation. Longer incubation time alone will not resolve keystone species away from less relevant "cheater" taxa.

Each concentration had a very different microbial community structure. Some evidence shows that the DOM concentration and quality can influence the community structure in a wide variety of inoculum (Docherty et al., 2006) and can have a more noticeable effect on oligotrophic communities, like the ocean (Eiler et al., 2003). Our results with the swapped microbial community indicated substrate concentration was limiting in our tested concentrations. The swapped microbial community, despite possessing active xylan-degrading microbes, was unable to mineralize lower concentrations suggesting concentration may be a larger constrain than the microbial community.

The "cheater" taxa may not have extracellular xylanolytic enzymes, but they could still play an important role in the microbial community. In general, saccharolytic microbes may be converting sugars into volatile fatty acids, alcohols and molecular hydrogen, or acetate, which in turn support the polymer-degrading microbes (Bayer et al., 1994). Further research could investigate the role of "cheater" taxa and the seemingly altruistic xylan-degrading microbes to determine if the relationship is mutualistic to any degree. This type of research may be best done in pure cultures rather than in complex microbial communities.

In conclusion, we have experimental evidence that the marine microbial community degrading xylan as a sole carbon source possessed a significant population of "cheaters". Using the microbial community in our monosaccharide xylose microcosms as our pool of xylose "cheaters", we conservatively interpreted the dominant taxa in our polysaccharide xylan microcosms as keystone species. Two taxa in the active 0.05% xylan seawater microcosm, *Muricauda* and *Pseudoalteromonas*, could be keystone species. These taxa have not been extensively studied for hemicellulose degradation before. As keystone species, they may be capable of producing important extracellular enzymes responsible for high molecular weight

carbon cycling in the ocean as well as provide stress tolerant and halotolerant enzymes with commercial value for the lignocellulosic biofuel industry.

Acknowledgements

This material is based upon work supported by the National Science Foundation Graduate Research Fellowship Program under grant no. DGE-1452154. Anthony Rossi was supported by the NSF REU summer program at the University of Tennessee during the summer of 2015. The authors thank Julian Fortney for sampling the seawater sample from their BP oil research cruise in the Great Australian Bight.

Conflict of Interest

The authors declare no conflict of interest.

Appendix B: Figures and Tables

Table 2 Non-adjusted total production of carbon dioxide

The table shows the raw data of total carbon dioxide produced by the microcosms.

Treatment	Replicate	Total Production of Co2 over the incubation in µg (non-adjusted values)
Low Xylose	1	1351.65
Low Xylose	2	913.672
Low Xylose	3	1578.432
Med Xylose	1	12919.73
Med Xylose	2	12359.764
Med Xylose	3	11901.602
High Xylose	1	79295.695
High Xylose	2	64130.183
High Xylose	3	59962.748
Unamended	1	-1584.783
Unamended	2	-1829.229
Unamended	3	-1143.983
High Xylan Abiotic	1	-5100.685
High Xylan Abiotic	2	-3812.626
High Xylan Abiotic	3	-3662.143
Killed High Xylan	1	-1382.81
Killed High Xylan	2	-1910.368
Killed High Xylan	3	-2375.628
Low Xylan Abiotic	1	-5208.13
Low Xylan Abiotic	2	-4589.984
Low Xylan Abiotic	3	-4369.757
Med Xylan Abiotic	1	-5145.973
Med Xylan Abiotic	2	-4057.996
Med Xylan Abiotic	3	-3640.098

Table 2 Continued

Treatment	Replicate	Total Production of Co2 over the incubation in µg (non-adjusted values)
Sterile Media	2	-4726.624
Sterile Media	1	-4807.772
Sterile Media	3	-5583.914
High Xylan	1	179.795
High Xylan	2	8439.821
High Xylan	3	531.253
Low Xylan	1	-1491.789
Low Xylan	2	-1651.631
Low Xylan	3	-1312.828
Med Xylan	1	-1180.388
Med Xylan	2	-1218.729
Med Xylan	3	-981.275
Xylan to Xylan	1	-1634.271
Xylan to Xylan	2	-1500.129
Xylan to Xylan	3	-1511.829
Xylose to Xylan	1	-1795.155
Xylose to Xylan	2	-1625.264
Xylose to Xylan	3	-1610.796

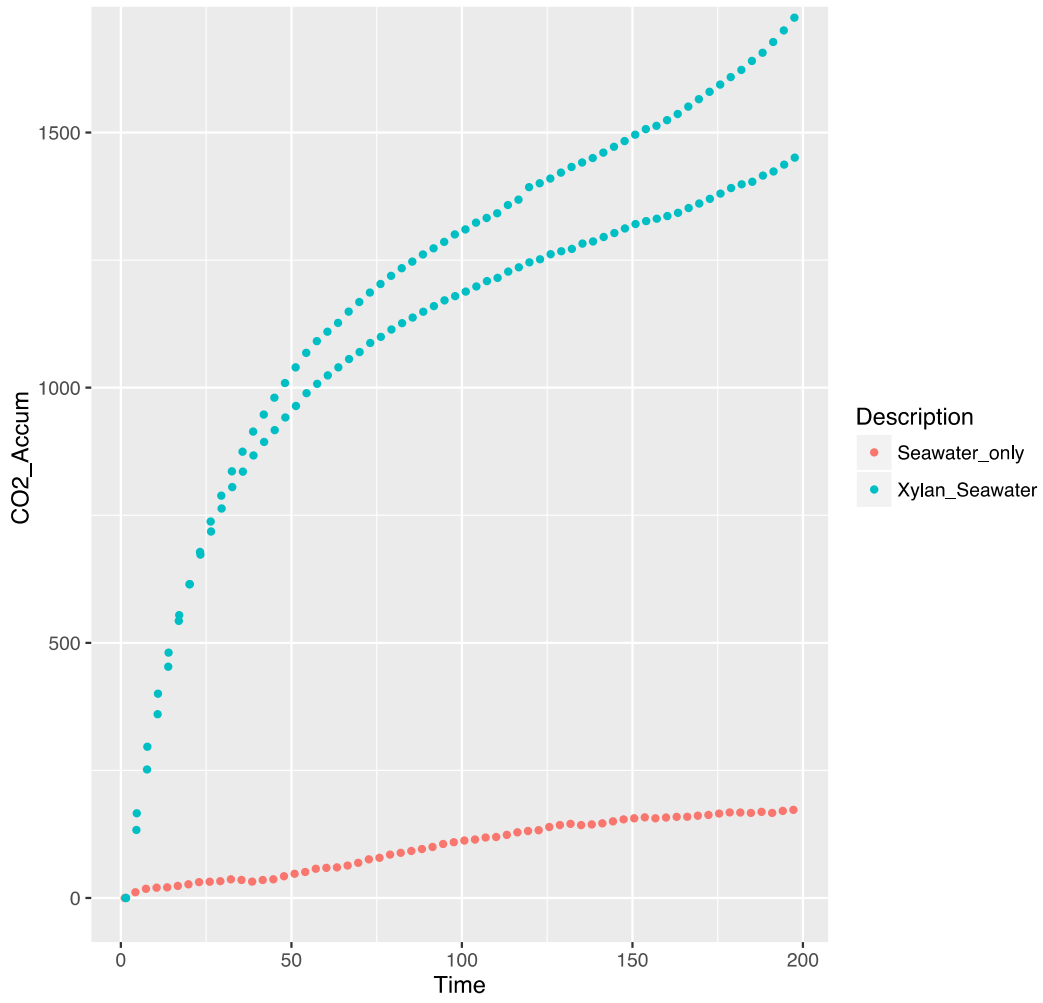

Figure 22 Carbon dioxide production from initial xylan-amended Australian Bight seawater

The xylan-amended seawater was tested in duplicate (turquoise). The seawater only control was unamended seawater (coral red). Carbon dioxide production was measured over 200 hours.

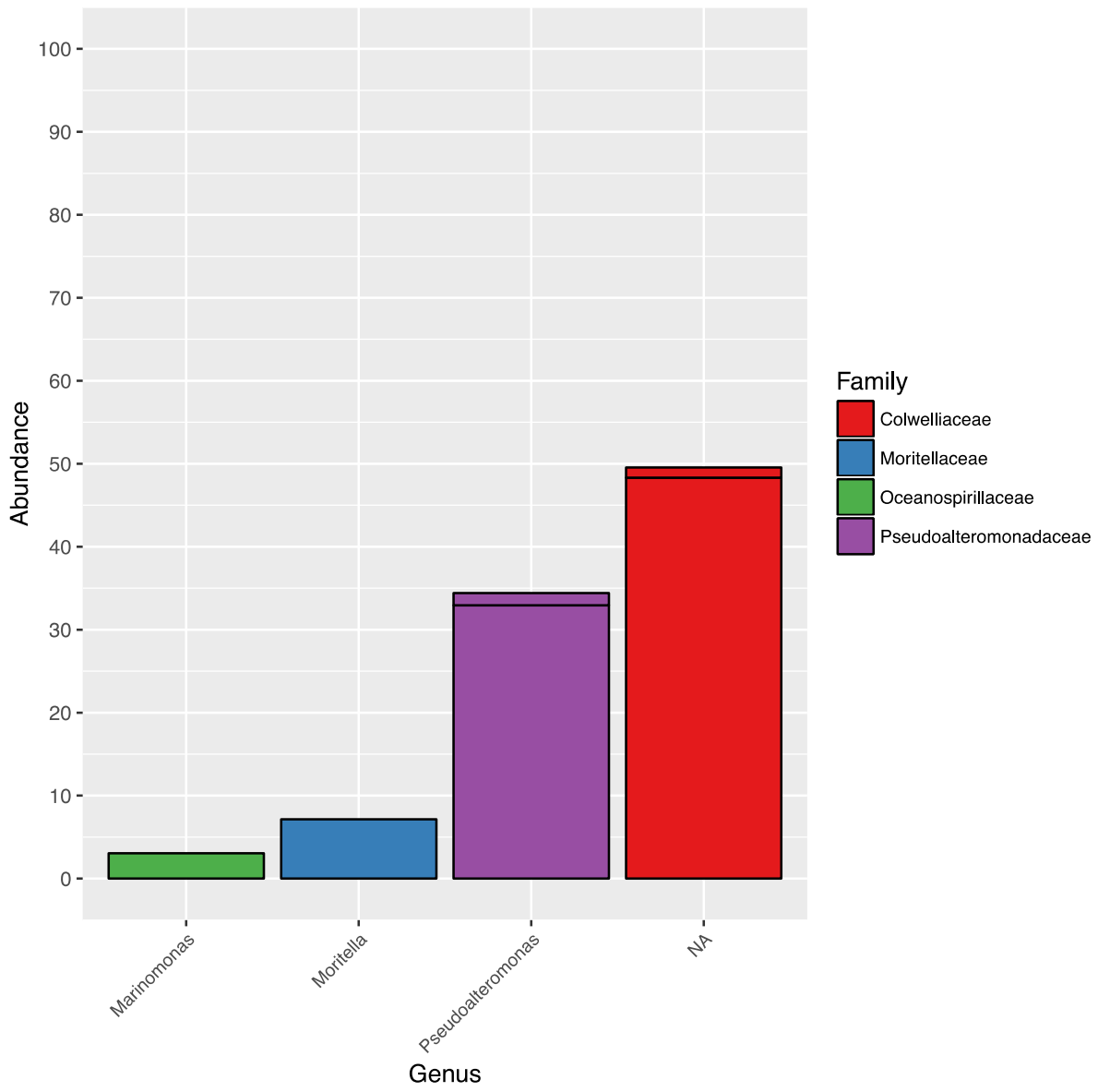

Figure 23 Dominant taxa in initial xylan-amended Australian Bight seawater

Dominant taxa within the xylan-amended Australian Bight seawater were *Marinomonas*, *Moritella*, *Pseudoalteromonas* and a genus of *Colwelliaceae* (in increasing order). Dominant taxa greater than 1% relative abundance are shown. Stacked bar plots for each genus indicate the number of distinct OTUs at 97% similarity.

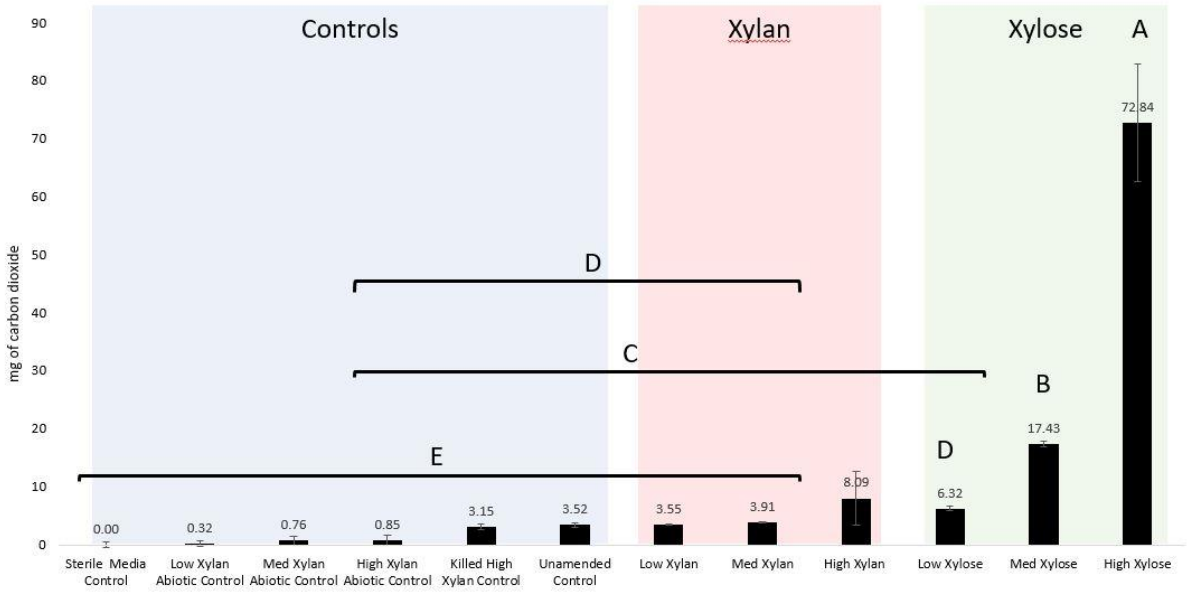

Figure 24 Production of carbon dioxide by substrate-amended microcosms

The mg of carbon dioxide produced by xylan-amended (red), xylose-amended (green), and various control microcosms (blue) were adjusted so that the sterile media control was exactly 0.00 mg. The adjusted value is shown above each plotted bar. The error bars indicate standard deviation between triplicate microcosm replicates of each treatment. Letters indicate the results from a pairwise student's t test where samples not connected by a letter are considered statistically different at $\alpha = 0.05$.

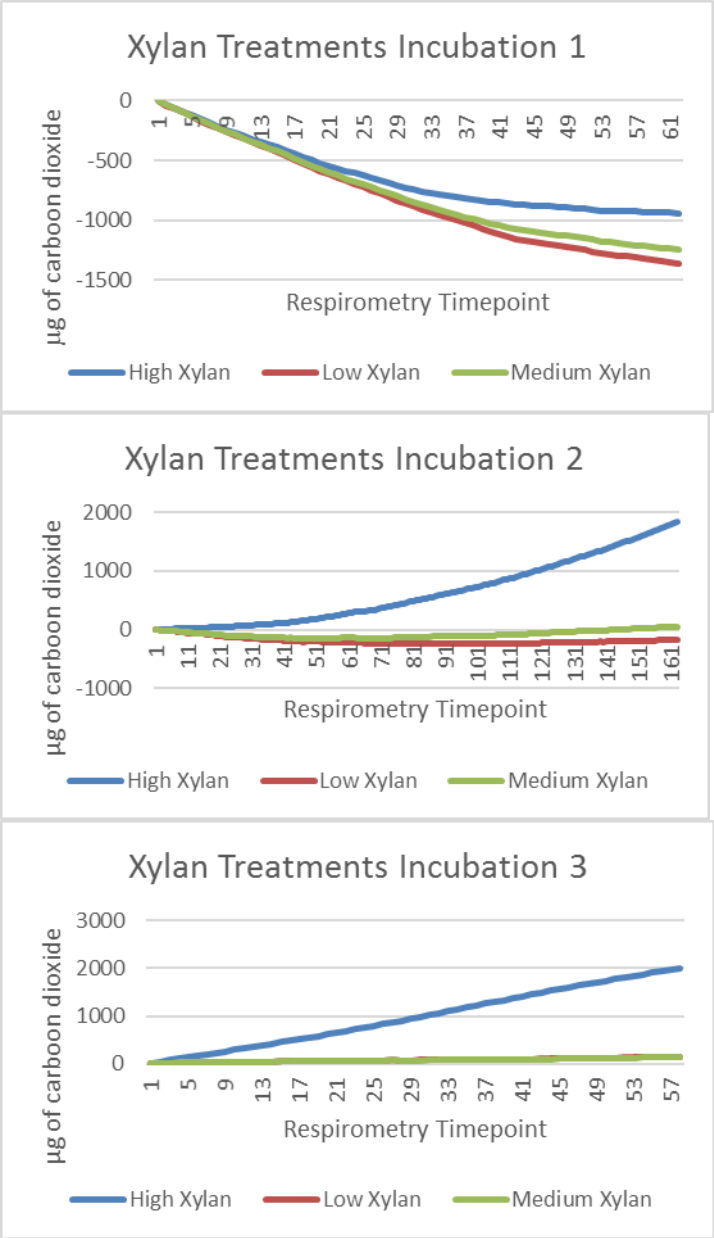

Figure 25 Xylan adapted consortia during the three consecutive incubations periods

Plots show µg of carbon dioxide accumulated over the course of the experiment that was divided into 3 consecutive incubations. "Incubation 1" refers to approximately the first week, or more precisely 180 h. "Incubation 2" is the following two weeks or 351 h. "Incubation 3" is the final week or 137 h. Horizontal axis shows the respirometry timepoints which are approximately 3 hours apart. Curves are the average of three biological replicates.

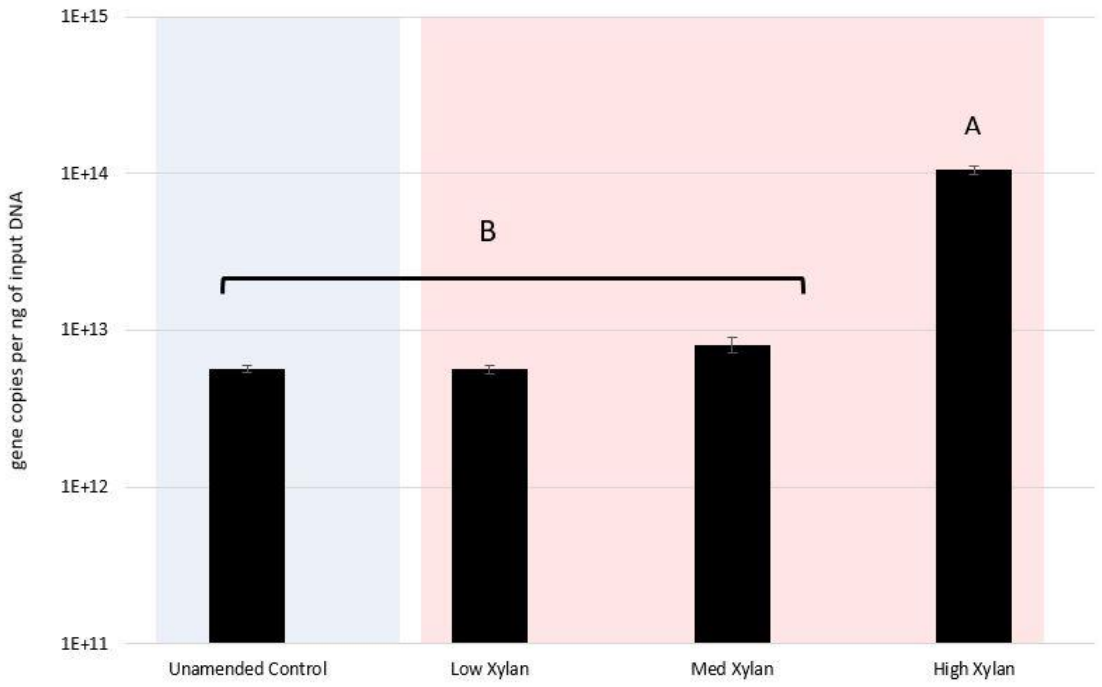

Figure 26 Quantification of bacterial 16S rRNA gene copies in xylan-amended microcosms

The total bacterial rRNA gene copies in the unamended control (blue) and all 3 concentrations of xylan-amended microcosms (red) were determined using qPCR with universal bacterial primers. The total reported is the sum of 3 timepoint measurements. Gene copies were calculated based on a qPCR standard curve and then normalized by the amount of input DNA. The gene copies per ng of input DNA was averaged using 3 replicates of a 10-fold and 100-fold dilution of input DNA for 6 replicates total. Standard deviations are indicated by the error bars. Letters indicate the results from a pairwise student's t test where samples not connected by a letter are considered statistically different at an alpha of 0.05.

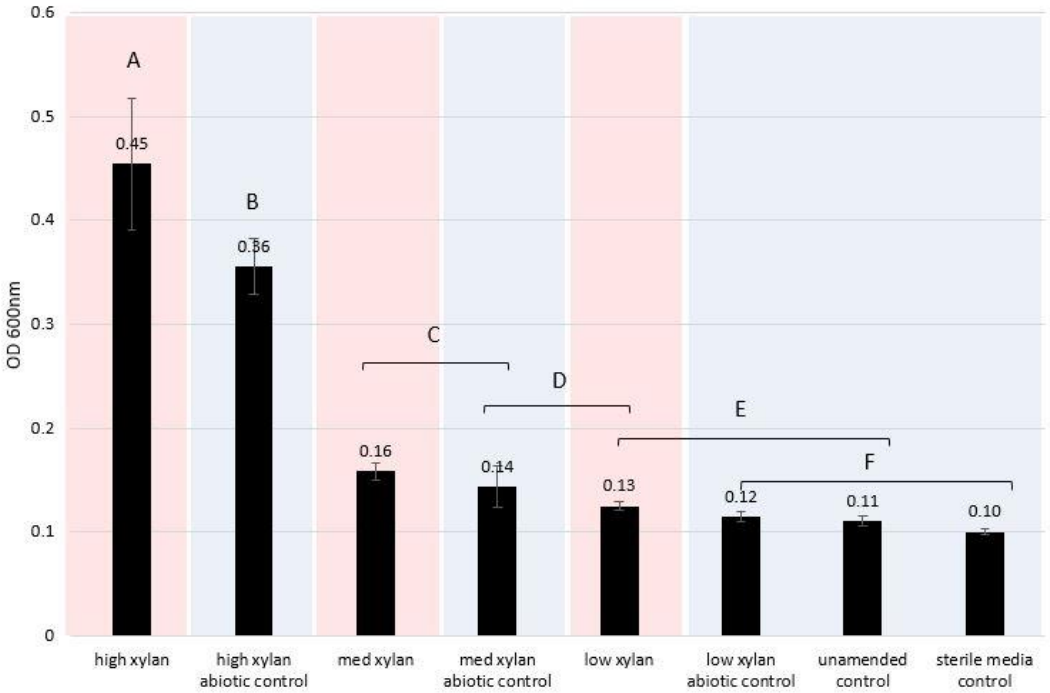

Figure 27 Optical Density at 600 nm (OD 600 nm) of xylan-amended and control microcosms

The OD 600 nm shown is the average of 9 replicates for each microcosm treatment. The error bars indicate the standard deviation. The value is shown above each bar. Letters indicate the results from a pairwise student's t test where samples not connected by a letter are considered statistically different at $\alpha = 0.05$. The red colored bars are xylan amended microcosm. Blue colored bars are the controls.

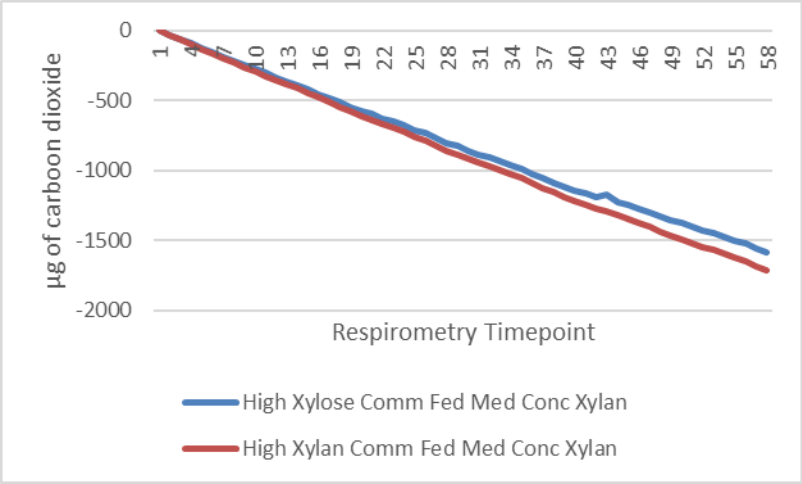

Figure 28 Swapped Community Test Carbon Dioxide Production

After the 2nd incubation, the high xylose and high xylan microbial communities were each transferred to a fresh medium (0.01%w/v) concentration of xylan in defined media. The vertical axis is µg of carbon dioxide accumulated. Horizontal axis shows the respirometry timepoints which are approximately 3 hours apart. The curves are the average of three biological replicates.

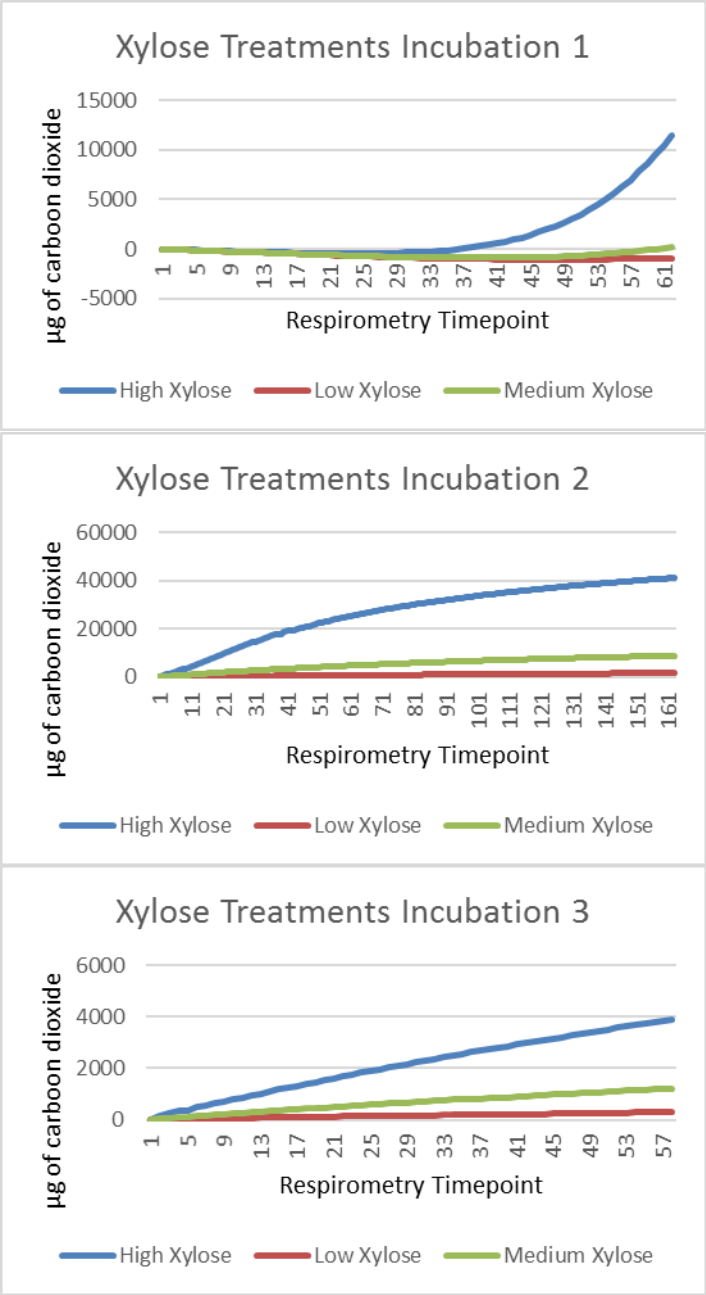

Figure 29 Xylose adapted consortia during the three consecutive incubations periods

Plots show µg of carbon dioxide accumulated over the course of the experiment that was divided into 3 consecutive incubations. Horizontal axis shows the respirometry timepoints which are approximately 3 hours apart. Curves are the average of three biological replicates.

Table 3 Sequencing Reads of 16S rRNA gene amplicons

The table shows the number of sequencing reads per sample.

Treatment	Timepoint	Number of Reads
Cryptic_Growth_Control	1	12534
Cryptic_Growth_Control	2	6359
Cryptic_Growth_Control	3	4986
High_Xylan	1	14293
High_Xylan	2	8935
High_Xylan	3	7160
High_Xylose	1	15079
High_Xylose	2	8099
High_Xylose	3	8230
Medium_Xylan	1	13960
Medium_Xylan	2	5210
Medium_Xylan	3	7724
Medium_Xylose	1	18004
Medium_Xylose	2	8973
Medium_Xylose	3	6007
Low_Xylan	1	15730
Low_Xylan	2	10062
Low_Xylan	3	10676
Low_Xylose	1	14192
Low_Xylose	2	6104
Low_Xylose	3	8932

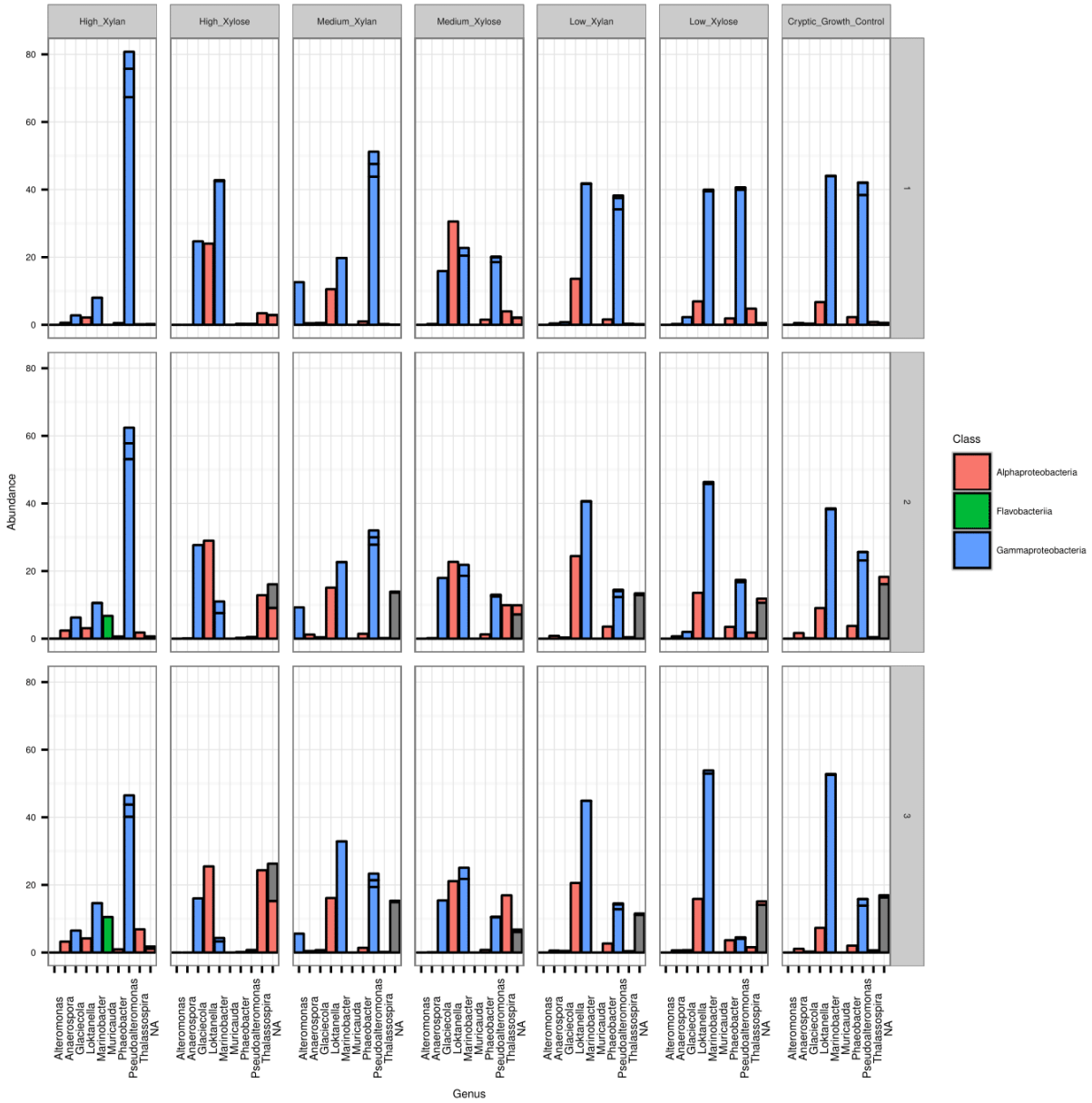

Figure 30 Relative abundances of dominant taxa

Taxa greater than 10% relative abundance are shown. Sub-plots are ordered horizontally by decreasing concentration of substrate and vertically by timepoint. Within each sub-plot, individual units of the stacked bars correspond to the relative abundance of each OTU classified as that genus. Bars are colored by their taxonomic class. Gray bars indicate OTUs without class- or genus- level classification.

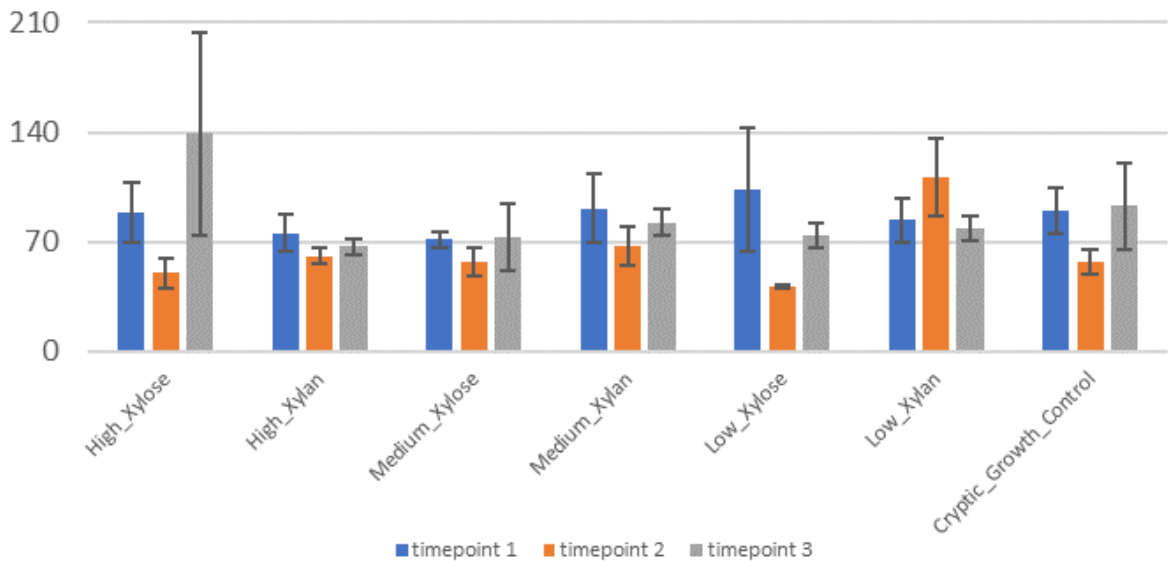

Figure 31 Chao1 Richness

The error bars for Chao1 indicate the standard error.

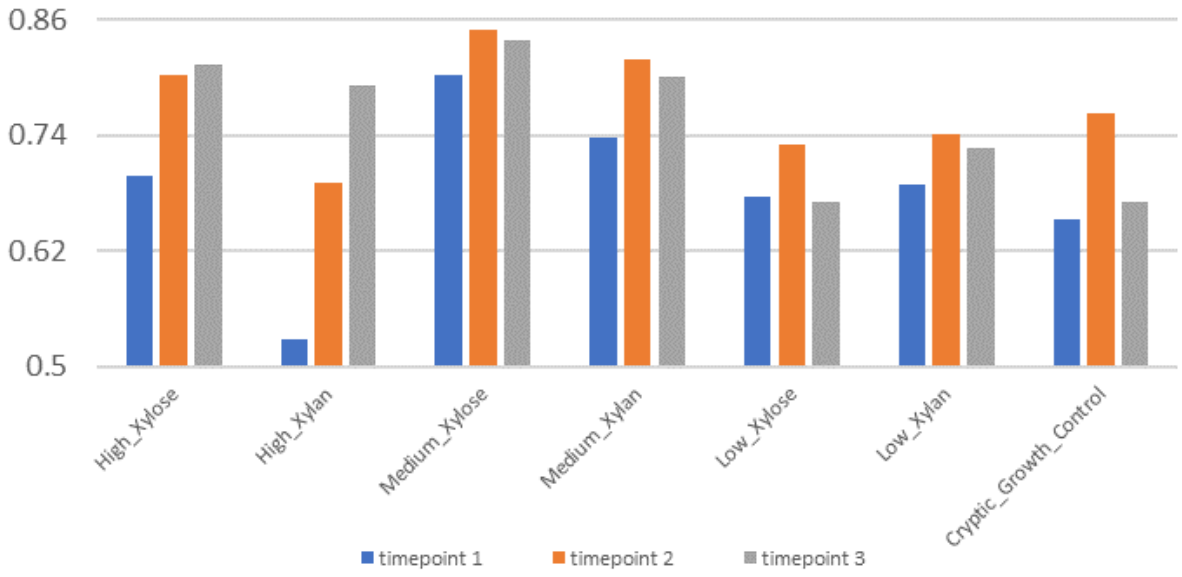

Figure 32 Simpson Diversity

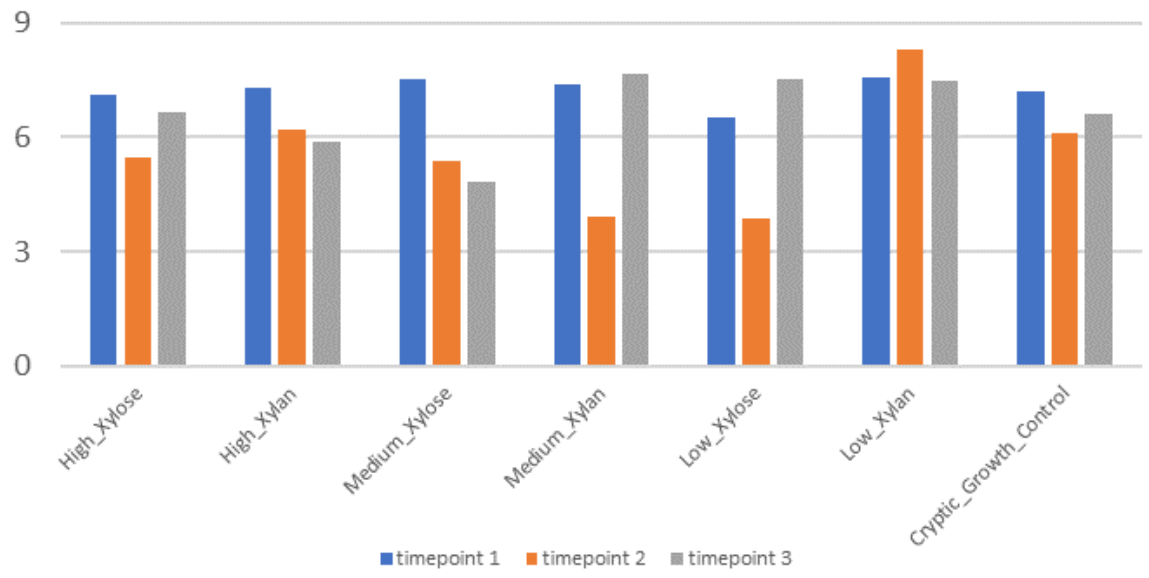

Figure 33 Faith's phylogenetic diversity

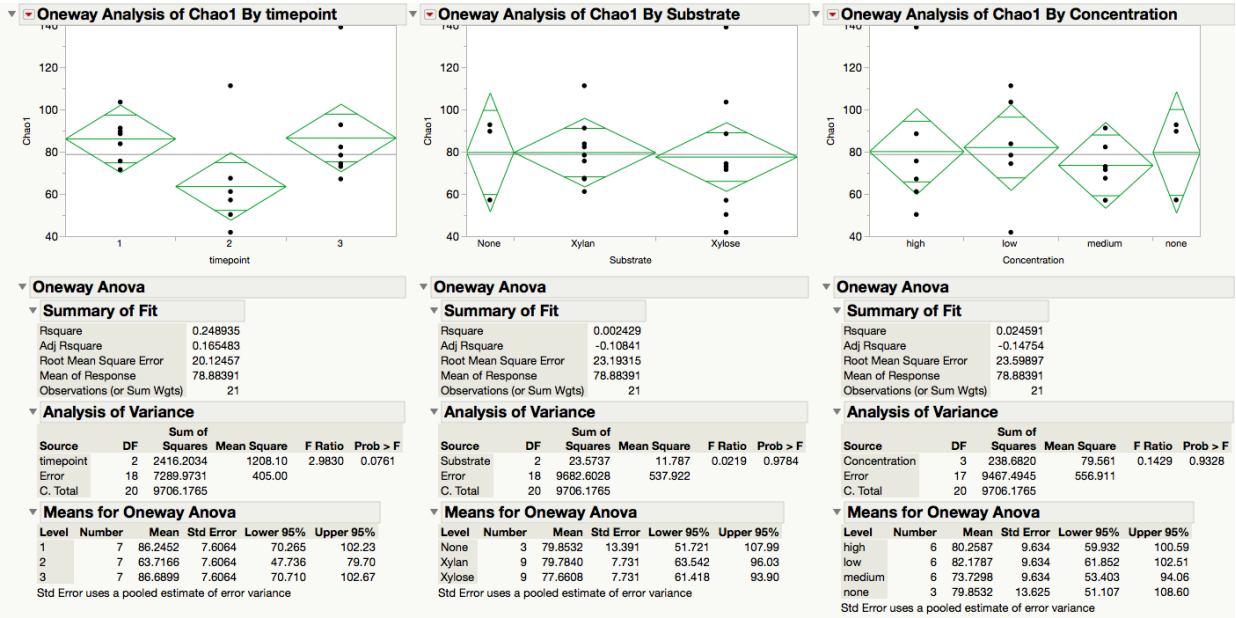

Figure 34 One-way ANOVA analysis of timepoint, substrate and concentration on Chao1 Richness Index

ANOVA reports are generated by JMP 12 Pro Fit X by Y function. ANOVA reports are generated by JMP 12 Pro Fit X by Y function. Analysis was run on each factor, timepoint, substrate and concentration. Reports include summary of fit, analysis of variance and means for each level of the factor tested.

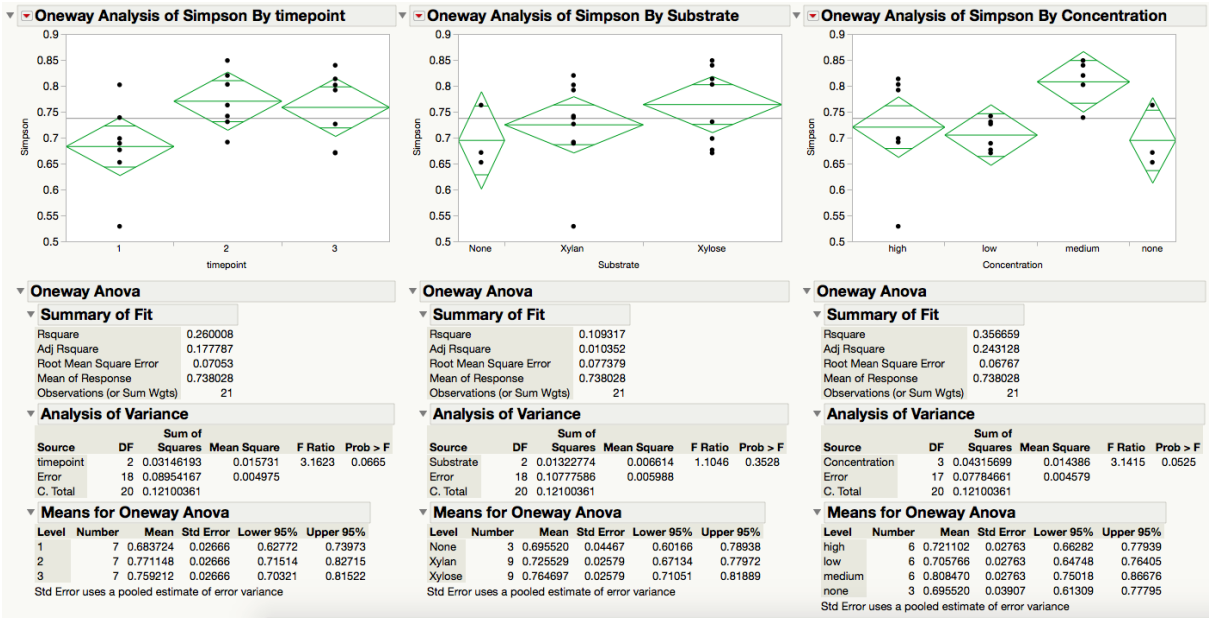

Figure 35 One-way ANOVA analysis of timepoint, substrate and concentration on Simpson Diversity Index

ANOVA reports are generated by JMP 12 Pro Fit X by Y function. Analysis was run on each factor, timepoint, substrate and concentration. Reports include summary of fit, analysis of variance and means for each level of the factor tested.

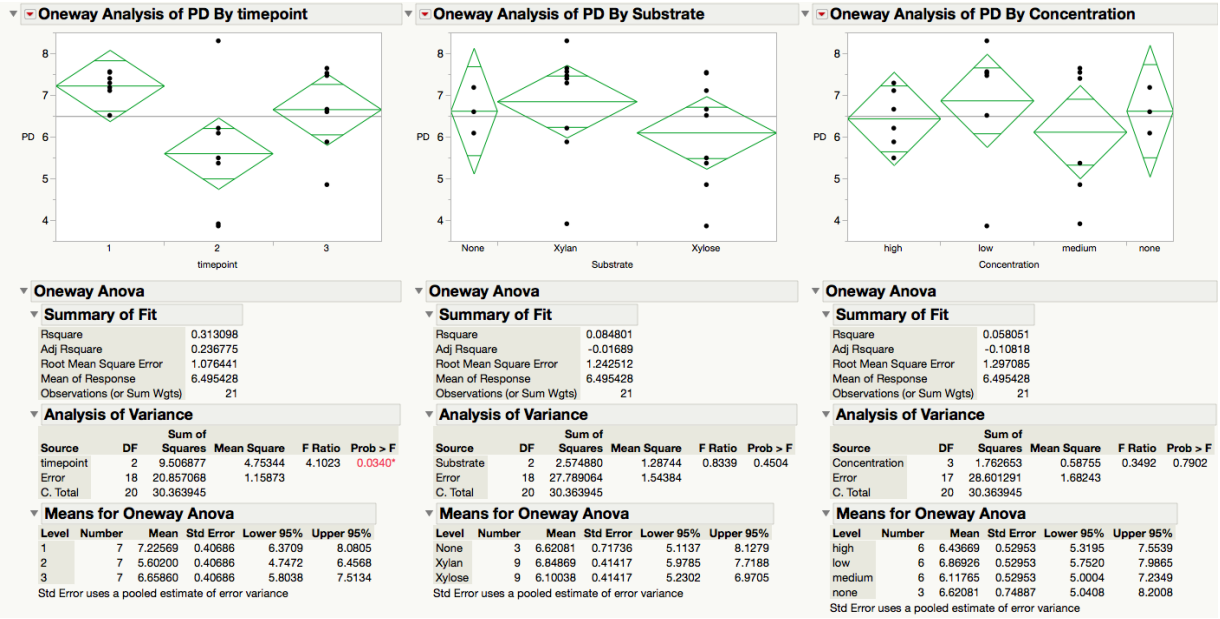

Figure 36 One-way ANOVA analysis of timepoint, substrate and concentration on Faith's Phylogenetic Diversity Index

ANOVA reports are generated by JMP 12 Pro Fit X by Y function. ANOVA reports are generated by JMP 12 Pro Fit X by Y function. Analysis was run on each factor, timepoint, substrate and concentration. Reports include summary of fit, analysis of variance and means for each level of the factor tested.

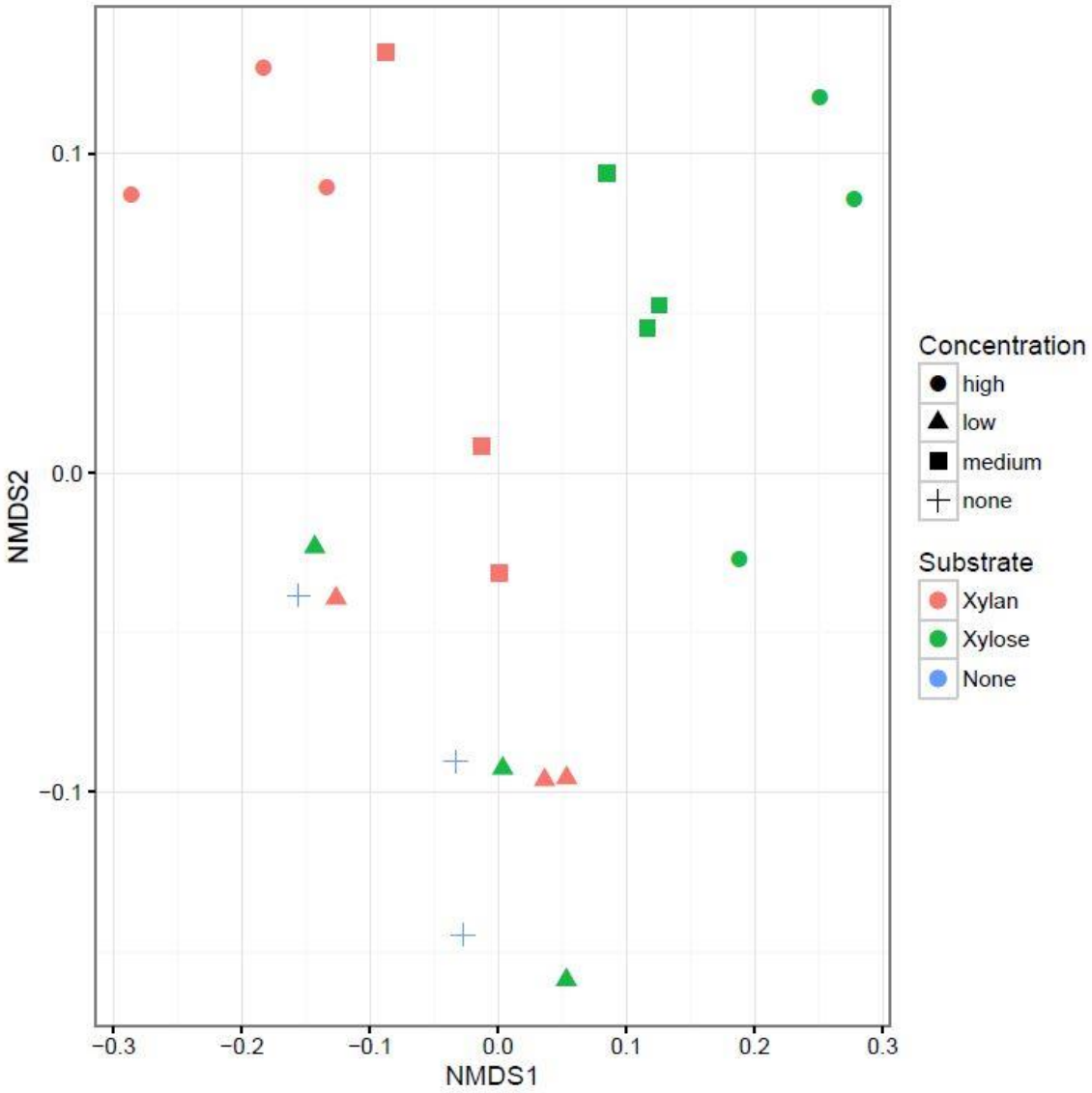

Figure 37 Non-Metric Multidimensional Scaling (NMDS) ordination analysis

NMDS analysis using weighted Unifrac distance was performed on the rarefied OTU table in the phyloseq R package. Stress of the ordination was 0.0850.

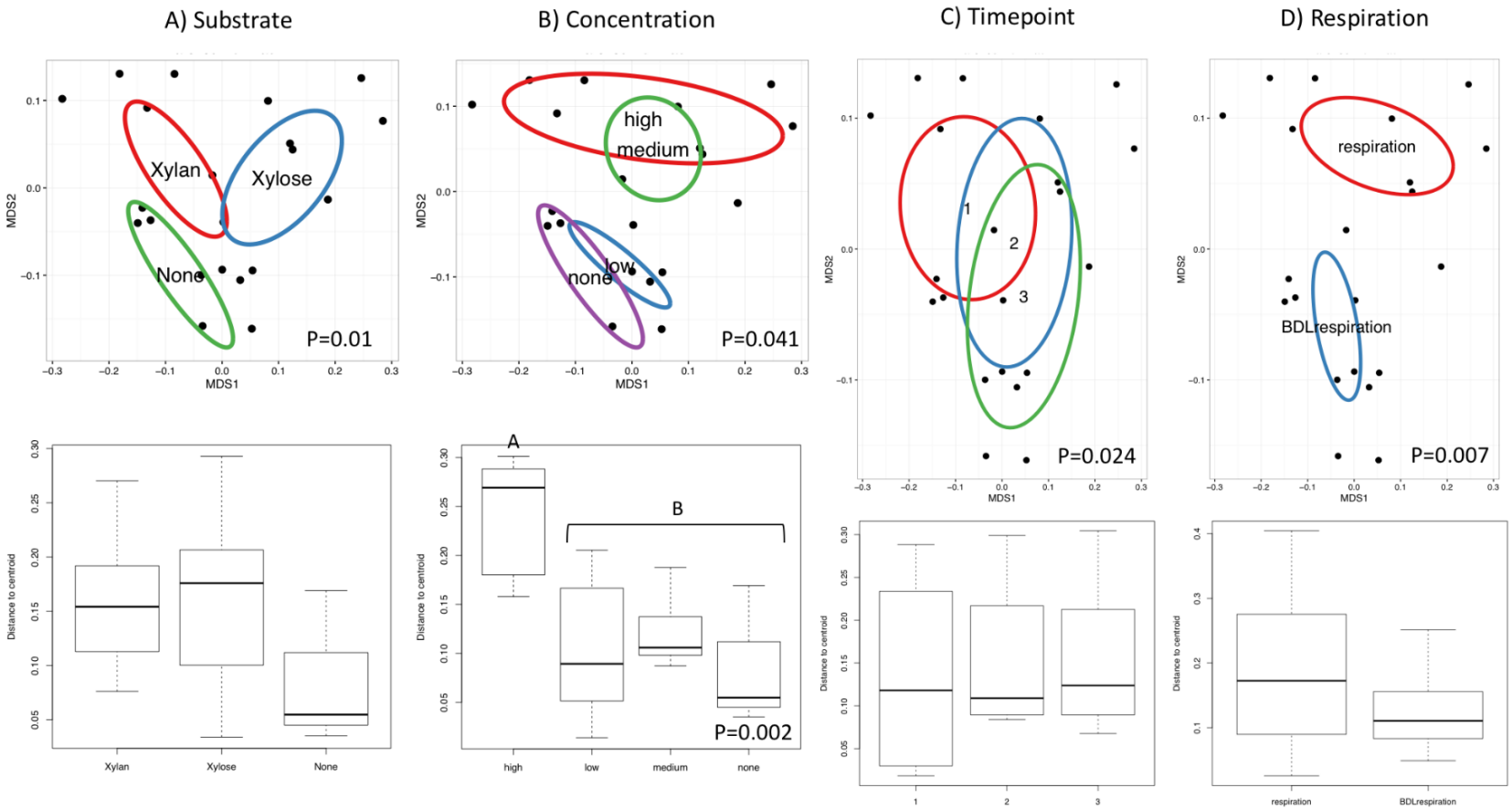

Figure 38 Non-Metric Multidimensional Scaling with confidence ellipses and variance boxplots

A) by Substrate, B) by Concentration, C) by Timepoint, D) by Respiration. 95% confidence intervals for each group are shown in ellipses. Boxplots show the variance of the dissimilarities. Respiration plot shows the dissimilarities between the treatments with positive respiration levels (the high xylan, high xylose and med xylose) and the other treatments below detection limit (BDL). ADONIS test and ANOVA test p-values are shown only if significant at α=0.05

Table 4 ADONIS tests of the main effects

The following are the ADONIS results generated by the vegan R package. ADONIS results indicate the effect of each factor, substrate, concentration and timepoint, on microbial community dissimilarity. Significance is indicated by the following: 0 ‘***’ 0.001 ‘**’ 0.01 ‘*’ 0.05 ‘.’ 0.1 ‘ ’

	Df	SumsOfSqs	MeanSqs	F.Model	R2	Pr(>F)	
Substrate	2	0.2426	0.121298	3.924	0.30362	0.008	**
Residuals	18	0.55641	0.030912	0.69638			
Total	20	0.799	1				

	Df	SumsOfSqs	MeanSqs	F.Model	R2	Pr(>F)	
Concentration	3	0.22715	0.075716	2.2509	0.28429	0.029	*
Residuals	17	0.57186	0.033639	0.71571			
Total	20	0.799	1				

	Df	SumsOfSqs	MeanSqs	F.Model	R2	Pr(>F)	
timepoint	2	0.18671	0.093353	2.7443	0.23367	0.038	*
Residuals	18	0.6123	0.034017	0.76633			
Total	20	0.799	1				

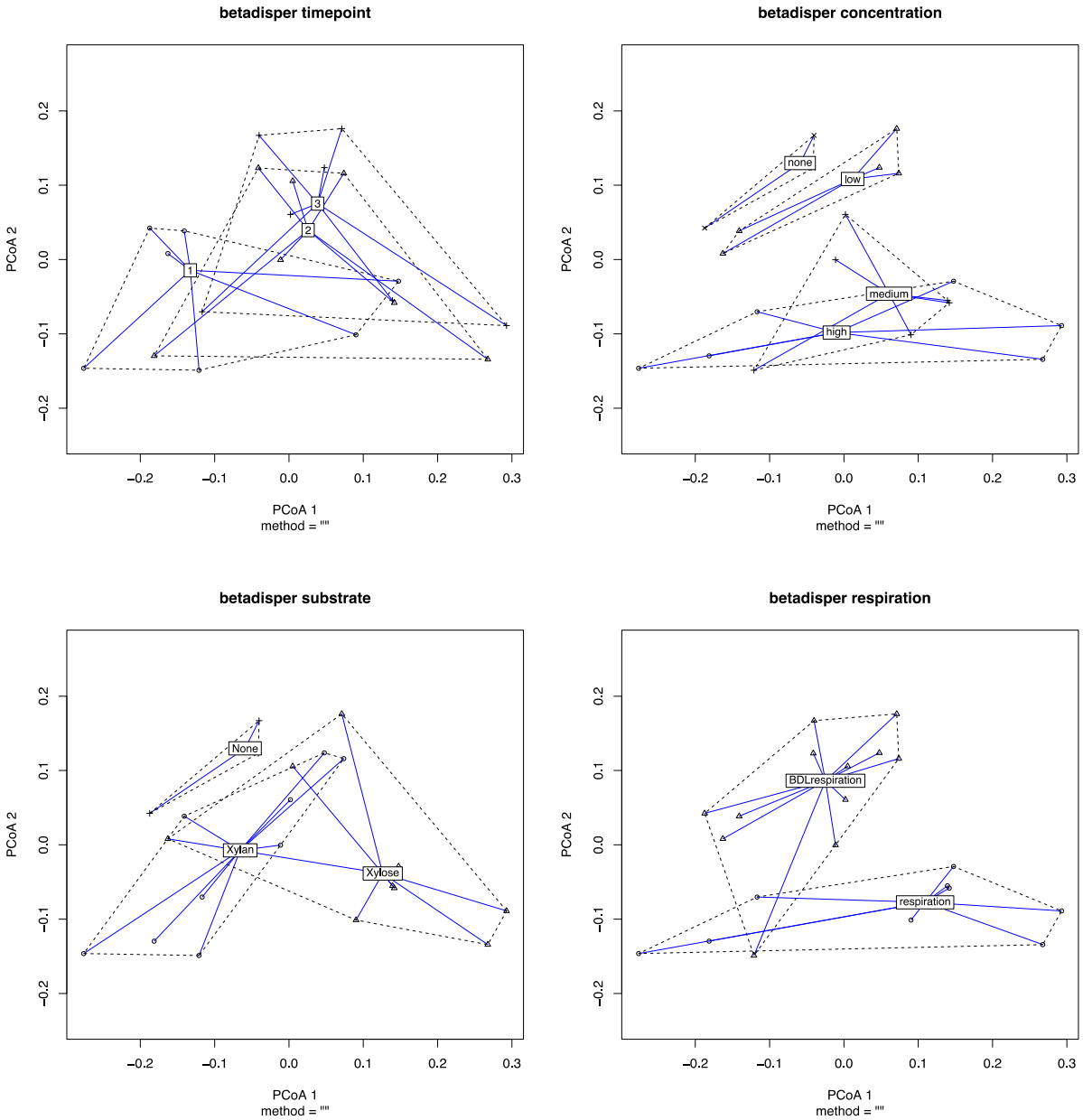

Figure 39 Multivariate homogeneity of group dispersions (variances) analysis

The dispersion of different levels of each experimental factor are shown. Dispersions were calculated using the vegan package *betadisper* function. Dispersions are plotted on the first two Principal Coordinate axes. Each subplot is a different factor: timepoint, concentration, substrate and respiration. Groupings are labelled at the centroid location.

Table 5 ADONIS tests of the interaction effects

ADONIS results indicate the effect of each factor, substrate, concentration and timepoint, on microbial community dissimilarity. Significance is indicated by the following: 0 '***' 0.001 '**' 0.01 '*' 0.05 '.' 0.1 ' '

	Df	SumsOfSqs	MeanSqs	F.Model	R2	Pr(>F)	
Substrate:Concentration	6	0.57399	0.095666	5.9523	0.71839	0.001	***
Residuals	14	0.22501	0.016072	0.28161			
Total	20	0.799	1				

	Df	SumsOfSqs	MeanSqs	F.Model	R2	Pr(>F)	
timepoint:Concentration	11	0.42464	0.038604	0.92806	0.53146	0.578	
Residuals	9	0.37436	0.041596	0.46854			
Total	20	0.799	1				

	Df	SumsOfSqs	MeanSqs	F.Model	R2	Pr(>F)	
Substrate:timepoint	8	0.43087	0.053859	1.7556	0.53926	0.07	.
Residuals	12	0.36814	0.030678	0.46074			
Total	20	0.799	1				

Table 6 ADONIS tests of focused tests between Substrate and Concentration

ADONIS results indicate the effect of each factor, substrate, concentration and timepoint, on microbial community dissimilarity. Significance is indicated by the following: 0 '***' 0.001 '**' 0.01 '*' 0.05 '.' 0.1 ' ' 7 cell means were in Description : low xylan, medium xylan, high xylan, low xylose, medium xylose, high xylose, unamended control.

Xylose only microcosms

	Df	SumsOfSqs	MeanSqs	F.Model	R2	Pr(>F)	
Concentration	2	0.17386	0.086931	5.2119	0.63467	0.015	*
Residuals	6	0.10008	0.01668	0.36533			
Total	8	0.27394	1				

Xylan only microcosms

	Df	SumsOfSqs	MeanSqs	F.Model	R2	Pr(>F)	
Concentration	2	0.15754	0.078768	4.8622	0.61843	0.016	*
Residuals	6	0.0972	0.0162	0.38157			
Total	8	0.25473	1				

	Df	SumsOfSqs	MeanSqs	F.Model	R2	Pr(>F)	
Description	6	0.57399	0.095666	5.9523	0.71839	0.001	***
Residuals	14	0.2251	0.016072	0.28161			
Total	20	0.799	1				

Table 7 Alpha Diversity and statistics of sampled based on respiration group

Respiration was created as another variable compare samples with significant respiration and non-significant respiration or respiration "below detectable limit" (BDL). Table shows each group's average Chao1, Simpson diversity and Faith's phylogenetic diversity at each timepoint.

diversity index	chao1			simpson			faiths		
group	respiration	bdl respiration		respiration	bdl respiration		respiration	bdl respiration	
	average +/- standard deviation		ttest pvalue	average +/- standard deviation		ttest pvalue	average +/- standard deviation		ttest pvalue
t1	78.53 +/- 8.87	92.03 +/- 8.29	0.09	0.68 +/- 0.14	0.69 +/- 0.04	0.86	7.31 +/- 0.22	7.16 +/- 0.46	0.63
t2	56.12 +/- 5.48	69.41 +/- 29.81	0.49	0.78 +/- 0.08	0.76 +/- 0.04	0.72	5.69 +/- 0.45	5.54 +/- 2.11	0.91
t3	93.03 +/- 39.92	81.93 +/- 7.90	0.60	0.81 +/- 0.02	0.72 +/- 0.06	0.05	5.79 +/- 0.91	7.31 +/- 0.48	0.03
	*ttest is a 2-tailed, homoscedastic								

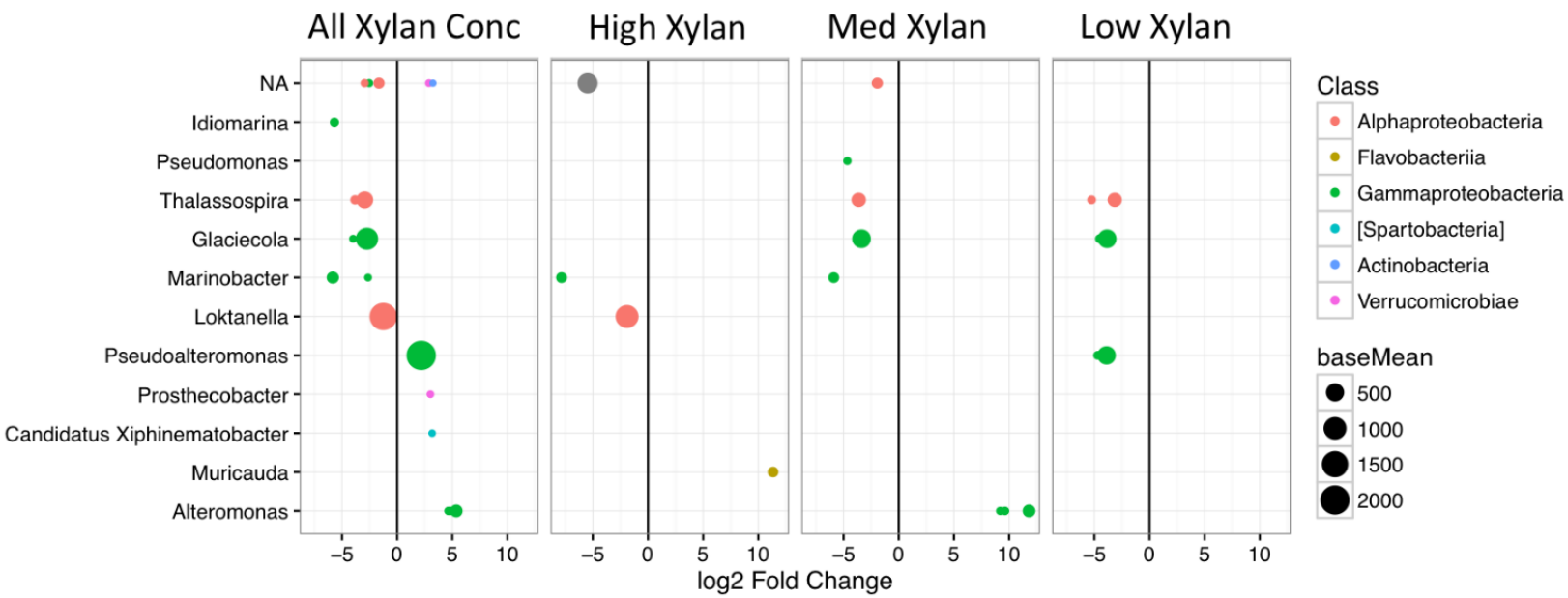

Figure 40 Log2-fold-change of OTUs in response to xylan amendment

Differential abundance analysis of the OTUs was conducted using the DESeq2 R package. OTUs plotted had a log-fold-change that was significant using a Wald test and an alpha of 0.1. OTUs with a positive log-fold-change increased in relative abundance in response to xylan. OTUs with a negative log-fold-change decreased in response to xylan, therefore they were more abundant in the control and xylose treatments. The size of the point indicates its normalized relative abundance (base mean). The color of the point indicates the taxonomic class of the OTU. Sub-plots are results from different DESeq2 analyses. "All Xylan Conc" indicates OTUs that were present in all microcosms of xylan regardless of concentration. "High Xylan", "Med Xylan", and "Low Xylan" show differentially abundant OTUs that were specific to the concentration of xylan.

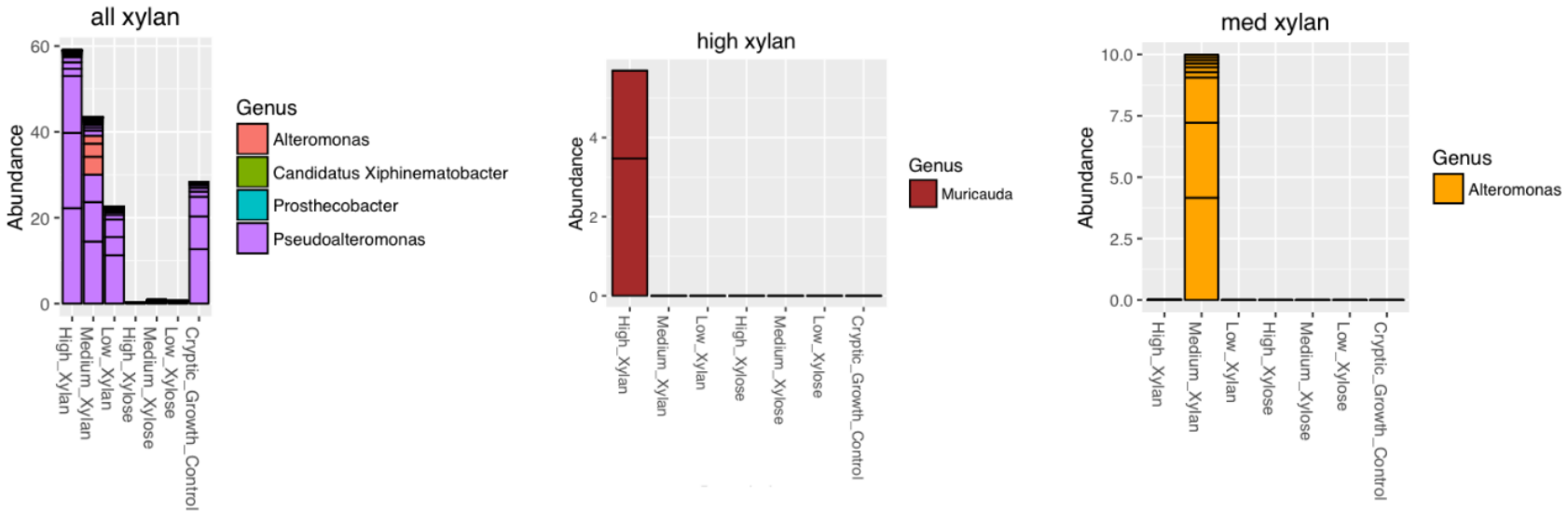

Figure 41 Differential abundant OTUs

Only OTUs that increased in relative abundance in response to xylan are shown in these taxa plots. DESeq2 analysis did not find any OTUs that exclusively increased in abundance in response to the low xylan amendment.

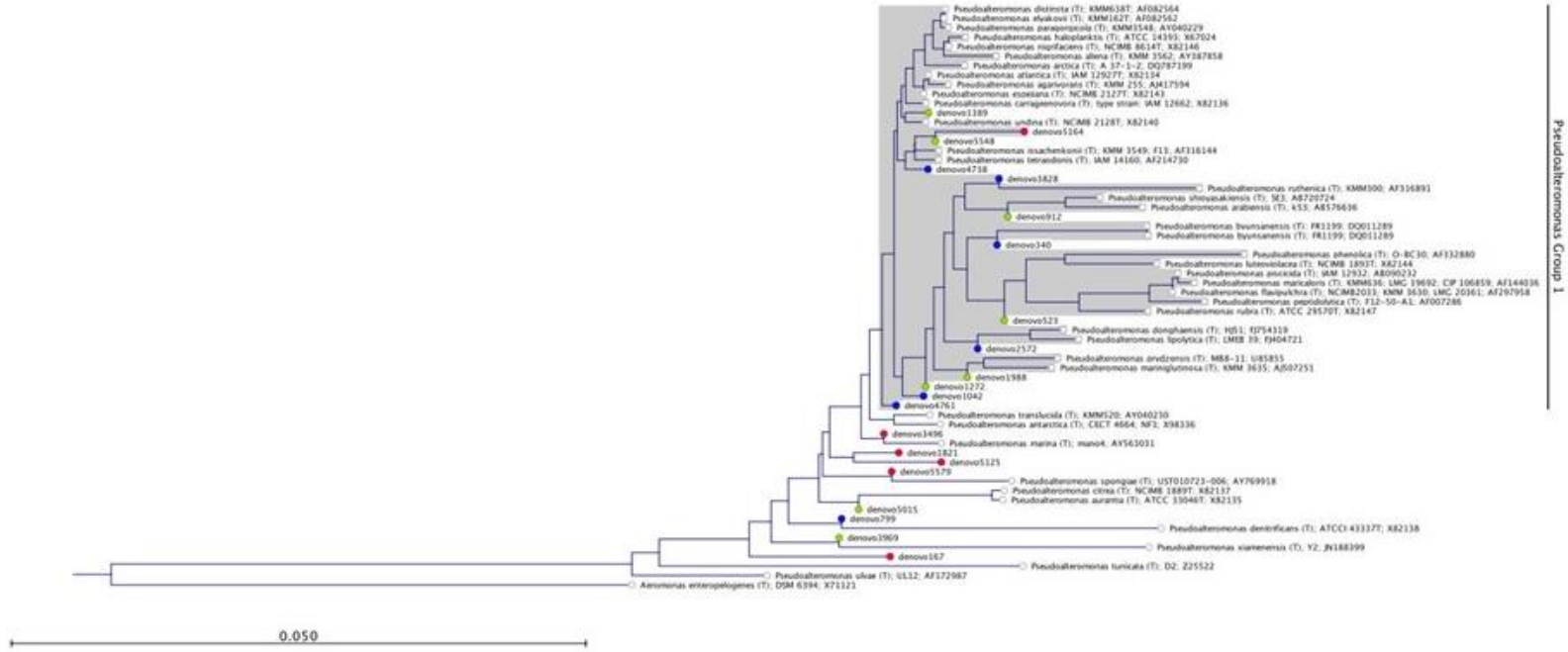

Figure 42 Phylogenetic tree of dominant Pseudoalteromonas OTUs

Representative sequences of the most abundant *Pseudoalteromonas* OTU clusters of 99.8% similarity are shown if they were greater than 3% relative abundance. OTUs were compared to type strain 16S rRNA gene sequences from the Ribosomal Database Project (RDP) in a Neighbor-joining tree using the Jukes-Cantor nucleotide distance measure and 100 replicates for bootstrapping. Strains from RDP are indicated by their genus and species name while OTUs are labelled with denovo and a unique numerical identifier. *Aeromonas enteropelogenes* was used as the outgroup. Color of the nodes indicate if the OTU was found in mostly xylan-amended (blue) or xylose-amended (red) microcosms. Nodes were green if they were found in all samples. *Pseudoalteromonas* Group 1 is the subtree that captures most of the OTUs that were associated with xylan-amended microcosms.

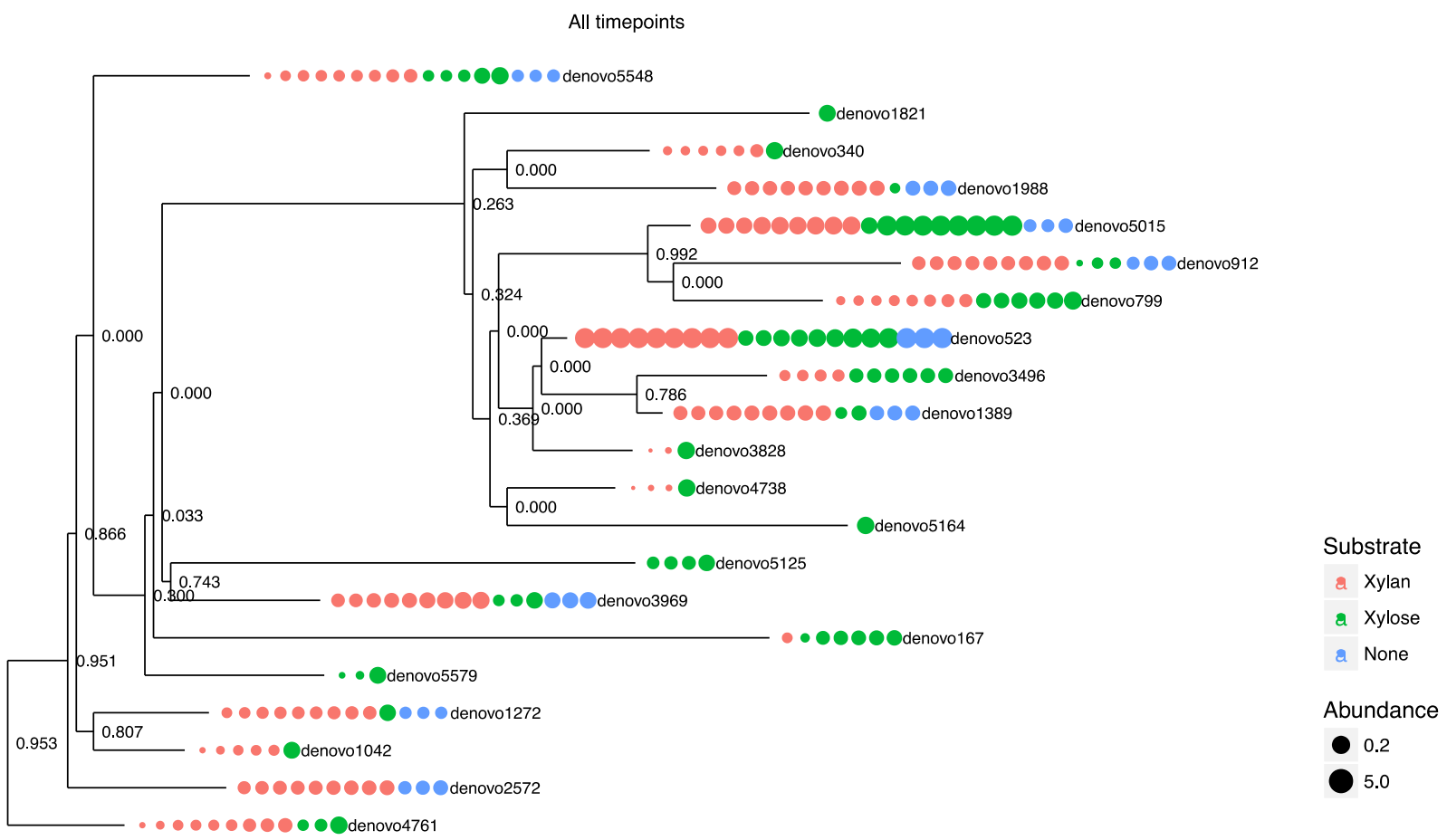

Figure 43 Phylogenetic tree analysis of Pseudoalteromonas denovo OTUs

Phylogenetic tree of denovo *Pseudoalteromonas* OTUs at 99.8% similarity. Denovo sequences were Fasttree method was used for tree building.

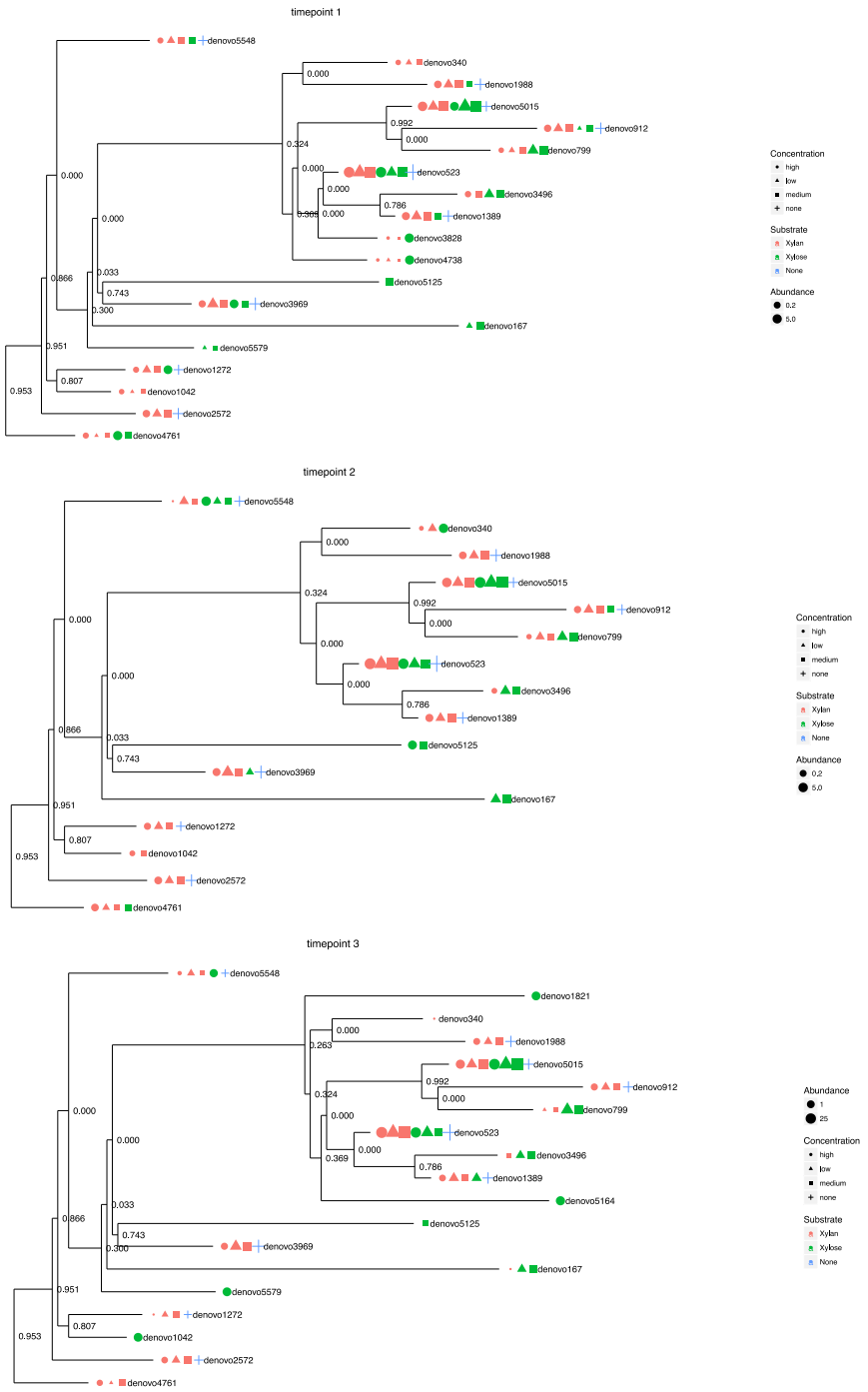

Figure 44 Phylogenetic tree analysis of Pseudoalteromonas denovo OTUs at each timepoint

Phylogenetic tree of denovo *Pseudoalteromonas* OTUs at 99.8% similarity. Denovo sequences were Fasttree method was used for tree building.

Chapter 4 Bacterial dominate lignin degradation via the phenylacetyl-CoA pathway in the Eastern Mediterranean Sea

Hannah L. Woo[1] and Terry C. Hazen[1,2,3,4]

[1]Civil and Environmental Engineering, University of Tennessee;

[2]Microbiology, University of Tennessee;

[3]Earth and Planetary Science, University of Tennessee

[4]Biosciences Division, Oak Ridge National Laboratory

Corresponding Author: Terry C. Hazen

507 SERF

University of Tennessee

Knoxville, Tennessee 37996-1605

Phone: 865-974-7709

E-mail: tchazen@utk.edu

Author Contributions

Hannah L Woo conceived and designed the experiments, performed the experiments in the lab, analyzed the data, and wrote the paper. Terry C Hazen also conceived and designed the experiments.

Submitted to ISMEJ

Abstract

The degradation of allochthonous terrestrial organic matter, such as recalcitrant lignin and hemicellulose from plants, occurs in the ocean. We hypothesize that bacteria instead of white-rot fungi, the model organisms of aerobic lignin degradation within terrestrial environments, are responsible for lignin degradation in the ocean due to the ocean's oligotrophy and hypersalinity. Warm oxic seawater from the Eastern Mediterranean Sea was enriched on lignin in laboratory microcosms. Lignin mineralization rates by the lignin-adapted consortia improved after two sequential incubations. Shotgun metagenomic sequencing detected a higher abundance of aromatic compound degradation genes in response to lignin, particularly phenylacetyl-CoA, which may be an effective strategy for marine microbes in fluctuating oxygen concentrations. 16S rRNA gene amplicon sequencing detected a higher abundance of *Gammaproteobacteria* and *Alphaproteobacteria* bacteria such as taxonomic families *Idiomarinaceae, Alcanivoraceae, and Alteromonadaceae* in response to lignin. Meanwhile, fungal *Ascomycetes* and *Basidiomycetes* remained at very low abundance. Our findings demonstrate the significant potential of bacteria and microbes utilizing the phenylacetyl-CoA pathway to contribute to lignin degradation in the Eastern Mediterranean where environmental conditions are unfavorable for fungi. Since very little is known about the biodiversity of bacterial lignin degraders, they may yield efficient lignin degrading enzymes for lignocellulosic biofuels.

Introduction

Terrestrial organic carbon cycling in the ocean occurs at significant rates despite most terrestrial organics being thermodynamically stable carbon sources such as cellulose, hemicellulose, and lignin of the plant cell wall (Hedges et al., 1997). About a third of the allochthonous organic carbon in the ocean entering through riverine input is found buried in the sediment (Burdige, 2005). The rest is putatively degraded within the water column. Of the many biogeochemical factors affecting terrestrial organic carbon utilization like photooxidation (Opsahl and Benner, 1998; Hernes, 2003; Lalonde et al., 2014), biomineralization by microbes is a significant factor (Fichot and Benner, 2014). We hypothesize that microbes of the open ocean must have efficient enzymes capable of attacking lignocellulose. Since little is known about the diversity of marine lignin degraders, we will identify microbial species tightly associated with lignin amendment using a combination of amplicon and shotgun DNA sequencing.

Few studies have tested for the presence of lignin degradation in the open ocean compared to more inland locations such as mangroves, ocean margins or rivers (Dittmar and Lara, 2001; Laurent et al., 2013; Ward et al., 2013; Fichot and Benner, 2014). The aromatic structure of phenylpropane units in lignin resembles the polyaromatic hydrocarbons originating from ocean seeps, therefore marine microbes could possess aromatic compound catabolism and enzymes such as ring-opening dioxygenases. So far, a link between the lignin and oil has been shown by fungal and bacteria only in isolates in pure culture (Arun and Eyini, 2011; Ohta et al., 2012).

Identifying marine enzymes for lignin degradation would aid the US lignocellulosic biofuel industry since one of the major challenges is enzymatically saccharifying the lignocellulosic biomass. The use of ionic liquids (salt-like solvents) in biomass pretreatment requires enzymes to operate in high ionic strength conditions that decrease efficiency (Turner et al., 2003). Marine enzymes will naturally be halotolerant and retain their conformation better in high ionic strength conditions.

Enzymes from marine microbes also have several practical advantages in addition to halotolerance. First, marine communities have less microbial diversity and species richness than soil, so less sequencing depth is required compared to soil communities. Second, the ocean's oligotrophy may select against fastidious fungi and allow bacteria to subsist on lignin. The extreme nutrient limitation of the ocean may trigger the secondary metabolism for microbes that is frequently associated with lignin degradation. Much less is known about bacterial lignin degradation despite bacteria being more amenable for commercial enzyme production (Brown and Chang, 2014) .

In this study, we will elucidate the microbial diversity of hemicellulose and lignin-adapted Eastern Mediterranean seawater using sequencing. Our consortia were originally sampled from the warm surface waters of the Eastern Mediterranean Sea. The Eastern Mediterranean (E.Med) is extremely oligotrophic particularly in phosphate, hypersaline, and well oxygenated even at bottom depths (Techtmann et al., 2015). All microcosms are aerobic because oxygen is not limiting in this ocean basin.

Sequencing substrate adapted consortia for microbial diversity insight is a common experimental approach when investigating the microbial degradation of lignocellulose (DeAngelis et al.,

2010). Lignin is challenging to quantify and characterize in environmental samples (Hatfield and Fukushima, 2005). A potential pitfall with a cultivation independent approach is that low levels of other carbon sources may serve as preferred labile carbon source that drastically affect community structure. To address the possibility of contaminant sources within our lignin directly, our experimental design includes a "contaminant carbon source" control of the hemicellulose polymer xylan, the most likely contaminant carbon source on the purified lignin used in this study. If we demonstrate that the lignin-adapted and xylan-adapted consortia have different community and functional profiles then the microbes in the lignin-adapted consortia are not utilizing the hemicellulose residues and are more likely utilizing lignin.

We utilize 16S rRNA gene amplicon sequencing and shotgun metagenomics to characterize the shifts in community structure and functional gene structure. Carbon dioxide production and oxygen utilization will be monitored during the enrichment for mineralization rates. Bacterial strains with exceptional ability to degrade lignin or xylan may be candidates for large-scale enzyme production. It is unclear how widely the ability to degrade terrestrial organic carbon is distributed amongst marine microbes. It may identify new species rarely studied for lignocellulose degradation or recalcitrant organic carbon cycling.

Material and Methods

Lignin and Xylan amended enrichments of Eastern Mediterranean Seawater

The seawater for enrichment culturing was collected in Niskin bottles at 50 m below the surface of the Eastern Mediterranean Sea, off the coast of the Nile Delta. The details of the sampling cruise are described by Techtmann et al. (Techtmann et al., 2015). Organosolv lignin for the enrichments was provided by Dr. Nicole Labbe of the University of Tennessee Center for Renewable Carbon. The Organosolv lignin was isolated at 140˚C for 90 min from switchgrass using a solvent mixture of Methyl Isobutyl Ketone/Ethanol/Water with 0.05M H_2SO_4. The fractionation method is similar to the control run described by Tao et al. (Tao et al., 2016). The Organosolv lignin would have had residual quantities of xylan still attached, less than 3% of the weight on a dry basis.

For the first enrichment "Microcosm 0", 60 mL of seawater were first enriched aerobically, in the dark, at 19°C on Organosolv lignin with an extra 1.5mM phosphate for 2 wk. The bottle was constantly shaked at 200 rpm to allow proper aeration and mixing of the insoluble lignin. After the 2 wk incubation, the lignin enrichment continued by creating the next lignin enrichment, "Lignin Microcosm I", where 1 mL of "Microcosm 0" was transferred to artificial seawater (ONR7a Medium pH 8.2 (Atlas, 2010) without bactopeptone, vitamins and trace elements) amended with 0.05% weight to volume of Organosolv lignin. In a likewise fashion, "Microcosm 0" was also transferred to xylan as a sole carbon source for the first xylan enrichment, "Xylan Microcosm I". Enrichments were created in duplicate and incubated for another 120 h. After the 120 h incubation, the enrichments were used to inoculate a fresh 0.05% loading of substrate and fresh ONR7a media for "Lignin Microcosm II" and "Xylan Microcosm II" and incubated for another 150 h. Figure 45 conceptually diagrams the experimental design (Figure 45).

Respirometry

During the incubation, carbon dioxide production was regularly monitored every 3 hours using a MicroOxymax respirometer (Columbus Instruments Columbus, Ohio). For the unamended controls of artificial seawater media only and abiotic controls of substrate-amended consortia, the cell inoculum in media was re-sterilized by autoclaving for 1 h, filtering through a 0.2 µm filter, and then inhibited from respiring using sodium azide before adding substrate.

DNA extraction

DNA was extracted from the lignin, xylan, and unamended enrichments. After the incubation, all particulates and cells were harvested into pellets by high speed centrifugation. DNA was extracted from each of the pellets using a ZR-Duet™ DNA/RNA MiniPrep Kit (Zymo Research Irvine, CA) following the manufacturer's instructions. DNA was cleaned of any contaminants using a OneStep™ PCR Inhibitor Kit (Zymo Research Irvine, CA) and then concentrated using a Genomic DNA Clean and Concentrate Kit (Zymo Research Irvine, CA). DNA was prepared into 2 libraries, one for 16s rRNA gene amplicon sequencing and the other for metagenomics.

Metagenomics

The functional gene structure of the enrichment was characterized using shotgun metagenomics. DNA libraries were prepared using the Nextera XT DNA Library Prep (Illumina San Diego, CA) kit following the manufacturer's instructions. The tagmentation and amplification was verified using a Bioanalyzer High Sensitivity chip (Agilent Santa Clara, CA). The quantity was determined using KAPA qPCR (Kapa Biosystems Wilmington, MA). Libraries were normalized by concentration and sequenced on the Illumina MiSeq sequencing platform using a 2x300 basepair kit. Unassembled reads were uploaded onto MG-RAST for automated annotation (Meyer et al., 2008). SEED subsystems annotation that possess 4 nested categories of functions was downloaded for analysis in the R package *DESeq2* (Love et al., 2014) and visualization using *ggplot2* (Wickham, 2009). Taxonomy was derived from the "representative hit classification" of the MG-RAST annotation using the M5NR database with max e-value cutoff of 10^{-5}, minimum identity cutoff of 60%, and minimum alignment length cutoff of 15.

16S rRNA gene amplicon sequencing

The microbial community structure and diversity was characterized using 16S rRNA gene amplicon sequencing. Sequencing libraries from the DNA were prepared, purified and quantified using the methods described in Techtmann et al (Techtmann et al., 2015). Once all libraries were multiplexed into a single sample, the sample was sequenced on an Illumina MiSeq sequencing platform using methods developed by Caporaso et al (Caporaso et al., 2012). The resulting 2x150 basepair Illumina reads were joined, demultiplexed, and annotated using an open picking method against the Greengenes database using Qiime (Caporaso et al., 2010). All OTUs were chimera checked before exporting into R for additional statistics and visualization using R packages *vegan* (Dixon and Palmer, 2003), *phyloseq* (McMurdie and Holmes, 2013), and *DESeq2*.

The OTU table was rarefied before alpha and beta diversity analysis using R packages *vegan* and *phyloseq*. Taxa bar plots were created also using *phyloseq*. *DESeq2* was used on the OTU abundances without any normalization as per the R package's instructions. The differential abundance of OTUs between lignin (n=2) and xylan amended microcosms (n=2) were using a local fitting. Indicator species of the 3 treatments of lignin, xylan and the control were determined using the R package *labsvd indval* function (Roberts, 2007).

Results

Mineralization of lignin and xylan as measured by carbon dioxide production

The mineralization rates of lignin to CO_2 by the microbial consortia increased with each transfer to fresh lignin and defined medium. The microbial consortia mineralization rates on hemicellulose were higher than on lignin, which suggests that hemicellulose is a more labile carbon source to the marine microbes. Residuals of hemicellulose attached to the lignin cannot be considered negligible. Other experimental controls such as an unamended control and abiotic control did not produce significant amounts of carbon dioxide. As expected of oxic cultures, a significant amount of oxygen was consumed by the substrate adapted consortia. The oxygen uptake (Figure 46) strongly correlated linearly with the carbon dioxide accumulation.

The xylan- and lignin-adapted consortia produced similar amounts of carbon dioxide during the first incubation of approximately one week. Both types of consortia produced about 2,500 µg of carbon dioxide within the first 120 h (Figure 47a) after a lag phase of 53 h of very low respiration. The next incubation took place immediately after the first incubation. A 1.6% inoculum of the first substrate-amended consortium was used to inoculate fresh substrate in fresh artificial seawater media. The second xylan-adapted consortia produced 12,000 µg of carbon dioxide within 150 h, which is nearly 5 times more carbon dioxide than the first consortia (Figure 47b). The second lignin-adapted consortia also improved in mineralization rate but not as greatly as the xylan-adapted consortia. The lignin enrichment produced about 4000 µg, which was nearly twice as much as the first incubation. In contrast to the first incubation, the second incubation of both substrates had a very brief lag phase. Approximately 0.3% of the lignin and 0.5% of the xylan was mineralized during the first incubation. More substrate was mineralized into CO_2 during the second incubation; 0.5% of the lignin and 2.5% of the xylan was mineralized.

Shifts in functional gene structure

The functional gene structures of the enrichments were characterized by shotgun metagenomes using the Illumina MiSeq. The unassembled reads were annotated by the automated MG-RAST pipeline (Table 8). Of the available annotations, the SEED Subsystems annotation was utilized for its hierarchical organization. The samples were compared in a Non-metric Multidimensional Scaling (NMDS) plot using Bray Curtis distance (Figure 48) at their finest level of functional annotation, which consisted of 4663 different functions. The first and second incubations of the lignin were more similar to each other than the incubations with xylan. The 2 incubations of the unamended control were very different.

The differential abundance of functional genes between the 2 xylan-amended consortia and the 2 lignin-amended consortia were analyzed using the negative binomial modeling of *DESeq2*. Positive $\log_2$-fold-changes indicated a greater abundance in the xylan amended microcosm. Calculated $\log_2$-fold-changes ranged from -0.6743 to 0.3077.

The functions associated with carbohydrates and aromatic compound catabolism were the most differentially abundant categories (Figure 49). The abundance of carbohydrate metabolism functions was higher in the xylan-amended microcosms. The average $\log_2$-fold-changes of the

1057 carbohydrate functional genes (Figure 50) were 0.245. Meanwhile, the lignin-amended microcosms had more aromatic catabolism genes. 237 genes of the aromatic compound metabolism category were on average -0.268.

Nearly all subcategories of genes related to carbohydrates were more abundant in the xylan-adapted consortia (Figure 51). Among the subcategories of genes in identifiable groups of functions related to carbohydrates, the polysaccharides, glycoside hydrolases, di- and oligosaccharides, monosaccharides were the most differentially abundant groupings. The only ones that were more abundant in the lignin-adapted consortia were the organic acids.

For the aromatic metabolism genes, functions that were more abundant in the lignin-adapted consortia were phenylacetyl-CoA catabolism pathway (Figure 52). Phenylpropanoid compound degradation is also more abundant in the lignin adapted consortia, which includes genes for vanillate and ferulate metabolism, two potential breakdown products from lignin. The most differentially abundant functional gene was 3,4-dihydroxyphenylacetate 2,3-dioxygenase (EC 1.13.11.15), which is essential for aromatic compound catabolism. Also catechol 1,2-dioxygenase was more abundant in lignin-adapted consortia.

Changes in microbial community composition

The microbial community composition of the lignin-, xylan-adapted and unamended consortia was characterized using 16S rRNA gene amplicon sequencing. DNA from the two replicates of each substrate amended enrichment were pooled before sequencing with an Illumina MiSeq. Using Qiime, all reads were processed into operational taxonomic units (OTUs) and annotated with the Greengenes database (DeSantis et al., 2006). Libraries were normalized by rarefying.

The community structure of the samples was compared by principal coordinate analysis (PCoA) using a weighted Unifrac distance (Figure 53a). The lignin- and xylan- adapted consortia were distinct communities. The two incubations of each substrate were similar in community while the two incubations of the control were different. The controls were likely very different between the incubations because of richness (Figure 53b). The substrate amended consortia had less observed OTUs than the controls. The control at the first timepoint had the highest number of distinct OTUs, nearly 350, while the second timepoint had less than half. The Shannon index which considers evenness in addition to richness indicates a decreasing trend for lignin-adapted consortia but an increasing trend for xylan-adapted consortia over time. Together these results indicate that a subset of species became dominant in the lignin-adapted consortia. Meanwhile, species became more evenly distributed within the xylan-adapted consortia.

The microbial communities of the unamended microcosms and xylan-adapted consortia were compared on 3 different levels of taxonomy: phylum, class and order. Rare OTUs with less than 1% of reads were excluded from visualization. At the phylum level, we observed more *Bacteroidetes, Planctomycetes, Acidobacteria and Actinobacteria* in the unamended and hemicellulose controls (Figure 54). Meanwhile, the lignin adapted consortia consisted mostly of *Proteobacteria* and some *Bacteroidetes*. Of the most abundant classes (Figure 55), *Gammaproteobacteria* increased in the lignin microcosms but decreased in the xylan microcosms. Of the *Gammaproteobacteria*, *Oceanospiralles* was the most dominant taxonomic family but found ubiquitously in all treatments (Figure 54). *Alphaproteobacteria*, particularly

the order *Kiloniellales*, increased in the xylan amended microcosms (Figure 54). *Flavobacteria* is important in xylan microcosms after the last incubation, particularly the genus *Salegentibacter* (Figure 54).

Archaea were very low in abundance despite being a dominant population contributing to ammonia oxidation in natural Eastern Mediterranean Seawater (Techtmann et al., 2015). Archaea were only present in the first unamended control (Figure 54). The orders *Nitrososphaerales* and *Cenarchaeales* of the phylum *Thaumarcheota* were the most abundant archaeal taxa in the first unamended control. Archaea were less than 0.1% in lignin-adapted and xylan-adapted consortia. The decrease in Archaea abundance corroborates other studies in the Eastern Mediterranean where Archaea became rare upon amendment of additional carbon (manuscript in preparation).

Fungi, like Archaea, were very low in abundance in the samples. Fungi were characterized using shotgun metagenomic unassembled reads. The fungal reads totaled less than 0.04% of any of the substrate-adapted or control metagenomes (Table 9). *Ascomycetes* were 0.04% or less; *Basidiomycetes* were 0.01% or less. In contrast, *Proteobacteria*, *Bacteroidetes*, *Actinobacteria* and *Firmicutes* constituted the majority at 97.98% of the total reads in the data set (Table 9). The most abundant *Ascomycetes* and *Basidiomycetes* were *Nectricia*, *Trichocomaceae*, *Debarymycetaceae*, *Ustilaginaceae*, *Schizosaccharamycetaceae*, *Sordariaceae* families (Figure 56).

Potential lignin-degrading species in lignin-adapted consortia

Differential abundance analysis was used to determine which taxa increased with lignin and hemicellulose amendment. The analysis was conducted using the R package *DESeq2*. Rare phyla with less than 0.005% relative abundance were excluded from further analysis. The shotgun metagenome captured a broad diversity of organisms including bacteria, fungi, archaea, plants and other larger eukaryotes. The phyla of invertebrates or vertebrates were excluded from the analysis.

More bacterial phyla than fungal phyla increased in response to lignin. The differences between the lignin-adapted consortia and the controls were small, only up to 0.6 $\log_2$-fold-change different. Phyla *Elusimicrobia*, *Synergistetes*, *Deferribacteres*, *Chrysiogenetes*, *Firmicutes*, *Thermotogae*, *Spirochaetes*, *Korarchaeota*, *Proteobacteria*, *Deinococcus-Thermus*, *Basidiomycota*, *Gemmatimonadetes*, *Tenericutes*, *Fusobacteria*, and various unclassifiable groups were found in higher abundance in the lignin-adapted consortia compared to xylan-adapted consortia or the unamended control (Figure 57). Two fungal phyla with white rot fungi, *Ascomycota* and *Basidiomycota*, were very low in relative abundance and were in more similar abundances between the controls and lignin-adapted consortia than Bacteria. *Ascomycota* was found in slightly higher abundance in hemicellulose and unamended controls, while *Basidiomycota* was slightly higher in the lignin adapted consortia. Among the families of the phyla that increased in response to lignin, *Idiomarinaceae* and other *Proteobacteria* were the most differentially abundant (Figure 58). Only two fungal families, *Ustilaginaceae* and *Trichocomaceae* were more abundant in the lignin-adapted consortia but did not increase as much as *Idiomarinaceae* or other *Proteobacteria*.

Indicator value of the taxa detected in the 16S rRNA gene amplicon data considers the fidelity and relative abundance of a taxa for lignin instead of log fold changes. *Caulobacteraceae, Colwelliaceae, Rhodocyclaceae, Oxalobacteraceae, Pseudoaltermonadaceae, Idiomarinaceae, Alcanivoraceae, Oceanospirallaceae, Erythrobacteraceae*, and *Clostridicaeae* had indicator values greater than 0.5, with 1.0 being the maximum possible value (Figure 59). In contrast, some families such as *Alteromonadaceae, Piscirickettsiaceae, Halomonadaceae*, and *Hyphomicrobiaceae* were ubiquitous in all consortia regardless of carbon source.

Discussion

The research objective was to discover the diversity of marine microbes from the Eastern Mediterranean Sea that are capable of degrading lignin and thereby potentially contributing to allochthonous terrestrial organic matter cycling. We believed oligotrophic and hypersaline marine microbial communities can provide insight into the untapped diversity of bacteria with efficient degradative enzymes for lignin. Evidence of increasing mineralization rates on lignin, changes in microbial community structure, and increases in abundance of aromatic catabolism gene abundance support the notion of the Eastern Mediterranean seawater possessing high potential for lignin degradation.

The lignin mineralization rates by the Eastern Mediterranean microbial consortia improved with transfers due to changes in the microbial community. The mineralization rates in the lignin-amended consortia nearly doubled between the first and second incubation. The mineralization rate at the end of the second incubation had not leveled off, indicating the potential to produce more carbon dioxide with more time. Abiotic causes could not have improved mineralization since the lignin and the defined media were fresh at each transfer and the incubation conditions remained constant. From the metagenome and 16S rRNA gene amplicon sequencing, the microbial community structure became less diverse between transfers on lignin as expected of substrate adapted consortia over time (DeAngelis et al., 2010). The alpha diversity shows decreasing species richness and less evenness in the lignin-adapted consortia.

Shifts in bacterial populations, rather than fungal, caused the increase in lignin mineralization rates. *Gammaproteobacteria* was the most abundant class of microorganism overall. Multiple taxonomic families of *Gammaproteobacteria* bacteria, such as the mesophilic and halophilic *Idiomarinaceae*, increased in abundance in the presence of lignin compared to the controls. Meanwhile, fungi remained low and static in abundance in all consortia from the Eastern Mediterranean. Among the few fungal taxa that were identified, *Basidiomycetes* slightly increased in the presence of lignin, while *Ascomycetes* slightly decreased. Relative abundance of *Ascomycetes* was slightly higher than *Basidiomycetes* in general. Fungi in deep-sea environments are rare and low in diversity in another cultivation independent study (Bass et al., 2007). Few marine white-rot basidiomycetes have been described in the literature, with much of the knowledge about lignocellulose marine fungi being from mangroves (Pointing and Hyde, 2000). Studies comparing bacterial and fungal impact on lignocellulose degradation in salt marsh sediment showed bacteria were dominant degraders of detritus (Benner et al., 1984).

Despite the improvements in mineralization rate, the Eastern Mediterranean consortia likely do not degrade lignin as quickly as white-rot fungi in pure culture. Under specific optimized conditions a soil basidiomycete white-rot fungus, *Phaenerochyte chrysosporium*, has been shown to mineralize 1% of a radiolabeled synthetic lignin into carbon dioxide every 24 h (Boyle et al., 1992). However, *P. chrysosporium* is an exceptional case as other white-rot fungal strains from marine environments have also been tested with radiolabeled lignin and had much lower mineralization rates, less than 5 % in 60 days (Sutherland et al., 1982).

Based on the functional gene structure of the lignin-adapted consortia, aerobic lignin degradation could occur via CoA thioesters instead of the dioxygenase-dependent Beta-ketoadipate pathways. The aromatic catabolism pathway with a phenylacetate CoA intermediate increased

the most after the amendment of lignin. The phenylacetyl-CoA pathway is considered an alternate to the more classical and well- studied Beta-ketoadipate pathways for aerobic aromatic catabolism (Ismail and Gescher, 2012). Unlike phenylacetyl-CoA, Beta-ketoadipate has been studied in relationship to lignin degradation in multiple bacterial strains (Bugg et al., 2011a), where peripheral pathways produce protocatechuate or catechol intermediates that are further degraded using ring-cleaving dioxygenases (Fuchs et al., 2011). CoA thioester pathways, in contrast, form non-aromatic ring-epoxide that may have several advantages in the marine environment (Fuchs et al., 2011). CoA thioesters are better retained by the cell which may be crucial in oligotrophic environments where more efficiency strategies are needed to survive. Also, CoA thioesters can enter both aerobic and anaerobic pathways allowing facultative anaerobic microbes to be flexible in fluctuating oxygen or low oxygen conditions. Phenylacetyl-CoA has not been extensively studied in connection with lignin but may be an important mechanism in lignin transformation in the ocean.

Our findings with hemicellulose demonstrate the utility of controls when heavily relying on cultivation independent techniques. The lignin-adapted and hemicellulose-adapted consortia had different functional gene abundances for key functions of aromatic and carbohydrate utilization. It is unlikely that we have a dominant hemicellulose degrading population within the lignin amended consortia, which is an important distinction since lignin is often tightly complexed with hemicellulose and cellulose even after chemical isolation. We observed much higher mineralization rates with hemicellulose than lignin. Hemicellulose may be preferentially utilized over lignin if both carbon sources are present, causing the community to become adapted for hemicellulose degradation. Combining the proper controls with ‘omics techniques will allow targeted studies into the biodiversity of lignin degradation in complex microbial communities.

In conclusion, the Eastern Mediterranean seawater microbial consortium utilized lignin as a sole carbon source in a defined media. *Gammaproteobacteria* dominated the lignin-adapted community structure rather than the white-rot fungi typically studied for lignin degradation in terrestrial environments. Bacteria may be the dominant lignin degrading species in open ocean environments. Genes corresponding to phenylacetyl CoA aromatic catabolism pathways increased in abundance the most after lignin amendment. Phenylacetyl CoA may be an effective strategy for marine microbes to utilize lignin in fluctuating oxygen conditions. Only one concentration of substrate was tested in this experiment. Recent evidence has shown that the low concentration rather than the structure of organic compounds in the ocean limit degradation rates (Arrieta et al., 2015). In the future, various concentrations should be tested to see if the microbial response is concentration dependent. Insight into the biodiversity of bacterial lignin degradation provides basic scientific knowledge into obtaining effective, salt-tolerant, and cheaper commercial lignin-degrading enzymes for industry and a systems-level understanding of carbon cycling in the ocean.

Acknowledgements

This material is based upon work supported by the National Science Foundation Graduate Research Fellowship Program under grant no. DGE-1452154. The authors thank Dr. Nicole Labbe from the University of Tennessee Center of Renewable Carbon for providing the purified Organosolv lignin. Also, the authors thank Dr. Stephen Techtmann and Julian Fortney for providing the seawater sample from their research cruise.

Conflict of Interest

The authors declare no conflict of interest.

Appendix C: Figures and Tables

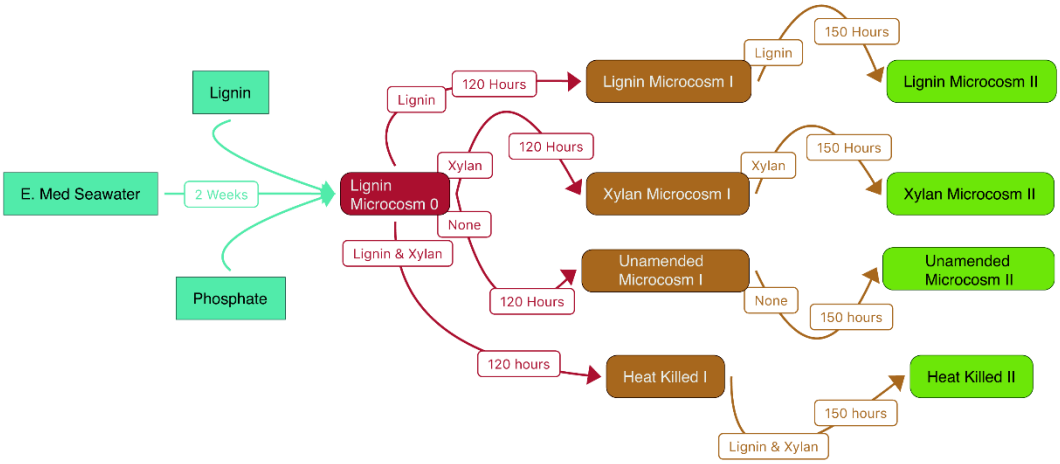

Figure 45 Experimental Design

The arrows indicate the inoculation of each substrate-adapted consortia. White Boxes on top of the arrow are the substrates amended in the microcosm and the length of the incubation.

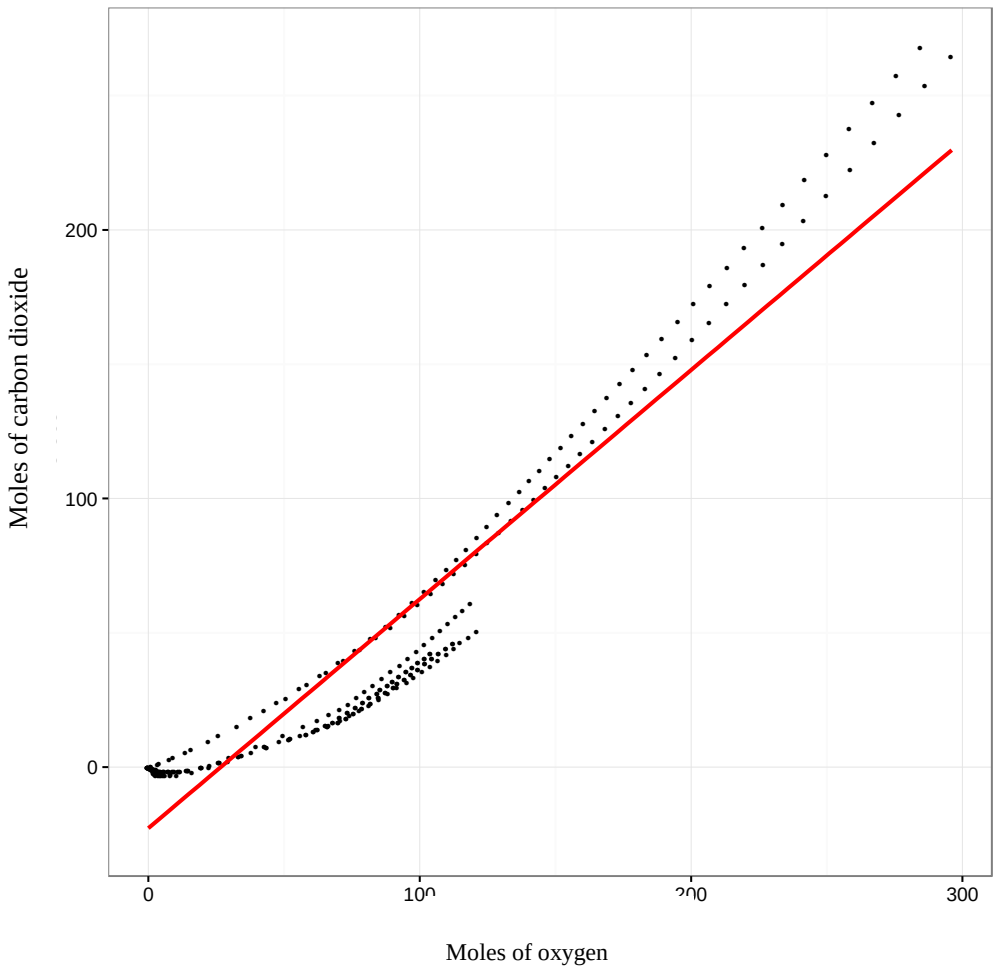

Figure 46 Regression of carbon dioxide and oxygen accumulation within xylan and lignin amended microcosms

The MicroOxyMax Respirometer monitored both carbon dioxide and oxygen accumulation in the xylan- and lignin amended microcosms. Carbon dioxide was positively correlated with oxygen utilization. A linear fit of the carbon dioxide and oxygen accumulation in moles had a high R-square of 0.90 and significant p-value less than 0.001.

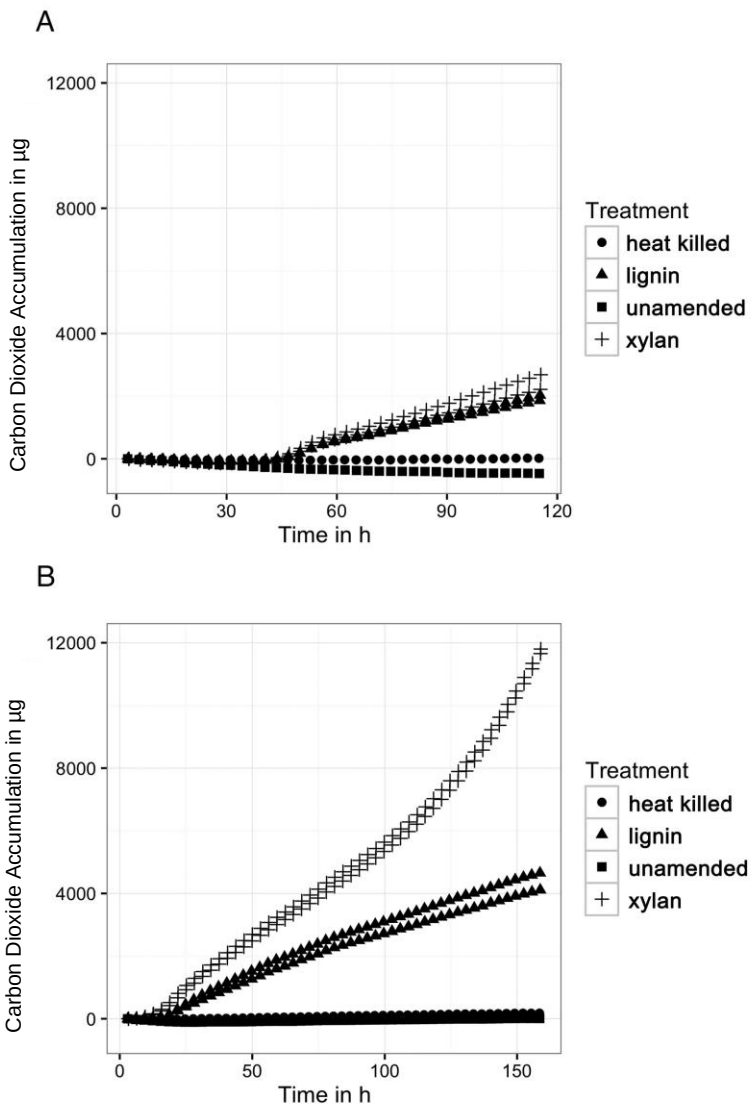

Figure 47 Carbon dioxide production

A) Carbon dioxide production from the first incubation of xylan and lignin The MicroOxyMax respirometer monitored carbon dioxide accumulation in the head space of the three different treatments: the xylan-amended seawater microcosms (n=2), lignin-amended seawater (n=2), unamended control (n=1), and abiotic control (n=1). **B) Carbon dioxide production from the second xylan and lignin incubation** The first xylan and lignin incubation was transferred to fresh media and substrate for a second incubation. The Microoxymax monitored carbon dioxide accumulation again.

Table 8 Metagenome sequencing results and accession numbers on MG-RAST

	Sequences*	%GC*
Lignin Microcosm I	5.20E+05	55
Lignin Microcosm II	9644143	56
Unamended Microcosm I	4.14E+06	55
Unamended Microcosm II	2.94E+06	57
Xylan Microcosm I	7.92E+06	55
Xylan Microcosm II	3879881	53

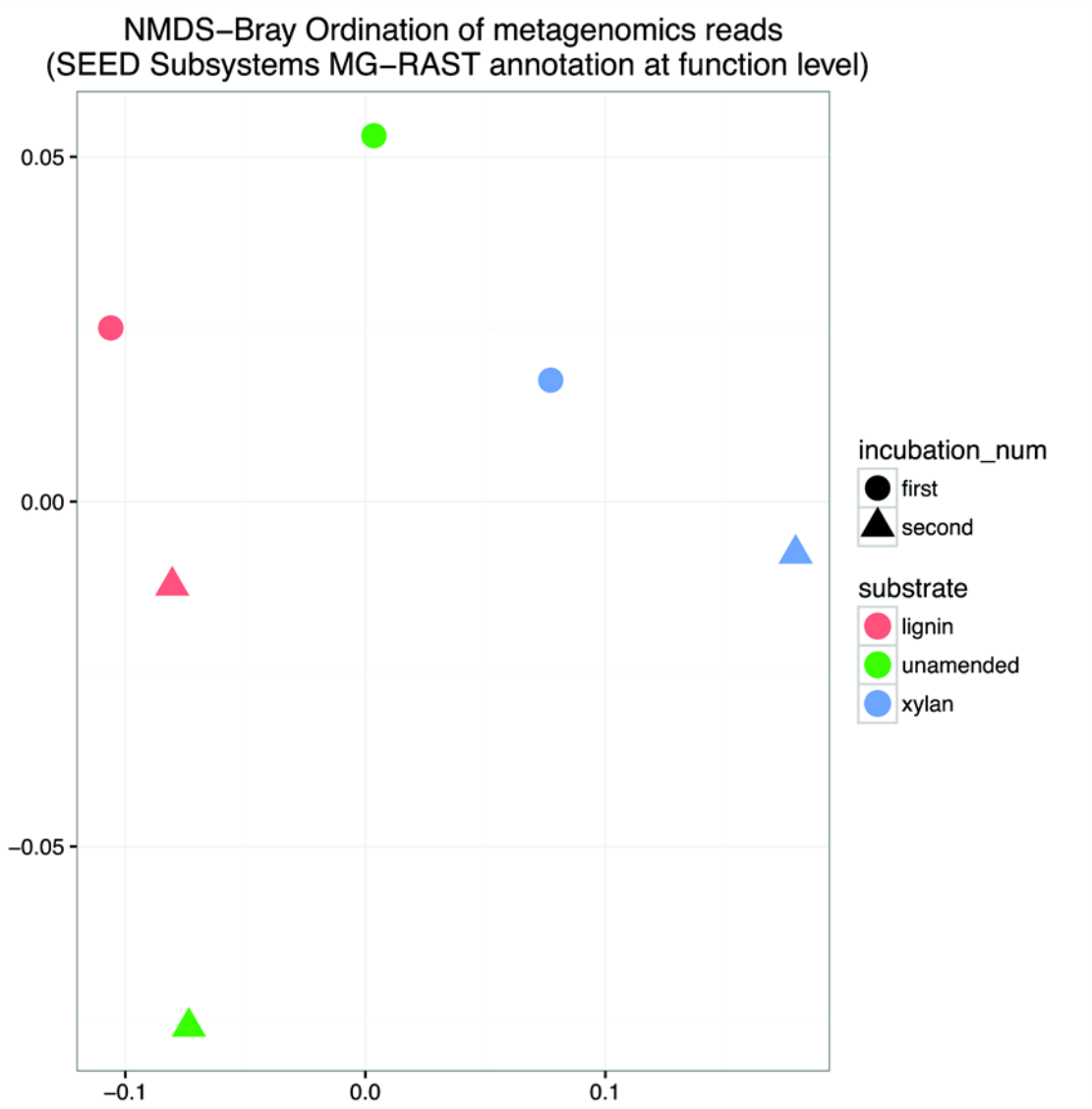

Figure 48 Non-metric Multidimensional Scaling (NMDS) Bray Ordination of functional gene structure

Functional genes were characterized by shotgun DNA sequencing and compared using Bray distance before NMDS. Stress was 3.25×10^{-14}. The substrate is indicated by the color of the point in the ordination plot: red for lignin, green for unamended, blue for xylan. The incubation is indicated by the shape of the point: circles for the first incubation, triangles for the second incubation.

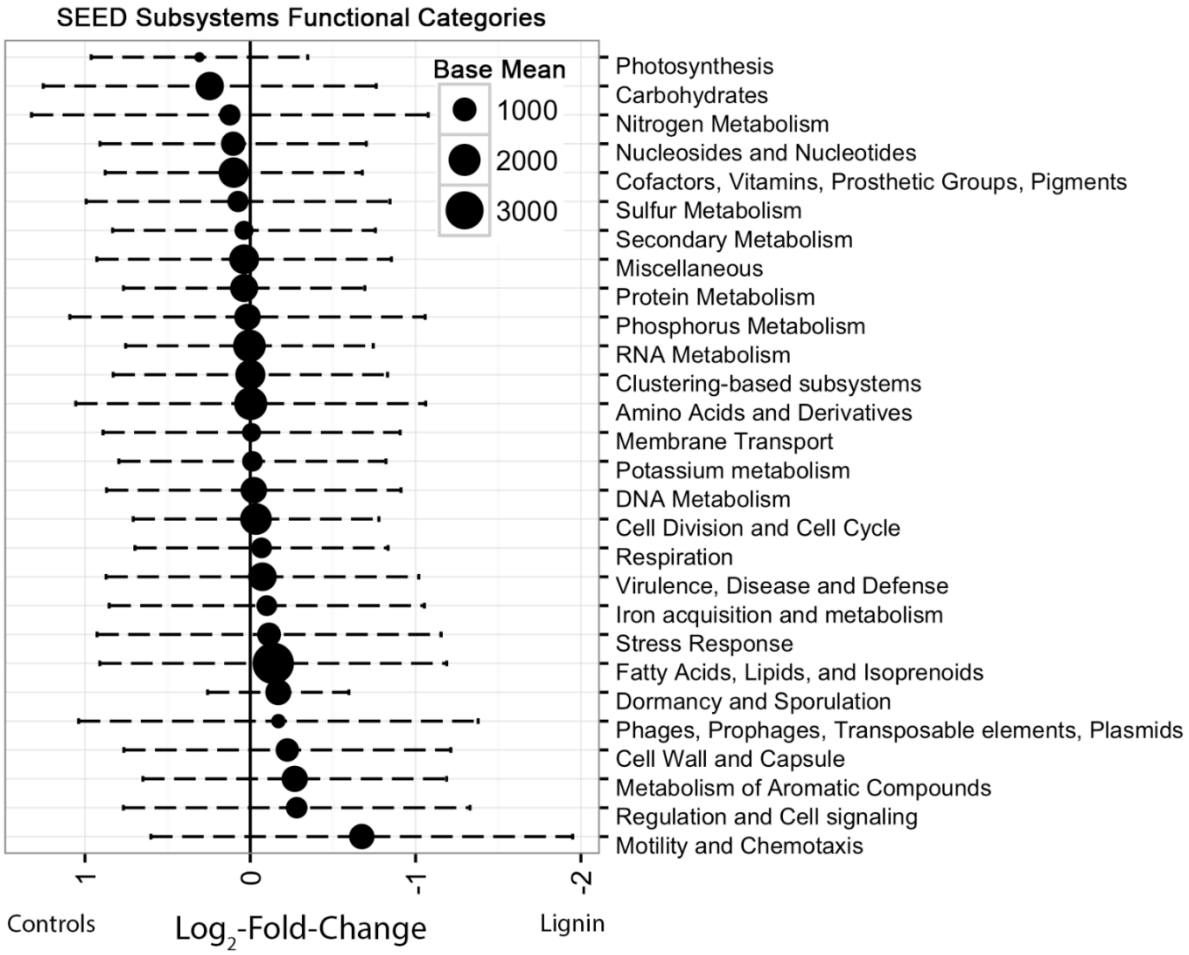

Figure 49 Average $\log_2$-fold change of differentially abundant functional categories between lignin and control microcosms

The log-fold change was determined by R package, DESeq2. Categories are based on SEED Subsystems annotation. Positive $\log_2$-fold change indicates functions in higher abundance in xylan-amended and unamended microcosms. Negative $\log_2$-fold change indicates functions in higher abundance in lignin-amended microcosms. Error bars represent the standard deviation. The size of the point indicates the normalized relative abundance of the functional category.

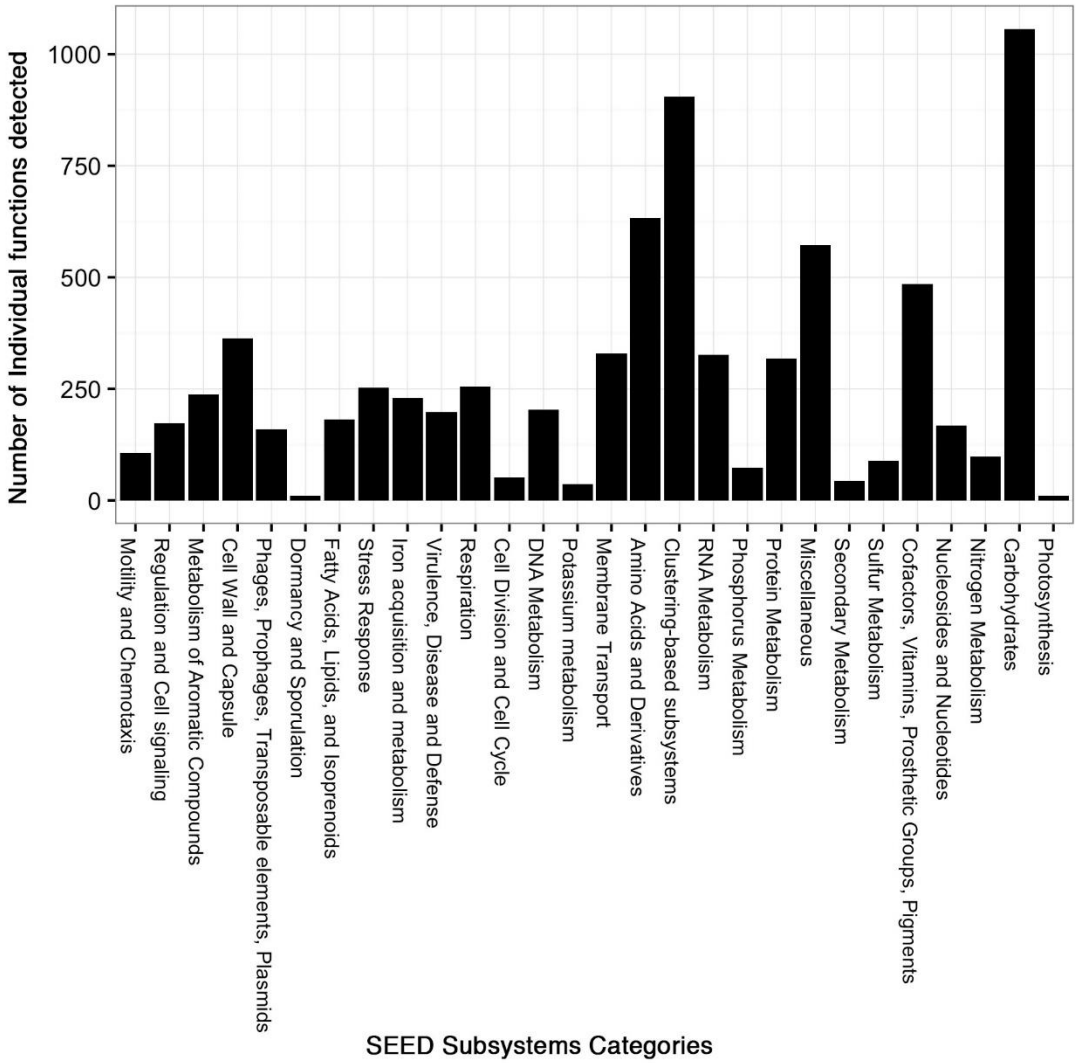

Figure 50 Number of detected functional genes in all metagenomes per SEED Subsystems category

Categories shown corresponding the broadest level of categorization by the SEED Subsystems curated database. Individual functions are the finest level of categorization. The height of bars indicates the number of distinct individual functions detected.

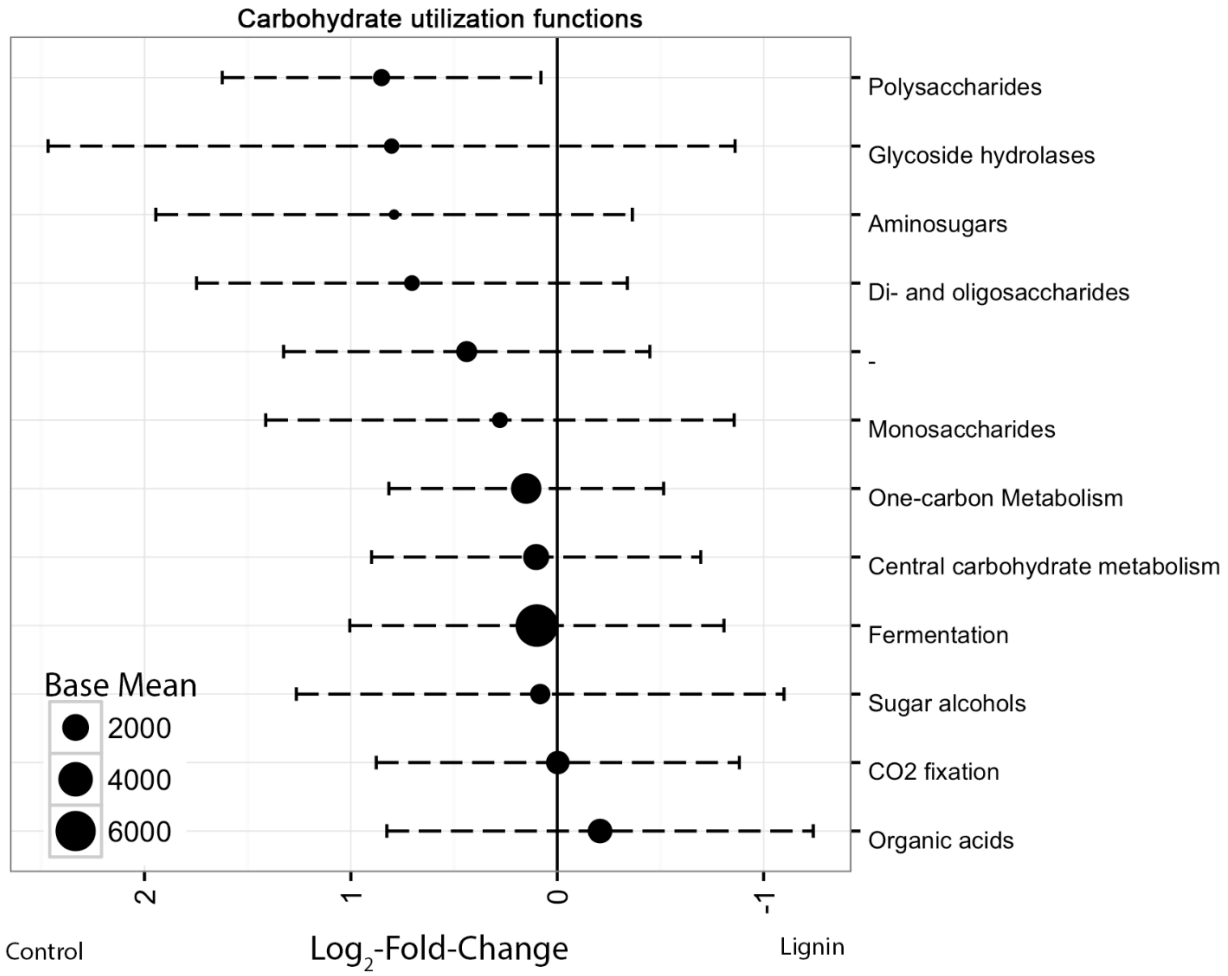

Figure 51 Average log_2-fold change of differentially abundant carbohydrate catabolism related functions between lignin and control microcosms

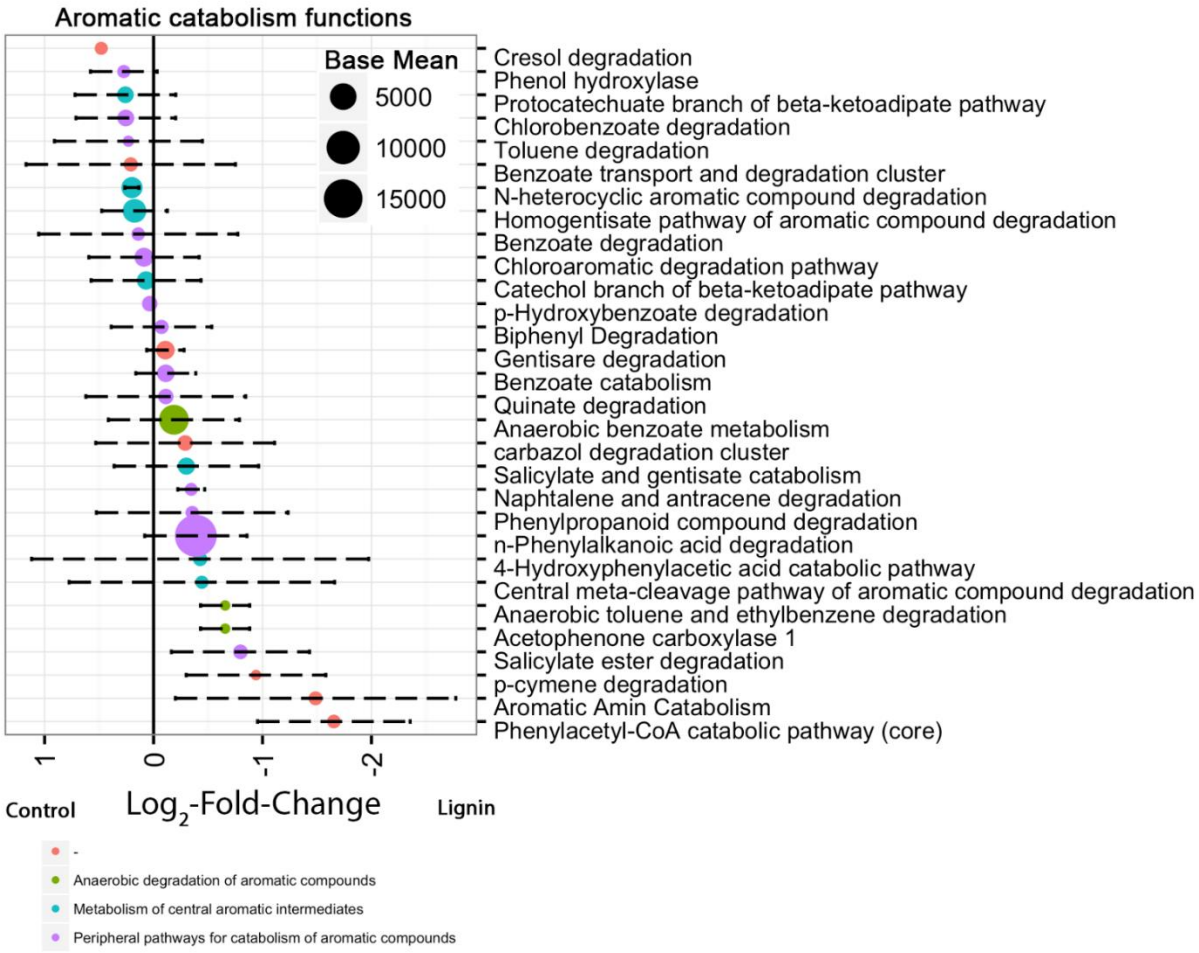

Figure 52 Average log_2-fold change of differentially abundant aromatic catabolism related functions between lignin and control microcosms

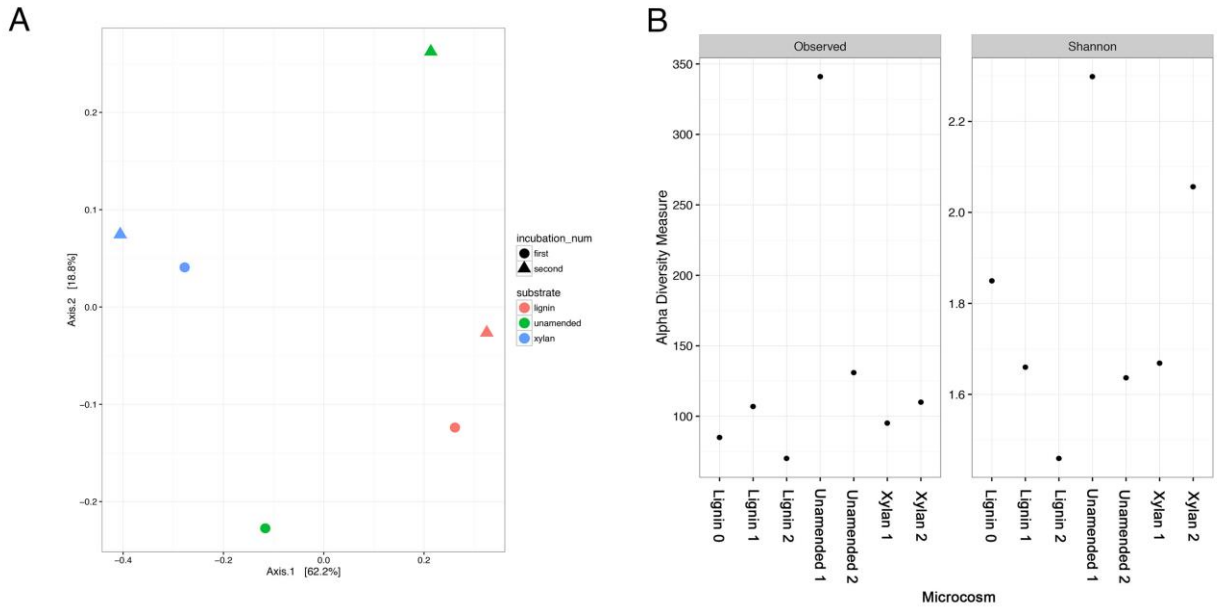

Figure 53 Beta-diversity and Alpha-diversity

A) Principal Coordinate Analysis (PCoA) of the microbial community structures from xylan and lignin amended microcosms. The microbial community structures of the microcosms were characterized by 16S rRNA gene amplicon sequencing. Microbial communities were compared using a weighted Unifrac distance before PCoA. The first two axes shown together describe about 80% of the variance between the samples. The incubation is indicated by the color of the point in the ordination plot: pink for the earlier incubation, turquoise from the latter. The amended substrate is indicated by the shape of the point: circles for lignin, squares for xylan, and triangles for controls with an added carbon source. B) Alpha diversity of the microbial community structure from xylan and lignin microcosms using observed number of species and Shannon diversity index. All indices were calculated using the phyloseq package in R.

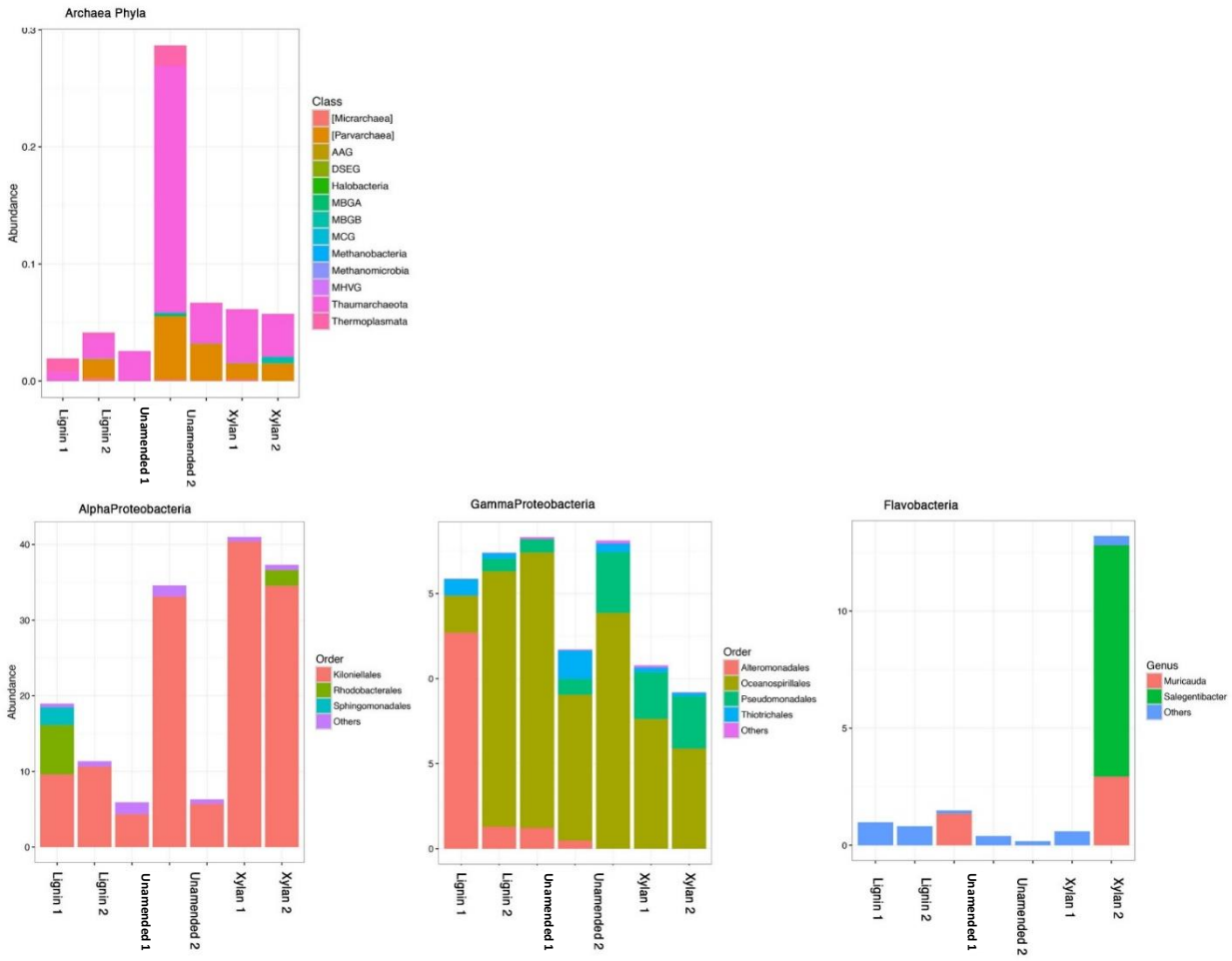

Figure 54 Taxa Bar plots of Archaea, Alphaproteobacteria, Gammaproteobacteria and Flavobacteria from the 16S rRNA gene amplicon sequencing

"Others" is used to represent taxa less than 1% relative abundance.

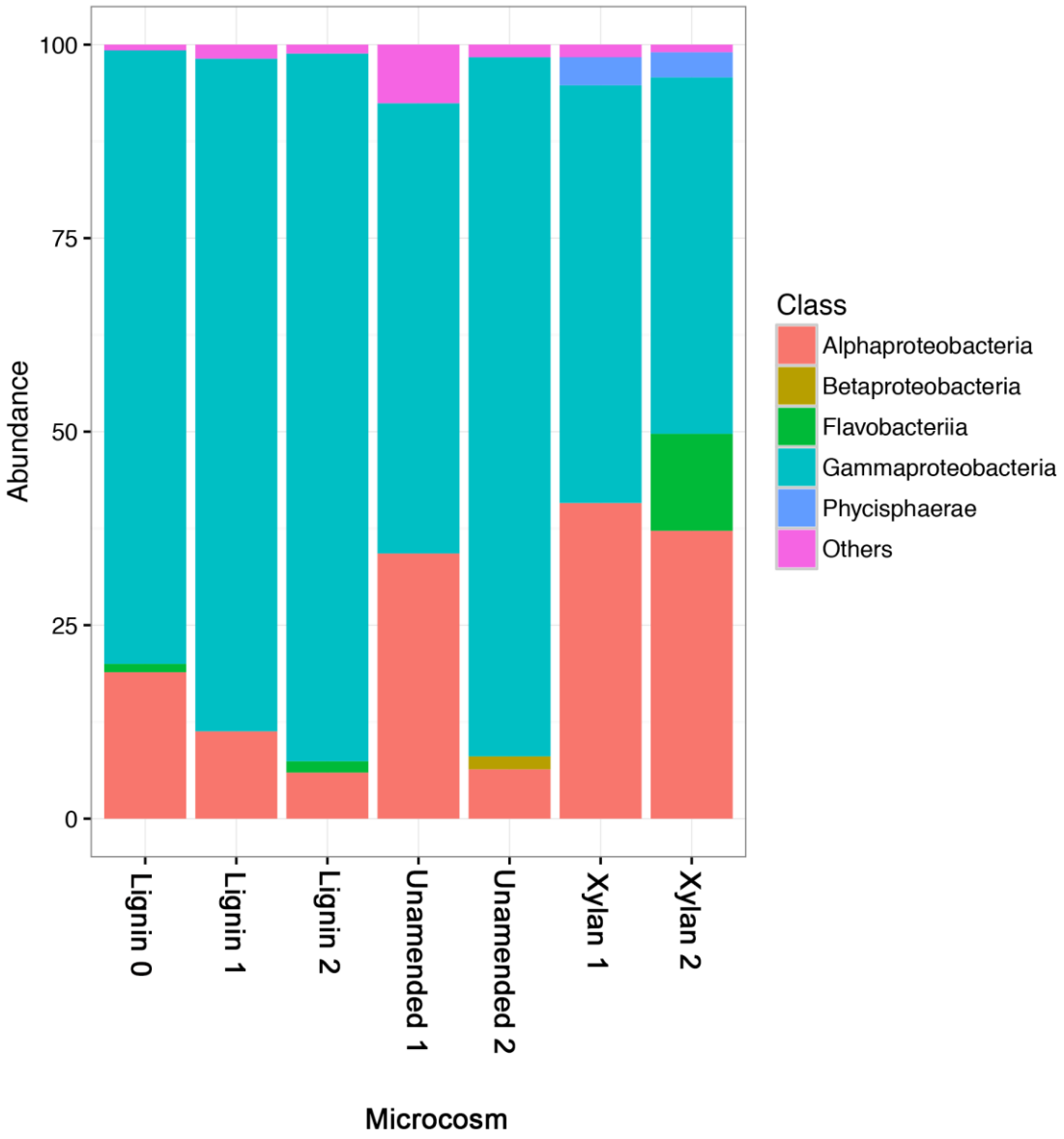

Figure 55 The relative abundances of taxonomic classes identified by 16S rRNA gene amplicon sequencing

Classes that are less than 1% relative abundances are aggregated as Others.

Table 9 The relative abundance of phyla detected in metagenomic shotgun reads

The reads were annotated using the MG-RAST automated annotation pipeline. Table uses the "representative hit classification" from the M5NR database with a maximum e-value cutoff of 1e-5, minimum % identity cutoff of 60%, and minimum alignment length cutoff of 15.

	Unamended I (%)	Unamended II (%)	Xylan I (%)	Xylan II (%)	Lignin I (%)	Lignin II (%)	Grand Total (%)
Acidobacteria	0.092	0.075	0.112	0.158	0.081	0.100	0.108
Actinobacteria	1.839	1.308	0.914	0.857	1.079	0.999	1.119
Apicomplexa	0.001	0.001	0.001	0.001	0.001	0.001	0.001
Aquificae	0.025	0.014	0.020	0.022	0.018	0.013	0.018
Arthropoda	0.020	0.016	0.024	0.021	0.025	0.017	0.020
Ascomycota	0.041	0.028	0.042	0.036	0.037	0.030	0.036
Bacillariophyta	0.009	0.004	0.007	0.007	0.002	0.003	0.006
Bacteroidetes	0.783	0.448	8.116	23.830	2.083	4.656	7.280
Basidiomycota	0.007	0.005	0.006	0.005	0.006	0.005	0.006
Chlamydiae	0.011	0.005	0.012	0.010	0.006	0.004	0.008
Chlorobi	0.158	0.100	0.145	0.124	0.110	0.112	0.128
Chloroflexi	0.132	0.085	0.109	0.101	0.100	0.092	0.103
Chlorophyta	0.012	0.006	0.009	0.015	0.007	0.005	0.009
Chordata	0.073	0.038	0.065	0.069	0.050	0.048	0.058
Chrysiogenetes	0.038	0.028	0.029	0.023	0.035	0.029	0.030
Cnidaria	0.019	0.025	0.033	0.040	0.017	0.021	0.027
Crenarchaeota	0.012	0.012	0.015	0.012	0.006	0.012	0.013
Cyanobacteria	0.486	0.356	0.468	0.422	0.363	0.370	0.419
Deferribacteres	0.015	0.014	0.012	0.021	0.022	0.015	0.015
Deinococcus-Thermus	0.140	0.110	0.119	0.102	0.122	0.114	0.117
Dictyoglomi	0.001	0.001	0.001	0.001	0.002	0.001	0.001
Echinodermata	0.000	0.000	0.001	0.001	0.001	0.001	0.001
Elusimicrobia	0.003	0.005	0.005	0.003	0.009	0.005	0.004
Euglenida	0.000	0.000	0.000	0.000	0.000	0.000	0.000
Euryarchaeota	0.102	0.076	0.088	0.088	0.078	0.081	0.087

Table 9 Continued

	Unamended I (%)	Unamended II (%)	Xylan I (%)	Xylan II (%)	Lignin I (%)	Lignin II (%)	Grand Total (%)
Fibrobacteres	0.001	0.001	0.001	0.003	0.001	0.001	0.001
Firmicutes	0.745	0.781	0.758	0.766	0.952	0.709	0.747
Fusobacteria	0.017	0.015	0.007	0.013	0.012	0.013	0.012
Gemmatimonadetes	0.009	0.011	0.012	0.014	0.012	0.012	0.012
Glomeromycota	0.000	0.000	0.000	0.000	0.000	0.000	0.000
Hemichordata	0.001	0.000	0.000	0.001	0.001	0.000	0.001
Korarchaeota	0.005	0.004	0.003	0.003	0.005	0.004	0.004
Lentisphaerae	0.006	0.007	0.009	0.011	0.007	0.005	0.007
Microsporidia	0.000	0.000	0.000	0.000	0.000	0.000	0.000
Mollusca	0.008	0.005	0.002	0.001	0.004	0.002	0.003
Nematoda	0.008	0.004	0.008	0.007	0.007	0.006	0.007
Nitrospirae	0.027	0.016	0.040	0.034	0.019	0.023	0.029
Phaeophyceae	0.000	0.000	0.000	0.001	0.002	0.001	0.000
Placozoa	0.001	0.000	0.002	0.002	0.001	0.001	0.001
Planctomycetes	0.132	0.083	0.127	0.147	0.096	0.088	0.113
Platyhelminthes	0.000	0.000	0.000	0.000	0.000	0.000	0.000
Poribacteria	0.001	0.002	0.000	0.001	0.003	0.001	0.001
Proteobacteria	94.341	95.730	87.993	72.387	94.022	91.875	88.836
Sipuncula	0.000	0.000	0.000	0.000	0.000	0.000	0.000
Spirochaetes	0.033	0.026	0.031	0.035	0.037	0.030	0.031
Streptophyta	0.104	0.060	0.089	0.077	0.084	0.057	0.076
Synergistetes	0.032	0.029	0.031	0.022	0.043	0.028	0.029
Tenericutes	0.003	0.002	0.001	0.006	0.005	0.003	0.003
Thaumarchaeota	0.003	0.001	0.000	0.001	0.002	0.003	0.002
Thermotogae	0.011	0.006	0.011	0.013	0.014	0.009	0.010
unassigned	0.154	0.127	0.144	0.117	0.132	0.128	0.135
unclassified (derived from Archaea)	0.003	0.001	0.004	0.001	0.002	0.002	0.003

Table 9 Continued

	Unamended I (%)	Unamended II (%)	Xylan I (%)	Xylan II (%)	Lignin I (%)	Lignin II (%)	Grand Total (%)
unclassified (derived from Bacteria)	0.112	0.137	0.144	0.127	0.094	0.083	0.115
unclassified (derived from Eukaryota)	0.021	0.011	0.021	0.019	0.014	0.014	0.017
unclassified (derived from Fungi)	0.000	0.001	0.001	0.001	0.001	0.000	0.001
unclassified (derived from other sequences)	0.013	0.021	0.024	0.016	0.019	0.020	0.019
unclassified (derived from unclassified sequences)	0.053	0.035	0.042	0.040	0.040	0.038	0.041
unclassified (derived from Viruses)	0.047	0.072	0.056	0.044	0.041	0.047	0.051
Verrucomicrobia	0.089	0.055	0.080	0.121	0.070	0.064	0.079

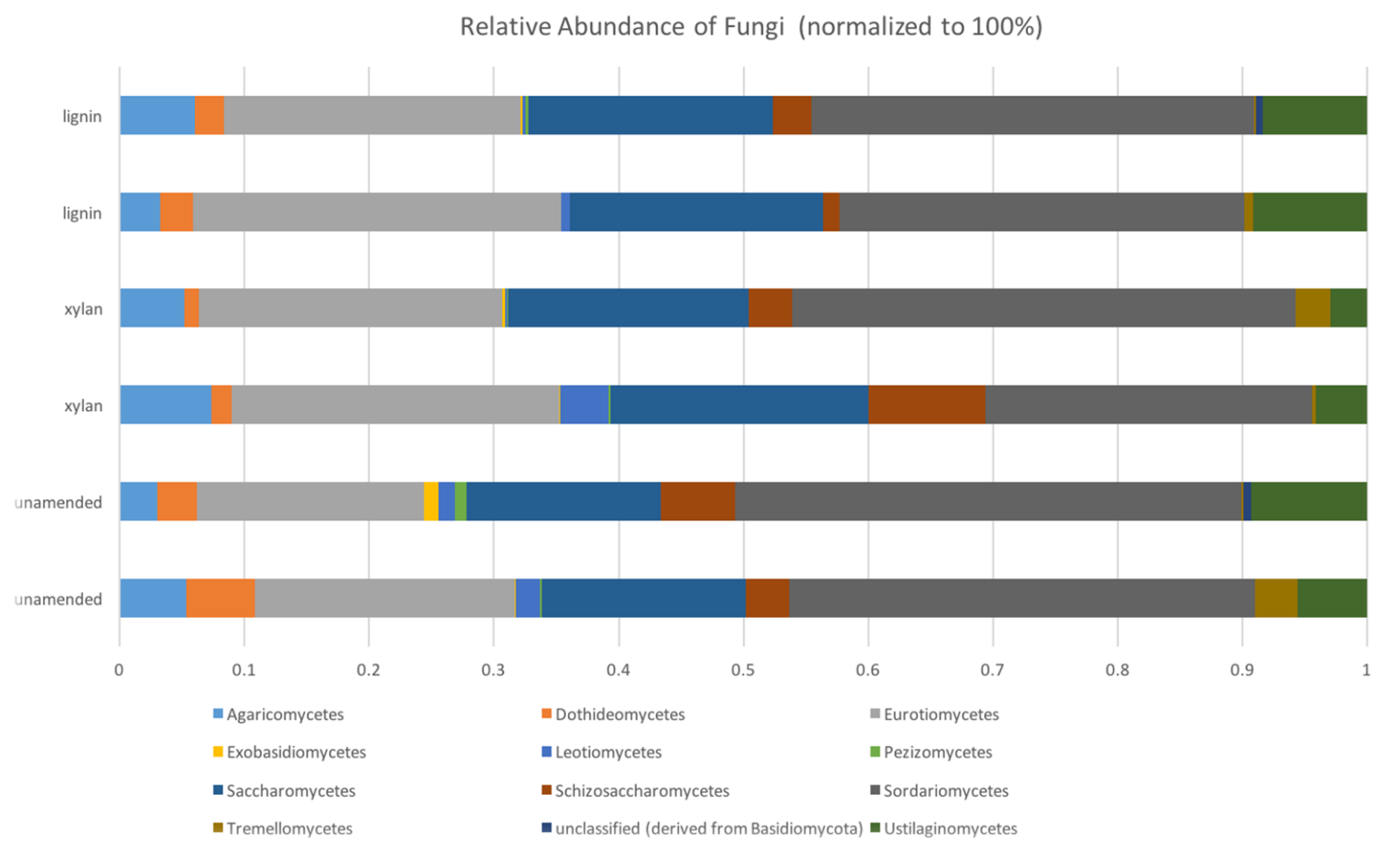

Figure 56 The relative abundance of fungal taxa within the metagenomic reads

The abundances of fungal taxa from each sample were normalized so that their sum would be 1.

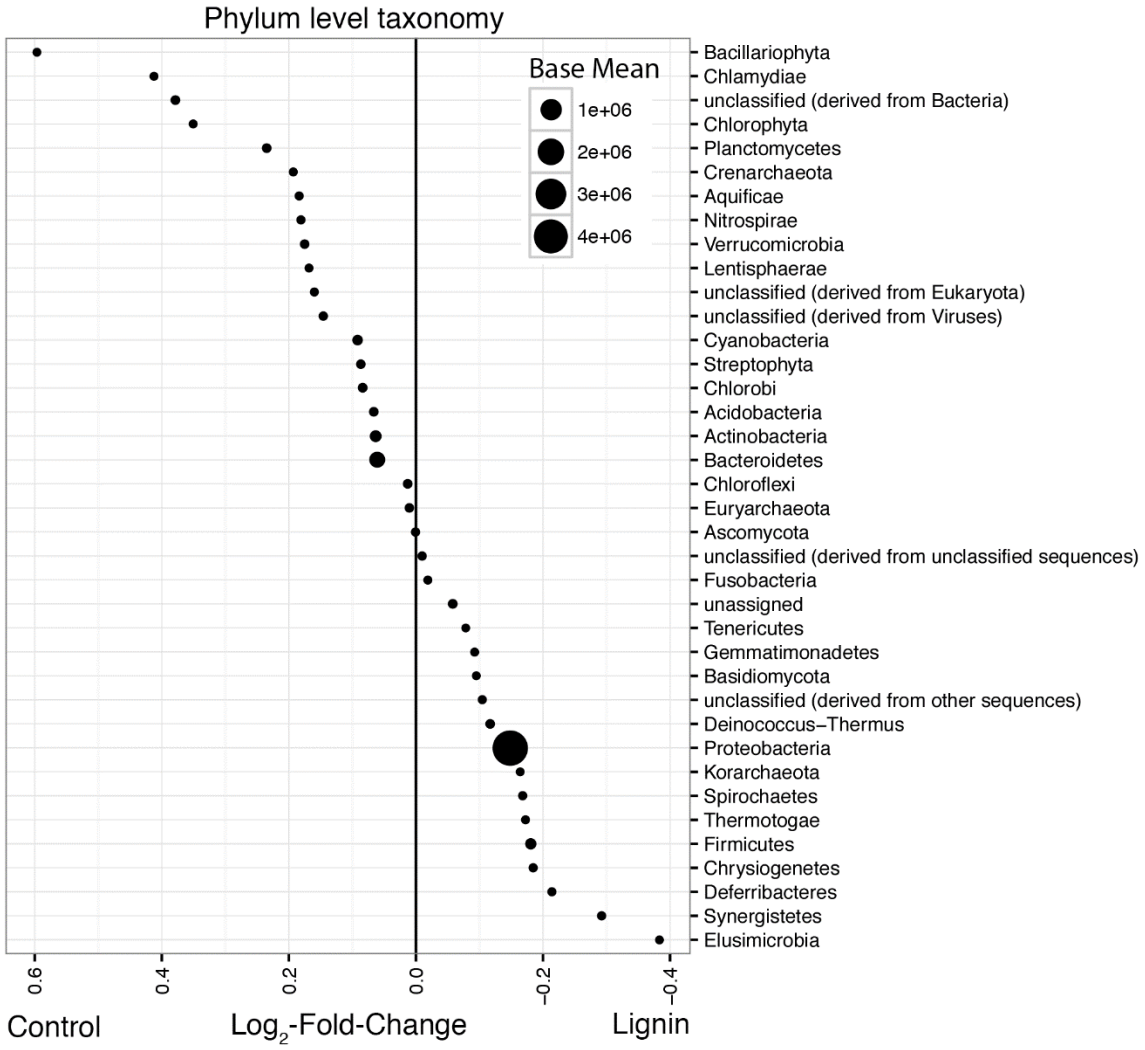

Figure 57 Average log_2-fold changes of phyla between lignin-adapted consortia and the controls

Abundances from the MG-RAST annotation were compared between the lignin-adapted consortia and the non-lignin controls. The first and second incubations were combined for each substrate. The non-lignin controls included both the unamended control and the xylan-adapted consortia. The size of the point indicates its normalized relative abundance. A negative log2-fold change indicates higher abundance in lignin-adapted consortia while a positive log2-fold change indicates higher abundance in the controls. Phyla that were less than 0.005% or macrofauna were excluded.

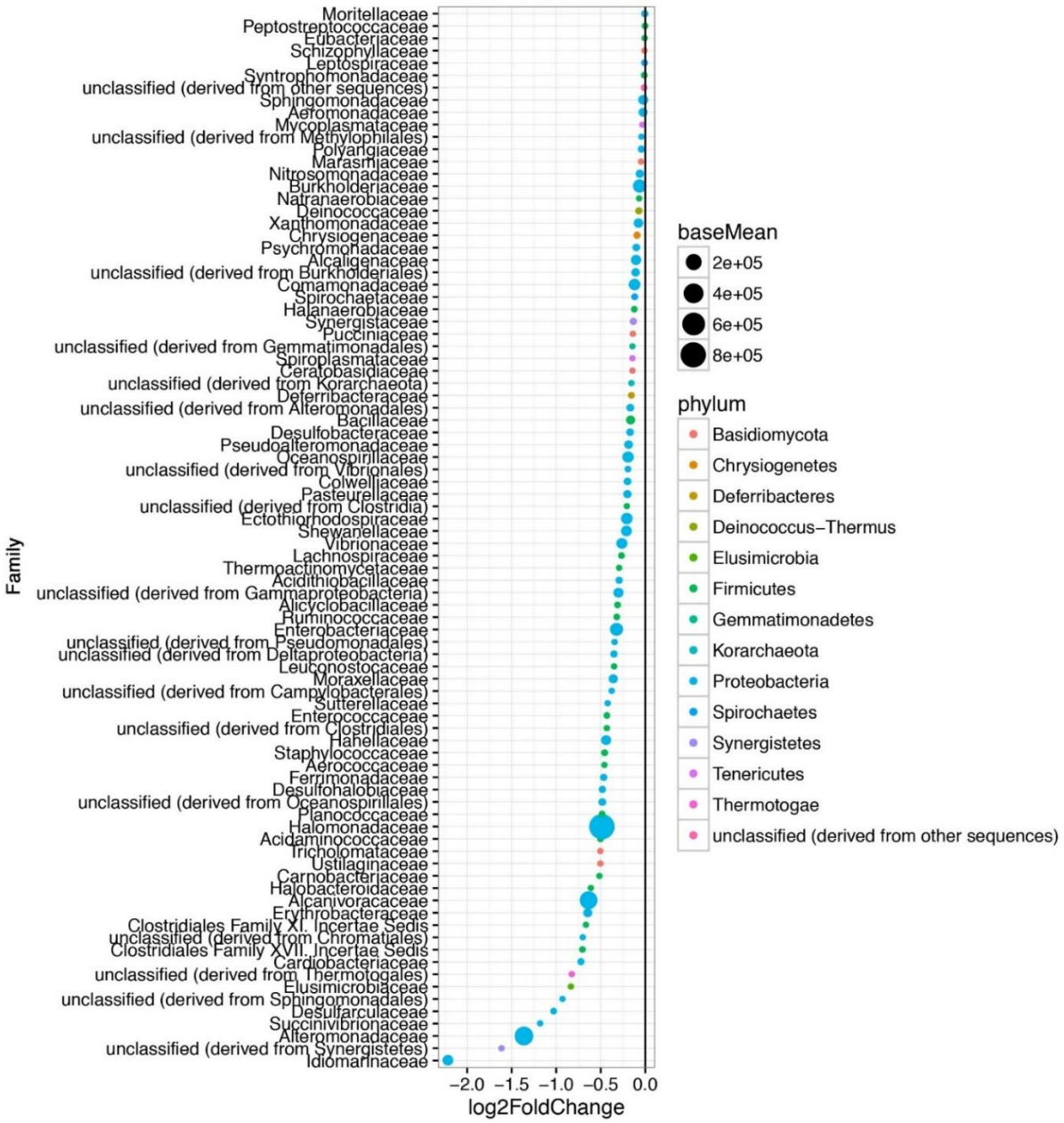

Figure 58 Taxonomic families from phyla that became higher in abundance in response to lignin

Taxonomy was derived from the metagenome annotation. A more negative $\log_2$-fold-change indicates a greater increase in response to lignin. Points indicate the average log-fold-change for the taxonomic family. Points are colored to show the phylum level taxonomy. Size of the point is proportional to the normalized relative abundance.

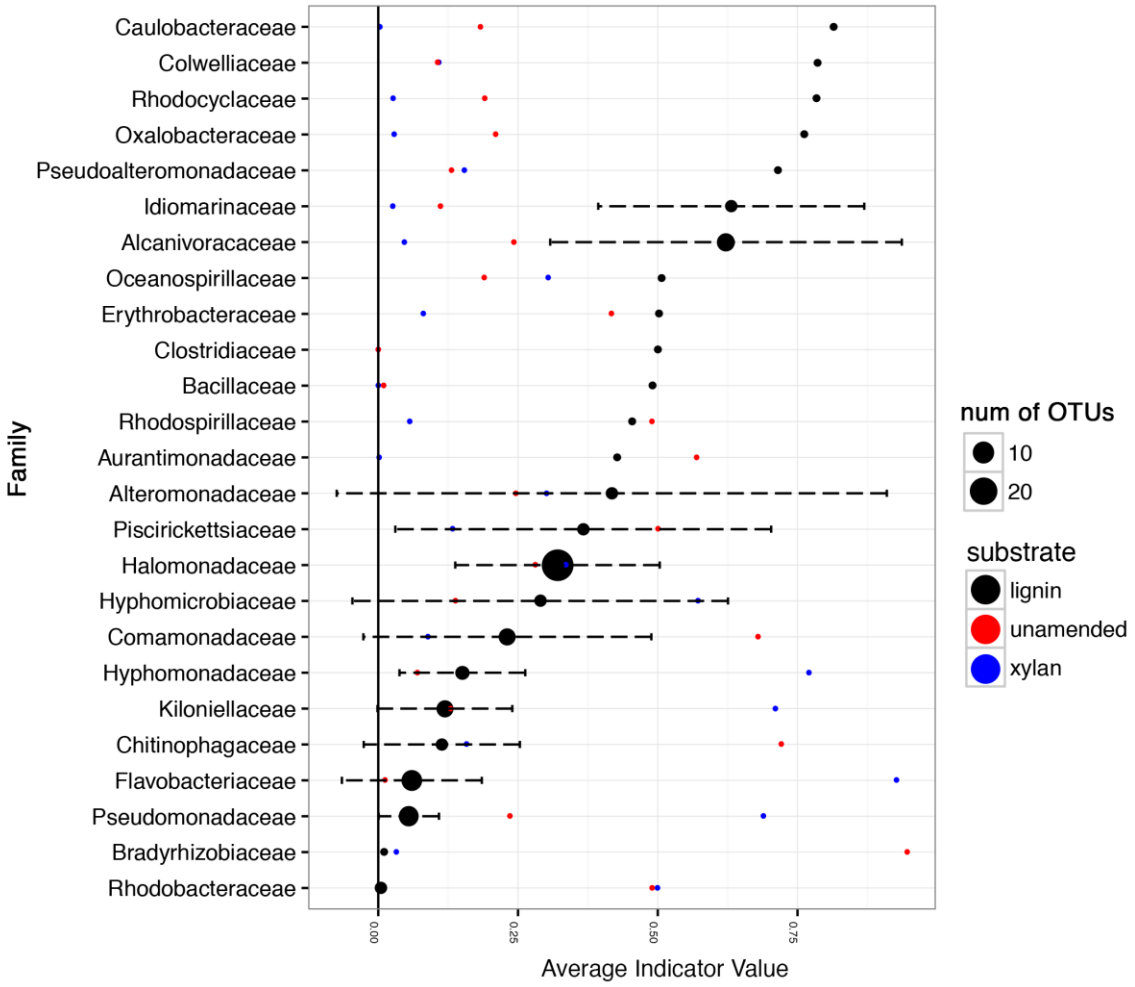

Figure 59 Average Indicator Values of taxonomic families for lignin amendment

The abundances of the OTUs in the 16S rRNA gene amplicon data were used to calculate the indicator value using the R package labsdv indval function. The first and second incubations were combined for each substrate. The average of the indicator value for lignin is shown by the black points. The error bars indicate the standard deviation of the indicator values. The size of the point indicates how many distinct OTUs are represented in the dataset. Taxonomic families with Indicator values less than 0.1 for lignin were excluded from visualization. The red points and blue points indicate indicator value for the unamended control and xylan amendment, respectively.

Chapter 5 Conclusions

Chapter 2 tested the hypothesis that sediment and seawater microbial communities would respond differently to lignin amendment. The results did not clearly support or reject the hypothesis. Microbial activities were similar between lignin-amended sediment and seawater while the microbial communities were very different. The organic carbon data showed some differences between sediment and seawater. The potential to degrade lignin may be widely distributed amongst different microbial taxa which allowed lignin to be remineralized efficiently in both the sediment and seawater. Since the organics released or utilized by the different microbial communities were different, the long-term carbon cycling in these two depths may become more distinct over the long-term.

Chapter 3 addressed a classic knowledge gap in microbial ecology, which is the identification of keystone species in microbial communities growing on high molecular weight carbon like hemicellulose. The keystone species responsible for the degradation of hemicellulose are difficult to identify because of the uncharacterized presence of "cheaters". We define "cheaters" as microbes capable of utilizing the released monosaccharide without producing any degradative extracellular enzymes. "Cheaters" are a commonly raised issue but is rarely experimentally investigated to determine its true relevance. The relevance of "cheaters" can dictate if the microbial community is "hemicellulose-degrading" or only "hemicellulose-associated".

The main finding was that "cheaters" exist in xylan degradation. Therefore, prediction of keystones species must be conservative to avoid false positives. We found two taxa as potential keystone species, *Muricauda* and *Pseudoalteromonas*. Little information is available on these two taxa as hemicellulose degraders. We believe our results are generalizable enough to set a precedent for inclusion of more monosaccharide or monomer controls in various high molecular weight carbon degradation studies (i.e. cellulose, lignin, crude oil). This is especially relevant for researchers interested in 'omics-based approaches like 16S rRNA gene amplicon sequencing, 16S rRNA gene DNA-SIP (stable isotope probing), and RNA-SIP.

Within the Chapter 4, experimental evidence implicated bacteria, not the typical white-rot fungi, in lignin degradation in the open ocean and the dominance of phenylacetyl CoA for aerobic aromatic catabolism in the ocean rather than the classical b-ketoadipate pathways. This new evidence ebbs at the long-held paradigms that fungi and Beta-ketoadipate pathways are the only significant biotic factors for lignin biodegradation. The work provides insight into the utilization of "recalcitrant" organic matter, a subject of growing interest in aquatic and marine systems. Lastly, the bacterial keystone species for lignin degradation identified in experiment has implications on the field of lignin valorization and lignocellulosic biofuels.

In conclusion, this dissertation supports the notion of bacteria in the ocean significantly contributing to terrestrial organic carbon cycling. The bacteria may be novel sources of lignin degrading enzymes for commercial use in biofuels and lignin valorization.

References

Ajanovic, A., and Haas, R. (2014) On the future prospects and limits of biofuels in Brazil, the US and EU. *Applied Energy* **135**: 730-737.

Allgaier, M., Reddy, A., Park, J.I., Ivanova, N., D'Haeseleer, P., Lowry, S. et al. (2010) Targeted discovery of glycoside hydrolases from a switchgrass-adapted compost community. *PLoS One* **5**: e8812.

Andersson, J.H., Wijsman, J.W.M., Herman, P.M.J., Middelburg, J.J., Soetaert, K., and Heip, C. (2004) Respiration patterns in the deep ocean. *Geophysical Research Letters* **31**: L03304.

Arnosti, C. (2011) Microbial extracellular enzymes and the marine carbon cycle. *Annual Review of Marine Science* **3**: 401-425.

Arrieta, J.M., Mayol, E., Hansman, R.L., Herndl, G.J., Dittmar, T., and Duarte, C.M. (2015) Dilution limits dissolved organic carbon utilization in the deep ocean. *Science*: 1258955.

Arun, A., and Eyini, M. (2011) Comparative studies on lignin and polycyclic aromatic hydrocarbons degradation by basidiomycetes fungi. *Bioresource Technology* **102**: 8063-8070.

Atlas, R.M. (2010) *Handbook of Microbiological Media, Fourth Edition*: Taylor & Francis.

Bach, C.E., Warnock, D.D., Van Horn, D.J., Weintraub, M.N., Sinsabaugh, R.L., Allison, S.D., and German, D.P. (2013) Measuring phenol oxidase and peroxidase activities with pyrogallol, l-DOPA, and ABTS: Effect of assay conditions and soil type. *Soil Biology and Biochemistry* **67**: 183-191.

Bass, D., Howe, A., Brown, N., Barton, H., Demidova, M., Michelle, H. et al. (2007) Yeast forms dominate fungal diversity in the deep oceans. *Proceedings of the Royal Society B: Biological Sciences* **274**: 3069.

Bayer, E.A., Morag, E., and Lamed, R. (1994) The cellulosome — A treasure-trove for biotechnology. *Trends in Biotechnology* **12**: 379-386.

Benner, R., Newell, S.Y., Maccubbin, A.E., and Hodson, R.E. (1984) Relative Contributions of Bacteria and Fungi to Rates of Degradation of Lignocellulosic Detritus in Salt-Marsh Sediments. *Applied and Environmental Microbiology* **48**: 36-40.

Bianchi, T.S. (2011a) The role of terrestrially derived organic carbon in the coastal ocean: a changing paradigm and the priming effect. *Proceedings of the National Academy of Sciences* **108**: 19473-19481.

Bianchi, T.S. (2011b) The role of terrestrially derived organic carbon in the coastal ocean: A changing paradigm and the priming effect. *Proceedings of the National Academy of Sciences* **108**: 19473-19481.

Bienhold, C., Pop Ristova, P., Wenzhofer, F., Dittmar, T., and Boetius, A. (2013) How deep-sea wood falls sustain chemosynthetic life. *PLoS One* **8**: e53590.

Birdwell, J.E., and Engel, A.S. (2010) Characterization of dissolved organic matter in cave and spring waters using UV–Vis absorbance and fluorescence spectroscopy. *Organic Geochemistry* **41**: 270-280.

Blair, N.E., and Aller, R.C. (2012) The fate of terrestrial organic carbon in the marine environment. *Annual Review of Marine Science* **4**: 401-423.

Boyle, C.D., Kropp, B.R., and Reid, I.D. (1992) Solubilization and mineralization of lignin by white rot fungi. *Applied and Environmental Microbiology* **58**: 3217-3224.

Brannen-Donnelly, K., and Engel, A.S. (2015) Bacterial diversity differences along an epigenic cave stream reveal evidence of community dynamics, succession, and stability. *Frontiers in Microbiology* **6**: 729.

Brodie, E., Edwards, S., and Clipson, N. (2002) Bacterial Community Dynamics across a Floristic Gradient in a Temperate Upland Grassland Ecosystem. *Microbial Ecology* **44**: 260-270.

Brown, M.E., and Chang, M.C. (2014) Exploring bacterial lignin degradation. *Current Opinion in Chemical Biology* **19**: 1-7.

Bruns, A., Rohde, M., and Berthe-Corti, L. (2001a) Muricauda ruestringensis gen.nov., sp. nov., a facultatively anaerobic, appendaged bacterium from German North Sea intertidal sediment. *Int J Syst Evol Microbiol* **51**.

Bruns, A., Rohde, M., and Berthe-Corti, L. (2001b) Muricauda ruestringensis gen. nov., sp. nov., a facultatively anaerobic, appendaged bacterium from German North Sea intertidal sediment. *International journal of systematic and evolutionary microbiology* **51**: 1997-2006.

Bugg, T.D., and Rahmanpour, R. (2015a) Enzymatic conversion of lignin into renewable chemicals. *Current Opinion in Chemical Biology* **29**: 10-17.

Bugg, T.D., Ahmad, M., Hardiman, E.M., and Rahmanpour, R. (2011a) Pathways for degradation of lignin in bacteria and fungi. *Natural Product Reports* **28**: 1883-1896.

Bugg, T.D.H., and Rahmanpour, R. (2015b) Enzymatic conversion of lignin into renewable chemicals. *Current Opinion in Chemical Biology* **29**: 10-17.

Bugg, T.D.H., Ahmad, M., Hardiman, E.M., and Rahmanpour, R. (2011b) Pathways for degradation of lignin in bacteria and fungi. *Natural Product Reports* **28**: 1883.

Burdige, D.J. (2005) Burial of terrestrial organic matter in marine sediments: A re-assessment:Terrestrial organic matter in marine sediments. *Global Biogeochemical Cycles* **19**: n/a-n/a.

Campbell, M.M., and Sederoff, R.R. (1996) Variation in Lignin Content and Composition (Mechanisms of Control and Implications for the Genetic Improvement of Plants). *Plant physiology* **110**: 3.

Cantarel, B.L., Coutinho, P.M., Rancurel, C., Bernard, T., Lombard, V., and Henrissat, B. (2009) The Carbohydrate-Active EnZymes database (CAZy): an expert resource for Glycogenomics. *Nucleic Acids Research* **37**: D233-238.

Caporaso, J.G., Lauber, C.L., Walters, W.A., Berg-Lyons, D., Huntley, J., Fierer, N. et al. (2012) Ultra-high-throughput microbial community analysis on the Illumina HiSeq and MiSeq platforms. *ISME J* **6**: 1621-1624.

Caporaso, J.G., Kuczynski, J., Stombaugh, J., Bittinger, K., Bushman, F.D., Costello, E.K. et al. (2010) QIIME allows analysis of high-throughput community sequencing data. *Nature Methods* **7**: 335-336.

Colberg, P.J., and Young, L.Y. (1985) Anaerobic Degradation of Soluble Fractions of [14C-Lignin]Lignocellulose. *Applied and Environmental Microbiology* **49**: 345-349.

Cole, J.R., Wang, Q., Fish, J.A., Chai, B., McGarrell, D.M., Sun, Y. et al. (2014) Ribosomal Database Project: data and tools for high throughput rRNA analysis. *Nucleic Acids Research* **42**: D633-642.

Collins, T., Gerday, C., and Feller, G. (2005) Xylanases, xylanase families and extremophilic xylanases. *FEMS Microbiology Reviews* **29**: 3-23.

Consortium, U. (2014) UniProt: a hub for protein information. *Nucleic Acids Research* **43**: D204-D212.

Cottrell, M.T., and Kirchman, D.L. (2000) Natural assemblages of marine proteobacteria and members of the Cytophaga-Flavobacter cluster consuming low- and high-molecular-weight dissolved organic matter. *Applied and Environmental Microbiology* **66**: 1692-1697.

Dalmaso, G.Z., Ferreira, D., and Vermelho, A.B. (2015) Marine extremophiles: a source of hydrolases for biotechnological applications. *Marine Drugs* **13**: 1925-1965.

Davis, R. (2013) Process design and economics for the conversion of lignocellulosic biomass to hydrocarbons: Dilute acid and enzymatic Deconstruction of biomass to sugars and biological conversion of Sugars to Hydrocarbons. In. Golden, CO: NREL.

DeAngelis, K.M., Fortney, J.L., Borglin, S., Silver, W.L., Simmons, B.A., and Hazen, T.C. (2012) Anaerobic Decomposition of Switchgrass by Tropical Soil-Derived Feedstock-Adapted Consortia. *mBio* **3**.

DeAngelis, K.M., Allgaier, M., Chavarria, Y., Fortney, J.L., Hugenholtz, P., Simmons, B. et al. (2011a) Characterization of trapped lignin-degrading microbes in tropical forest soil. *PLoS One* **6**: e19306.

DeAngelis, K.M., Gladden, J.M., Allgaier, M., D'haeseleer, P., Fortney, J.L., Reddy, A. et al. (2010) Strategies for Enhancing the Effectiveness of Metagenomic-based Enzyme Discovery in Lignocellulolytic Microbial Communities. *BioEnergy Research* **3**: 146-158.

Deangelis, K.M., D'Haeseleer, P., Chivian, D., Fortney, J.L., Khudyakov, J., Simmons, B. et al. (2011b) Complete genome sequence of "Enterobacter lignolyticus" SCF1. *Standards in Genomic Sciences* **5**: 69-85.

DeSantis, T.Z., Hugenholtz, P., Larsen, N., Rojas, M., Brodie, E.L., Keller, K. et al. (2006) Greengenes, a Chimera-Checked 16S rRNA Gene Database and Workbench Compatible with ARB. *Applied and Environmental Microbiology* **72**: 5069-5072.

Dittmar, T., and Lara, R.J. (2001) Molecular evidence for lignin degradation in sulfate-reducing mangrove sediments (Amazônia, Brazil). *Geochimica et Cosmochimica Acta* **65**: 1417-1428.

Dixon, P., and Palmer, M.W. (2003) VEGAN, a package of R functions for community ecology. *Journal of Vegetation Science* **14**: 927-930.

Docherty, K.M., Young, K.C., Maurice, P.A., and Bridgham, S.D. (2006) Dissolved Organic Matter Concentration and Quality Influences upon Structure and Function of Freshwater Microbial Communities. *Microbial Ecology* **52**: 378-388.

Dodd, D., and Cann, I.K.O. (2009) Enzymatic deconstruction of xylan for biofuel production. *Global Change Biology Bioenergy* **1**: 2-17.

Domozych, D.S. (2016) Biosynthesis of the Cell Walls of the Algae. In *The Physiology of Microalgae*. Borowitzka, M.A., Beardall, J., and Raven, J.A. (eds). Cham: Springer International Publishing, pp. 47-63.

Eichorst, S.A., Joshua, C., Sathitsuksanoh, N., Singh, S., Simmons, B.A., and Singer, S.W. (2014) Substrate-Specific Development of Thermophilic Bacterial Consortia by Using Chemically Pretreated Switchgrass. *Applied and Environmental Microbiology* **80**: 7423-7432.

Eichorst, S.A., Varanasi, P., Stavila, V., Zemla, M., Auer, M., Singh, S. et al. (2013) Community dynamics of cellulose-adapted thermophilic bacterial consortia. *Environmental Microbiology* **15**: 2573-2587.

Eiler, A., Langenheder, S., Bertilsson, S., and Tranvik, L.J. (2003) Heterotrophic Bacterial Growth Efficiency and Community Structure at Different Natural Organic Carbon Concentrations. *Applied and Environmental Microbiology* **69**: 3701-3709.

Ekşioğlu, S.D., Acharya, A., Leightley, L.E., and Arora, S. (2009) Analyzing the design and management of biomass-to-biorefinery supply chain. *Computers & Industrial Engineering* **57**: 1342-1352.

Fergus, B.J., and Goring, D.A.I. (1970) The Distribution of Lignin in Birch Wood as Determined by Ultraviolet Microscopy. In *Holzforschung - International Journal of the Biology, Chemistry, Physics and Technology of Wood*, p. 118.

Fernandez-Gomez, B., Richter, M., Schuler, M., Pinhassi, J., Acinas, S.G., Gonzalez, J.M., and Pedros-Alio, C. (2013) Ecology of marine Bacteroidetes: a comparative genomics approach. *ISME J* **7**: 1026-1037.

Fichot, C.G., and Benner, R. (2014) The fate of terrigenous dissolved organic carbon in a river-influenced ocean margin. *Global Biogeochemical Cycles* **28**: 300-318.

Fuchs, G., Boll, M., and Heider, J. (2011) Microbial degradation of aromatic compounds - from one strategy to four. *Nature Review Microbiology* **9**: 803-816.

Goñi, M.A., and Montgomery, S. (2000) Alkaline CuO Oxidation with a Microwave Digestion System: Lignin Analyses of Geochemical Samples. *Analytical Chemistry* **72**: 3116-3121.

Hall, S.J., Silver, W.L., Timokhin, V.I., and Hammel, K.E. (2015) Lignin decomposition is sustained under fluctuating redox conditions in humid tropical forest soils. *Global Change Biology*.

Haruta, S., Cui, Z., Huang, Z., Li, M., Ishii, M., and Igarashi, Y. (2002) Construction of a stable microbial community with high cellulose-degradation ability. *Applied Microbiology and Biotechnology* **59**: 529-534.

Hatfield, R., and Fukushima, R.S. (2005) Can Lignin Be Accurately Measured? *Crop Science* **45**: 832.

Hazen, T.C., Dubinsky, E.A., DeSantis, T.Z., Andersen, G.L., Piceno, Y.M., Singh, N. et al. (2010) Deep-Sea Oil Plume Enriches Indigenous Oil-Degrading Bacteria. *Science* **330**: 204-208.

Hedges, J.I., Keil, R.G., and Benner, R. (1997) What happens to terrestrial organic matter in the ocean? *Organic Geochemistry* **27**: 195-212.

Hernes, P.J. (2003) Photochemical and microbial degradation of dissolved lignin phenols: Implications for the fate of terrigenous dissolved organic matter in marine environments. *Journal of Geophysical Research* **108**.

Hernes, P.J., and Benner, R. (2003) Photochemical and microbial degradation of dissolved lignin phenols: Implications for the fate of terrigenous dissolved organic matter in marine environments. *Journal of Geophysical Research* **108**: 3291.

Hess, M., Sczyrba, A., Egan, R., Kim, T.-W., Chokhawala, H., Schroth, G. et al. (2011) Metagenomic Discovery of Biomass-Degrading Genes and Genomes from Cow Rumen. *Science* **331**: 463-467.

Holladay, J.E., Bozell, J.J., White, J.F., and Johnson, D. (2007) Top value-added chemicals from biomass. *Volume II–Results of Screening for Potential Candidates from Biorefinery Lignin, Report prepared by members of NREL, PNNL and University of Tennessee*.

Huntemann, M., Teshima, H., Lapidus, A., Nolan, M., Lucas, S., Hammon, N. et al. (2012) Complete genome sequence of the facultatively anaerobic, appendaged bacterium Muricauda ruestringensis type strain (B1T). *Standards in Genomic Sciences* **6**: 185-193.

Ilmberger, N., Meske, D., Juergensen, J., Schulte, M., Barthen, P., Rabausch, U. et al. (2012) Metagenomic cellulases highly tolerant towards the presence of ionic liquids—linking thermostability and halotolerance. *Applied Microbiology and Biotechnology* **95**: 135-146.

International, C.I. (2010) *Micro Oxymax Instruction Manual*. Columbus, Ohio: Columbus Instruments International.

Ishii, K., and Fukui, M. (2001) Optimization of Annealing Temperature To Reduce Bias Caused by a Primer Mismatch in Multitemplate PCR. *Applied and Environmental Microbiology* **67**: 3753-3755.

Ismail, W., and Gescher, J. (2012) Epoxy Coenzyme A Thioester pathways for degradation of aromatic compounds. *Applied and Environmental Microbiology* **78**: 5043-5051.

Jimenez, D.J., Dini-Andreote, F., and van Elsas, J.D. (2014) Metataxonomic profiling and prediction of functional behaviour of wheat straw degrading microbial consortia. *Biotechnology for biofuels* **7**.

Jogler, M., Chen, H., Simon, J., Rohde, M., Busse, H.-J., Klenk, H.-P. et al. (2013) Description of Sphingorhabdus planktonica gen. nov., sp. nov. and reclassification of three related members of the genus Sphingopyxis in the genus Sphingorhabdus gen. nov. *International journal of systematic and evolutionary microbiology* **63**: 1342-1349.

Jorgensen, S.L., Hannisdal, B., Lanzén, A., Baumberger, T., Flesland, K., Fonseca, R. et al. (2012) Correlating microbial community profiles with geochemical data in highly stratified sediments from the Arctic Mid-Ocean Ridge. *Proceedings of the National Academy of Sciences* **109**: E2846–E2855.

Kembel, S.W., Cowan, P.D., Helmus, M.R., Cornwell, W.K., Morlon, H., Ackerly, D.D. et al. (2010) Picante: R tools for integrating phylogenies and ecology. *Bioinformatics* **26**: 1463-1464.

Khudyakov, J.I., D'haeseleer, P., Borglin, S.E., DeAngelis, K.M., Woo, H., Lindquist, E.A. et al. (2012) Global transcriptome response to ionic liquid by a tropical rain forest soil bacterium, Enterobacter lignolyticus. *Proceedings of the National Academy of Sciences* **109**: E2173–E2182.

Kirk, T.K., and Farrell, R.L. (1987) Enzymatic "combustion": the microbial degradation of lignin. *Annual Reviews in Microbiology* **41**: 465-501.

Klein-Marcuschamer, D., Oleskowicz-Popiel, P., Simmons, B.A., and Blanch, H.W. (2012) The challenge of enzyme cost in the production of lignocellulosic biofuels. *Biotechnology and Bioengineering* **109**: 1083-1087.

Kline, L.M., Hayes, D.G., Womac, A.R., and Labbe, N. (2010) Simplified determination of lignin content in hard and soft woods via uv-spectrophotometric analysis of biomass dissolved in ionic liquids. *Bioresources* **5**: 1366-1383.

Krom, M.D., Emeis, K.C., and Van Cappellen, P. (2010) Why is the Eastern Mediterranean phosphorus limited? *Progress in Oceanography* **85**: 236-244.

Krom, M.D., Woodward, E.M.S., Herut, B., Kress, N., Carbo, P., Mantoura, R.F.C. et al. (2005) Nutrient cycling in the south east Levantine basin of the eastern Mediterranean: Results from a phosphorus starved system. *Deep Sea Research Part II: Topical Studies in Oceanography* **52**: 2879-2896.

Lalonde, K., Vähätalo, A.V., and Gélinas, Y. (2014) Revisiting the disappearance of terrestrial dissolved organic matter in the ocean: a δ13C study. *Biogeosciences* **11**: 3707-3719.

Laurent, M.C.Z., Le Bris, N., Gaill, F., and Gros, O. (2013) Dynamics of wood fall colonization in relation to sulfide concentration in a mangrove swamp. *Marine Environmental Research* **87-88**: 85-95.

Lee, D.-J., Show, K.-Y., and Wang, A. (2013a) Unconventional approaches to isolation and enrichment of functional microbial consortium – A review. *Bioresource Technology* **136**: 697-706.

Lee, R.A., Bedard, C., Berberi, V., Beauchet, R., and Lavoie, J.M. (2013b) UV-Vis as quantification tool for solubilized lignin following a single-shot steam process. *Bioresource Technology* **144**: 658-663.

Leung, H.T.C., Maas, K.R., Wilhelm, R.C., and Mohn, W.W. (2016) Long-term effects of timber harvesting on hemicellulolytic microbial populations in coniferous forest soils. *ISME J* **10**: 363-375.

Linger, J.G., Vardon, D.R., Guarnieri, M.T., Karp, E.M., Hunsinger, G.B., Franden, M.A. et al. (2014) Lignin valorization through integrated biological funneling and chemical catalysis. *Proceedings of the National Academy of Sciences* **111**: 12013-12018.

Love, M.I., Huber, W., and Anders, S. (2014) Moderated estimation of fold change and dispersion for RNA-seq data with DESeq2. *Genome Biology* **15**: 550.

Lozupone, C., and Knight, R. (2005) UniFrac: a new phylogenetic method for comparing microbial communities. *Applied and Environmental Microbiology* **71**: 8228-8235.

Lupoi, J.S., Singh, S., Simmons, B.A., and Henry, R.J. (2014) Assessment of Lignocellulosic Biomass Using Analytical Spectroscopy: an Evolution to High-Throughput Techniques. *BioEnergy Research* **7**: 1-23.

Lynd, L.R., Weimer, P.J., van Zyl, W.H., and Pretorius, I.S. (2002) Microbial Cellulose Utilization: Fundamentals and Biotechnology. *Microbiology and Molecular Biology Reviews* **66**: 506-577.

Mathews, S.L., Pawlak, J., and Grunden, A.M. (2015) Bacterial biodegradation and bioconversion of industrial lignocellulosic streams. *Applied Microbiology and Biotechnology* **99**: 2939-2954.

McClain, C., and Barry, J. (2014) Beta-diversity on deep-sea wood falls reflects gradients in energy availability. *Biology Letters* **10**: 20140129.

McMurdie, P.J., and Holmes, S. (2013) phyloseq: an R package for reproducible interactive analysis and graphics of microbiome census data. *PLoS One* **8**: e61217.

McMurdie, P.J., and Holmes, S. (2014) Waste Not, Want Not: Why Rarefying Microbiome Data Is Inadmissible. *PLoS Comput Biol* **10**: e1003531.

Meyer, F., Paarmann, D., D'Souza, M., Olson, R., Glass, E.M., Kubal, M. et al. (2008) The metagenomics RAST server - a public resource for the automatic phylogenetic and functional analysis of metagenomes. *BMC Bioinformatics* **9**: 386.

Nakamura, H. (1961) Chemical separation methods for common microbes. *Journal of Biochemical and Microbiological Technology and Engineering* **3**: 395-403.

Nguyen, N.-P., Warnow, T., Pop, M., and White, B. (2016) A perspective on 16S rRNA operational taxonomic unit clustering using sequence similarity. *Npj Biofilms And Microbiomes* **2**: 16004.

O'Dell, K.B., Woo, H.L., Utturkar, S., Klingeman, D., Brown, S.D., and Hazen, T.C. (2015) Genome sequence of Halomonas sp. strain KO116, an ionic liquid-tolerant marine bacterium isolated from a lignin-enriched seawater microcosm. *Genome announcements* **3**: e00402-00415.

Oh, J., Choe, H., Kim, B.K., and Kim, K.M. (2015) Complete genome of a coastal marine bacterium Muricauda lutaonensis KCTC 22339T. *Marine Genomics* **23**: 51-53.

Ohta, Y., Nishi, S., Haga, T., Tsubouchi, T., Hasegawa, R., Konishi, M. et al. (2012) Screening and Phylogenetic Analysis of Deep-Sea Bacteria Capable of Metabolizing Lignin-Derived Aromatic Compounds. *Open Journal of Marine Science* **02**: 177-187.

Ooshima, H., Burns, D.S., and Converse, A.O. (1990) Adsorption of cellulase from Trichoderma reesei on cellulose and lignacious residue in wood pretreated by dilute sulfuric acid with explosive decompression. *Biotechnology and Bioengineering* **36**: 446-452.

Opsahl, S., and Benner, R. (1998) Photochemical reactivity of dissolved lignin in river and ocean waters. *Limnology and Oceanography* **43**: 1297-1304.

Ovreås, L., Forney, L., Daae, F.L., and Torsvik, V. (1997) Distribution of bacterioplankton in meromictic Lake Saelenvannet, as determined by denaturing gradient gel electrophoresis of PCR-amplified gene fragments coding for 16S rRNA. *Applied and Environmental Microbiology* **63**: 3367-3373.

Park, J.I., Steen, E.J., Burd, H., Evans, S.S., Redding-Johnson, A.M., Batth, T. et al. (2012) A thermophilic ionic liquid-tolerant cellulase cocktail for the production of cellulosic biofuels. *PLoS One* **7**: e37010.

Pianka, E.R. (1970) On r-and K-selection. *The American Naturalist* **104**: 592-597.

Pointing, S.B., and Hyde, K.D. (2000) Lignocellulose-degrading marine fungi. *Biofouling* **15**: 221-229.

Pollegioni, L., Tonin, F., and Rosini, E. (2015) Lignin-degrading enzymes. *FEBS J* **282**: 1190-1213.

Ponce-Soto, G.Y., Aguirre-von-Wobeser, E., Eguiarte, L.E., Elser, J.J., Lee, Z.M.P., and Souza, V. (2015) Enrichment experiment changes microbial interactions in an ultra-oligotrophic environment. *Frontiers in Microbiology* **6**.

Prasad, M.P., and Sethi, R. (2013) Screening for xylanase producing microorganisms from marine sources. *International Journal of Current Microbiology and Applied Sciences* **2**: 489-492.

Ragauskas, A.J., Beckham, G.T., Biddy, M.J., Chandra, R., Chen, F., Davis, M.F. et al. (2014) Lignin valorization: improving lignin processing in the biorefinery. *Science* **344**: 1246843.

Richards, T.A., Jones, M.D.M., Leonard, G., and Bass, D. (2012) Marine Fungi: Their Ecology and Molecular Diversity. *Annual Review of Marine Science* **4**: 495-522.

Roberts, D. (2007) Labdsv: ordination and multivariate analysis for ecology. In.

Ruiz-Dueñas, F.J., and Martínez, Á.T. (2009) Microbial degradation of lignin: how a bulky recalcitrant polymer is efficiently recycled in nature and how we can take advantage of this. *Microbial Biotechnology* **2**: 164-177.

Sánchez-Porro, C., Martín, S., Mellado, E., and Ventosa, A. (2003) Diversity of moderately halophilic bacteria producing extracellular hydrolytic enzymes. *Journal of Applied Microbiology* **94**: 295-300.

Schellenberger, S., Kolb, S., and Drake, H.L. (2010) Metabolic responses of novel cellulolytic and saccharolytic agricultural soil Bacteria to oxygen. *Environmental Microbiology* **12**: 845-861.

Scheller, H.V., and Ulvskov, P. (2010) Hemicelluloses. *Annual Review of Plant Biology* **61**: 263-289.

Schlünz, B., and Schneider, R.R. (2000) Transport of terrestrial organic carbon to the oceans by rivers: re-estimating flux- and burial rates. *International Journal of Earth Sciences* **88**: 599-606.

Scully, E.D., Geib, S.M., Hoover, K., Tien, M., Tringe, S.G., Barry, K.W. et al. (2013) Metagenomic Profiling Reveals Lignocellulose Degrading System in a Microbial Community Associated with a Wood-Feeding Beetle. *PLoS One* **8**: e73827.

Sinsabaugh, R.L. (2010) Phenol oxidase, peroxidase and organic matter dynamics of soil. *Soil Biology and Biochemistry* **42**: 391-404.

Skovhus, T.L., HolmstrÃ¶m, C., Kjelleberg, S., and DahllÃ¶f, I. (2007) Molecular investigation of the distribution, abundance and diversity of the genus Pseudoalteromonas in marine samples: Abundance and diversity of Pseudoalteromonas. *FEMS Microbiology Ecology* **61**: 348-361.

Smith Jr., K.L., and Hinga, K.R. (1983) Sediment community respiration in the deep sea. In *Deep-Sea Biology The Sea*. Rowe, G. (ed). New York: WIley Interscience, pp. 331-370.

Strachan, C.R., Singh, R., VanInsberghe, D., Ievdokymenko, K., Budwill, K., Mohn, W.W. et al. (2014) Metagenomic scaffolds enable combinatorial lignin transformation. *Proceedings of the National Academy of Sciences* **111**: 10143-10148.

Sutherland, J.B., Crawford, D.L., and Speedie, M.K. (1982) Decomposition of C-Labeled Maple and Spruce Lignin by Marine Fungi. *Mycologia* **74**: 511-513.

Tao, J., Hosseinaei, O., Delbeck, L., Kim, P., Harper, D.P., Bozell, J.J. et al. (2016) Effects of organosolv fractionation time on thermal and chemical properties of lignins. *RSC Advances* **6**: 79228-79235.

Techtmann, S.M., Fortney, J.L., Ayers, K.A., Joyner, D.C., Linley, T.D., Pfiffner, S.M., and Hazen, T.C. (2015) The unique chemistry of Eastern Mediterranean water masses selects for distinct microbial communities by depth. *PLoS One* **10**: e0120605.

Thevenot, M., Dignac, M.-F., and Rumpel, C. (2010) Fate of lignins in soils: A review. *Soil Biology and Biochemistry* **42**: 1200-1211.

Turner, M.B., Spear, S.K., Huddleston, J.G., Holbrey, J.D., and Rogers, R.D. (2003) Ionic liquid salt-induced inactivation and unfolding of cellulase from Trichoderma reesei. *Green Chemistry* **5**: 443.

van der Lelie, D., Taghavi, S., McCorkle, S.M., Li, L.L., Malfatti, S.A., Monteleone, D. et al. (2012) The metagenome of an anaerobic microbial community decomposing poplar wood chips. *PLoS One* **7**: e36740.

Velicer, G.J. (2003) Social strife in the microbial world. *Trends in Microbiology* **11**: 330-337.

Vera, J., Alvarez, R., Murano, E., Slebe, J.C., and Leon, O. (1998) Identification of a Marine AgarolyticPseudoalteromonas Isolate and Characterization of Its Extracellular Agarase. *Applied and Environmental Microbiology* **64**: 4378-4383.

Wang, W., Yan, L., Cui, Z., Gao, Y., Wang, Y., and Jing, R. (2011) Characterization of a microbial consortium capable of degrading lignocellulose. *Bioresource Technology* **102**: 9321-9324.

Ward, N.D., Keil, R.G., Medeiros, P.M., Brito, D.C., Cunha, A.C., Dittmar, T. et al. (2013) Degradation of terrestrially derived macromolecules in the Amazon River. *Nature Geoscience* **6**: 530-533.

Wickham, H. (2009) *ggplot2: Elegant Graphics for Data Analysis*: Springer-Verlag New York.

Woo, H.L., Hazen, T.C., Simmons, B.A., and DeAngelis, K.M. (2014) Enzyme activities of aerobic lignocellulolytic bacteria isolated from wet tropical forest soils. *Systematic and Applied Microbiology* **37**: 60-67.

Xia, Y., Ju, F., Fang, H.H.P., and Zhang, T. (2013) Mining of Novel Thermo-Stable Cellulolytic Genes from a Thermophilic Cellulose-Degrading Consortium by Metagenomics. *PLoS One* **8**: e53779.

Zakrzewski, M., Proietti, C., Ellis, J.J., Hasan, S., Brion, M.J., Berger, B., and Krause, L. (2016) Calypso: a user-friendly web-server for mining and visualizing microbiome-environment interactions. *Bioinformatics*.

Zakzeski, J., Bruijnincx, P.C.A., Jongerius, A.L., and Weckhuysen, B.M. (2010) The Catalytic Valorization of Lignin for the Production of Renewable Chemicals. *Chemical Reviews* **110**: 3552-3599.

Vita

Hannah L. Woo grew up in the San Francisco East Bay Area, California. She graduated from Pinole Valley High School in 2005. She obtained her Bachelor of Science in Molecular Environmental Biology from the University of California, Berkeley in 2009. She was a research technician from 2009-2012 at Lawrence Berkeley National Laboratory and the Joint Bioenergy Institute. She then became an NSF iGERT fellow (2012-2014), an NSF GRFP fellow (2014-2017), an NSF EAPSI fellow (2016), and PEO scholar (2016-2017) at the University of Tennessee Civil and Environmental Engineering department. Since 2009, she has co-authored 10 publications, given talks and poster presentations at 31 regional, national, and international conferences.